

Phenomenology of virtual Compton scattering processes in the era of new experiments

Paweł Sznajder
National Centre for Nuclear Research, Poland

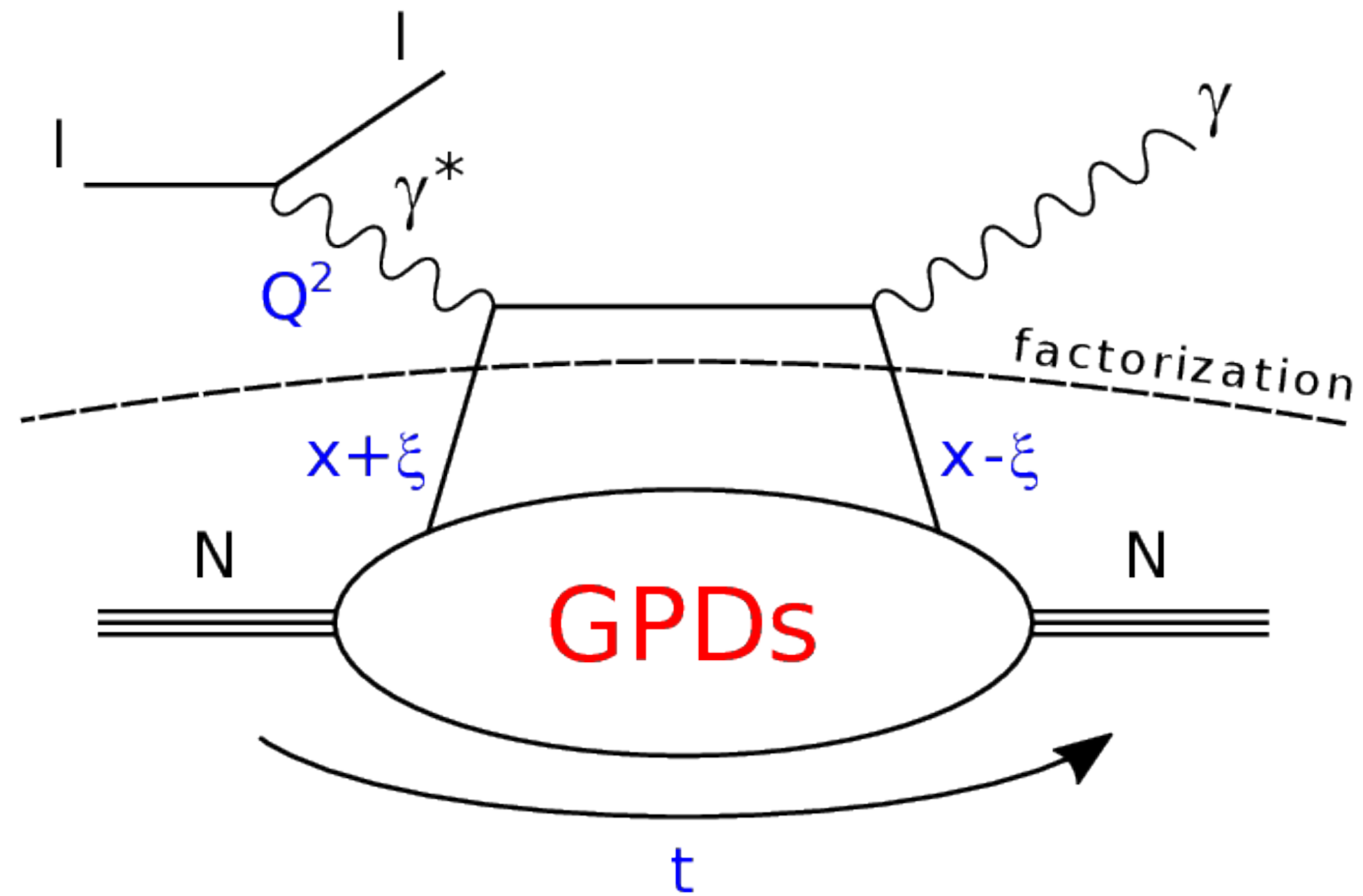


NATIONAL
CENTRE
FOR NUCLEAR
RESEARCH
ŚWIERK

3D Structure of the Nucleon via Generalized Parton Distributions,
Incheon, Republic of Korea, June 25th, 2024

- Introduction and motivation
- Virtual Compton scattering processes
- Deconvolution problem
- Double Deeply Virtual Scattering
- Inclusion lattice-QCD results
- Summary

Deeply Virtual Compton Scattering (DVCS)



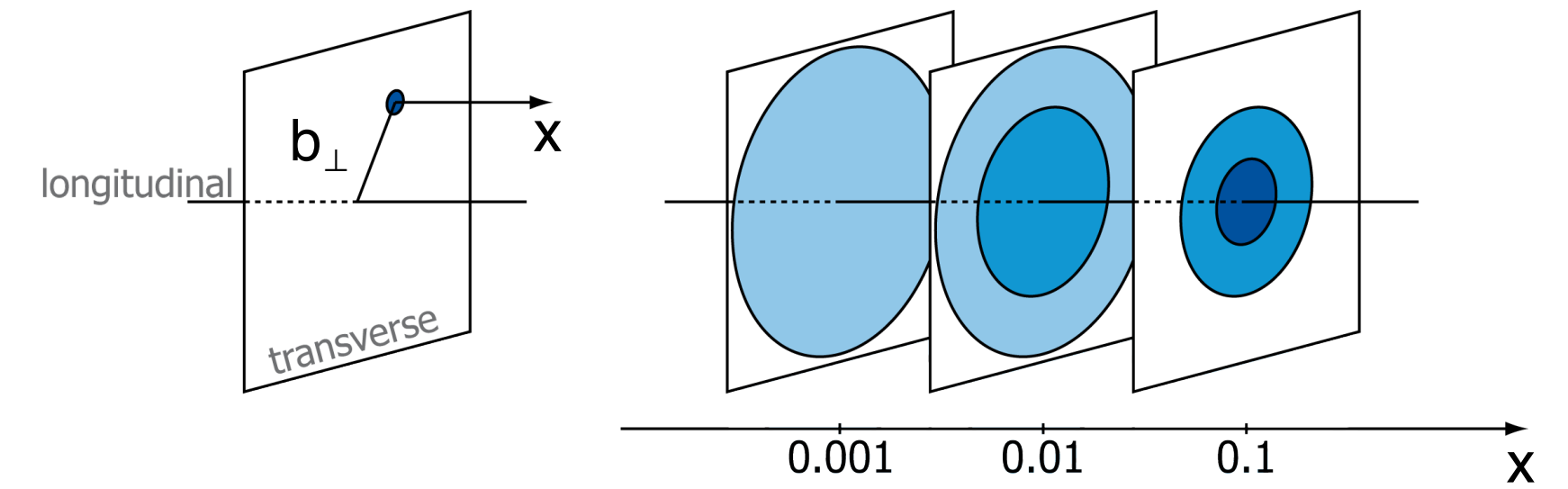
factorisation for $|t|/Q^2 \ll 1$

Chiral-even GPDs:
(helicity of parton conserved)

$H^{q,g}(x, \xi, t)$	$E^{q,g}(x, \xi, t)$	<i>for sum over parton helicities</i>
$\tilde{H}^{q,g}(x, \xi, t)$	$\tilde{E}^{q,g}(x, \xi, t)$	<i>for difference over parton helicities</i>
<i>nucleon helicity conserved</i>	<i>nucleon helicity changed</i>	

Nucleon tomography:

$$q(x, \mathbf{b}_\perp) = \int \frac{d^2 \Delta}{4\pi^2} e^{-i\mathbf{b}_\perp \cdot \Delta} H^q(x, 0, t = -\Delta^2)$$



Energy momentum tensor in terms of form factors (OAM and mechanical forces):

$$T^{\mu\nu} = \begin{bmatrix} \text{Energy density } T^{00} & \text{Momentum density } T^{01} & T^{02} & T^{03} \\ T^{10} & T^{11} & T^{12} & T^{13} \\ T^{20} & T^{21} & T^{22} & T^{23} \\ T^{30} & T^{31} & T^{32} & T^{33} \end{bmatrix}$$

Shear stress
Normal stress

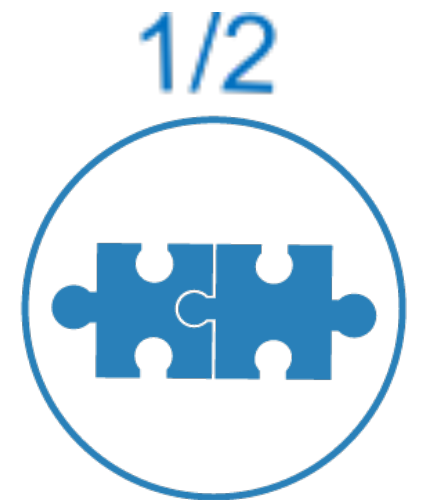
Energy flux Momentum flux

$$\langle p', s' | \hat{T}^{\mu\nu} | p, s \rangle = \bar{u}(p', s') \left[\frac{P^\mu P^\nu}{M} A(t) + \frac{\Delta^\mu \Delta^\nu - \eta^{\mu\nu} \Delta^2}{M} C(t) + M \eta^{\mu\nu} \bar{C}(t) + \frac{P^\mu i\sigma^{\nu\lambda} \Delta_\lambda}{4M} [A(t) + B(t) + D(t)] + \frac{P^\nu i\sigma^{\mu\lambda} \Delta_\lambda}{4M} [A(t) + B(t) - D(t)] \right] u(p, s)$$

Total angular momentum:

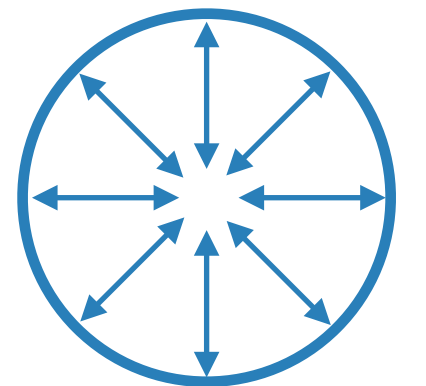
$$A^q(0) + B^q(0) = \int_{-1}^1 x [H^q(x, \xi, 0) + E^q(x, \xi, 0)] = 2J^q$$

Ji's sum rule

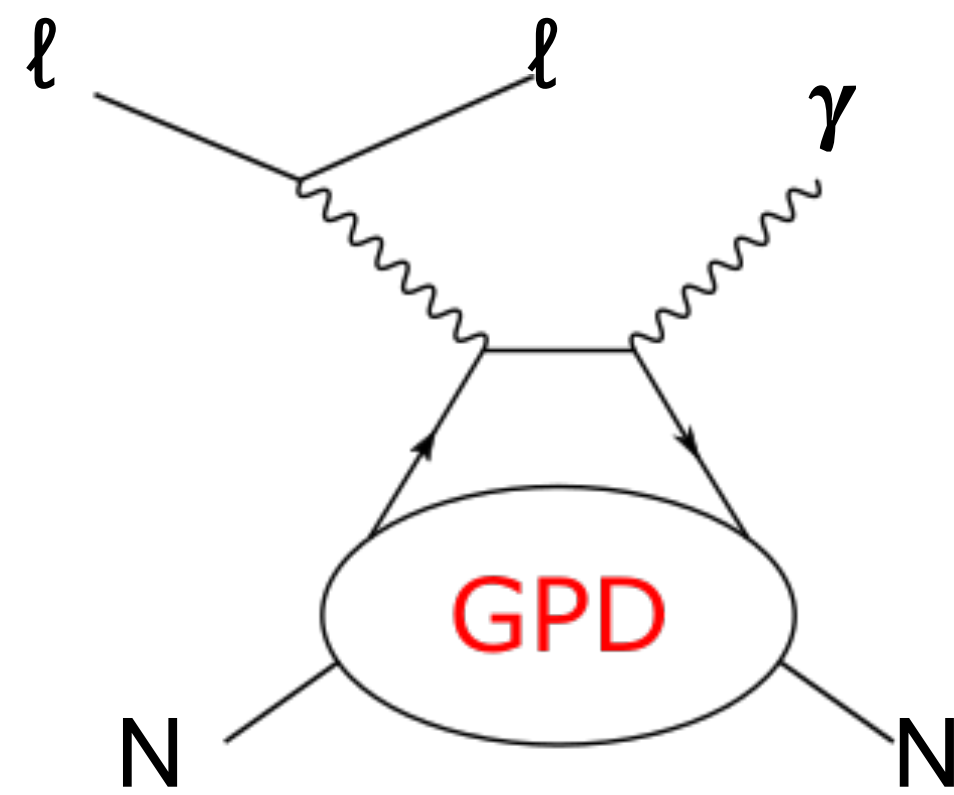


“Mechanical” forces acting on quarks, e.g. pressure in nucleon center:

$$p(0) = \frac{1}{6\pi^2 M} \int_{-\infty}^0 dt \sqrt{-t} C(t)$$



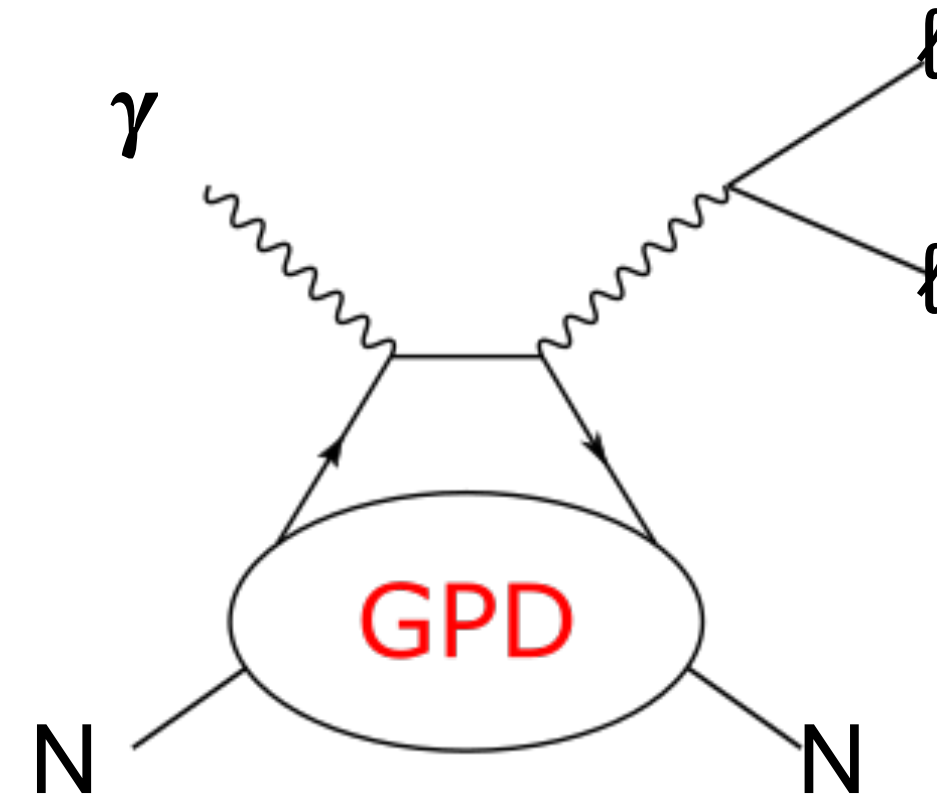
**VCS processes provide the most straightforward way to access GPDs
(at least from theory side...)**



DVCS

Deeply Virtual Compton Scattering

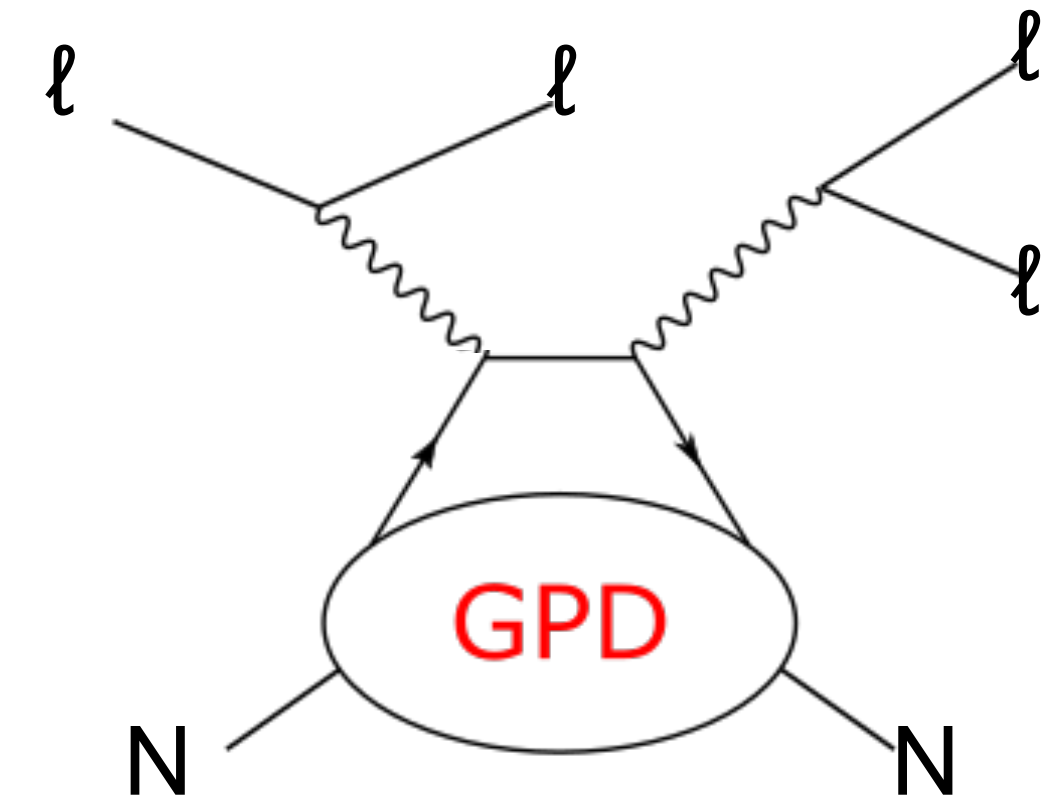
- many measurements, see e.g.:
[EPJA 52 \(2016\) 6, 157](#)
- description up to NNLO and twist-4 available
[PRL 129 \(2022\) 17, 172001](#)
[JHEP 01 \(2023\) 078](#)



TCS

Timelike Compton Scattering

- first measurement by CLAS
[PRL 127 \(2021\) 26, 262501](#)
- description up to NLO and twist-2 available
(preliminary tw-4)



DDVCS

Double Deeply Virtual Compton Scattering

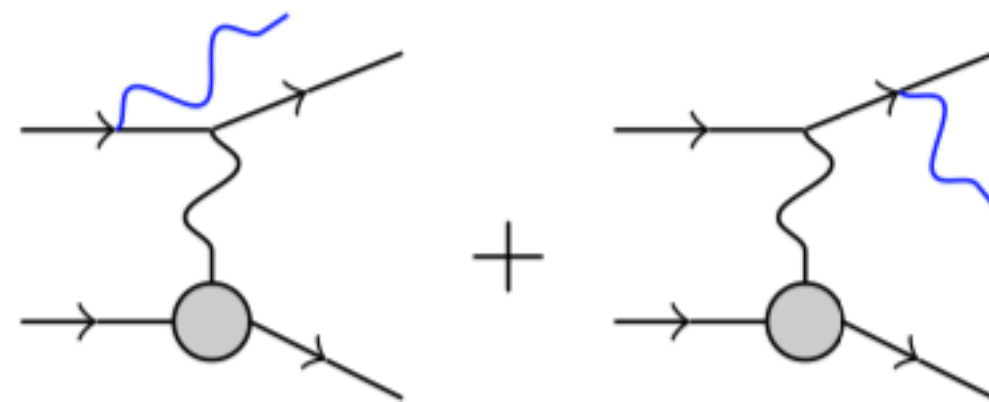
- never measured
- description up to NLO and twist-2 available
(preliminary tw-4)

more production channels sensitive to GPDs exist!

Cross-section for single photon production ($l + N \rightarrow l + N + \gamma$):

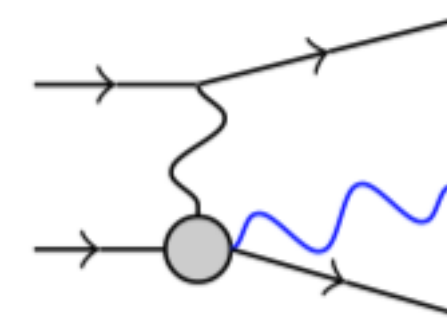
$$\sigma \propto |\mathcal{A}|^2 = |\mathcal{A}_{BH} + \mathcal{A}_{DVCS}|^2 = |\mathcal{A}_{BH}|^2 + |\mathcal{A}_{DVCS}|^2 + \mathcal{F}$$

Bethe-Heitler process



*calculable within QED
parametrised by elastic FFs*

DVCS



*calculable within QCD
parametrised by CFFs*

see e.g. NPB 878 (2014) 214
for more details

$$\text{Im}\mathcal{H}(\xi, t) \stackrel{\text{LO}}{=} \pi \sum_q e_q^2 H^{q(+)}(\xi, \xi, t)$$

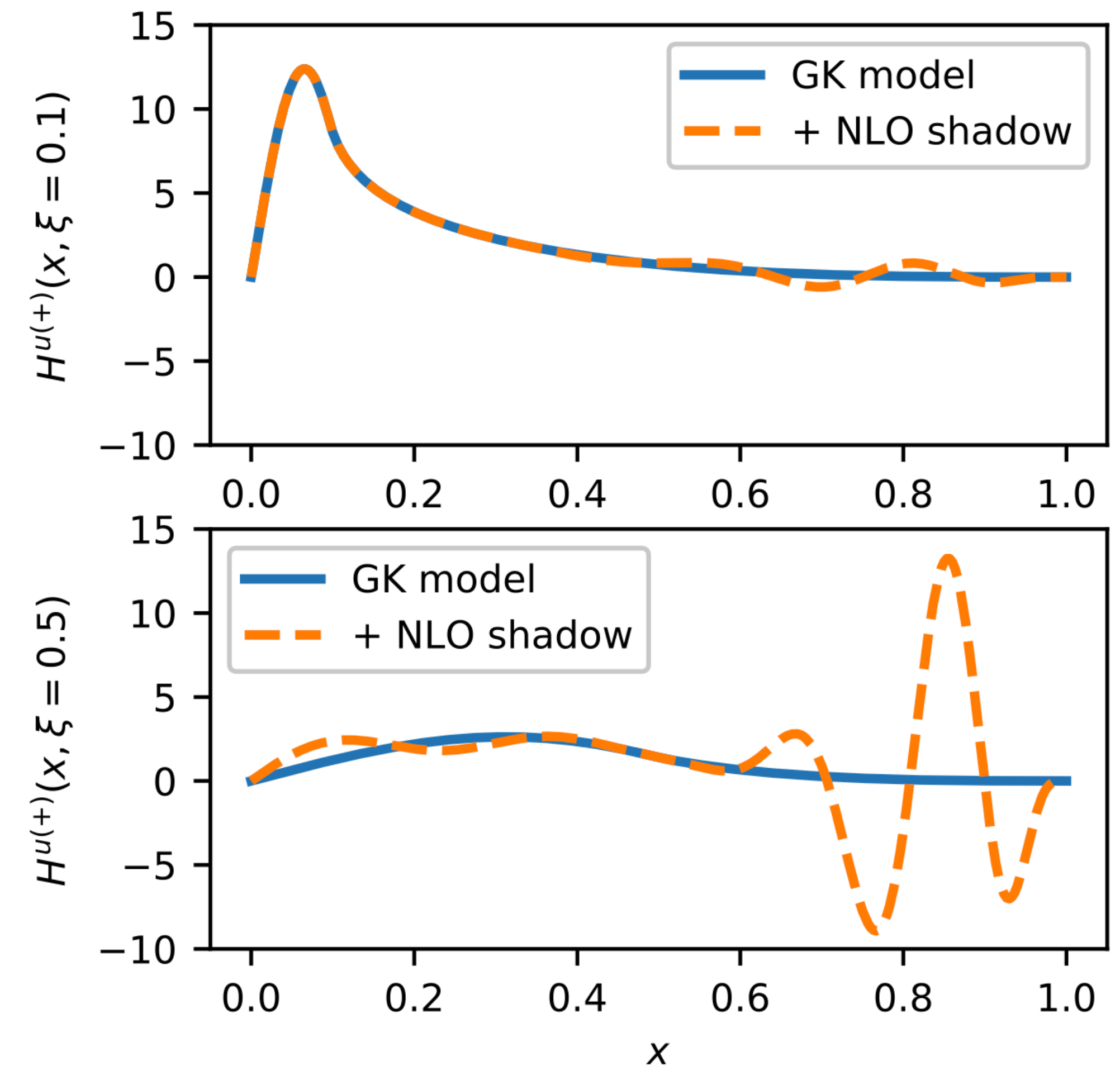
$$\text{Re}\mathcal{H}(\xi, t) = \text{PV} \int_0^1 \frac{d\xi'}{\pi} \text{Im}\mathcal{H}(\xi', t) \left(\frac{1}{\xi - \xi'} - \frac{1}{\xi + \xi'} \right) + C_H(t)$$

Shadow GPDs have considerable size, but:

- at arbitrary initial scale do not contribute to PDFs and CFFs
- at other scales contribute negligibly

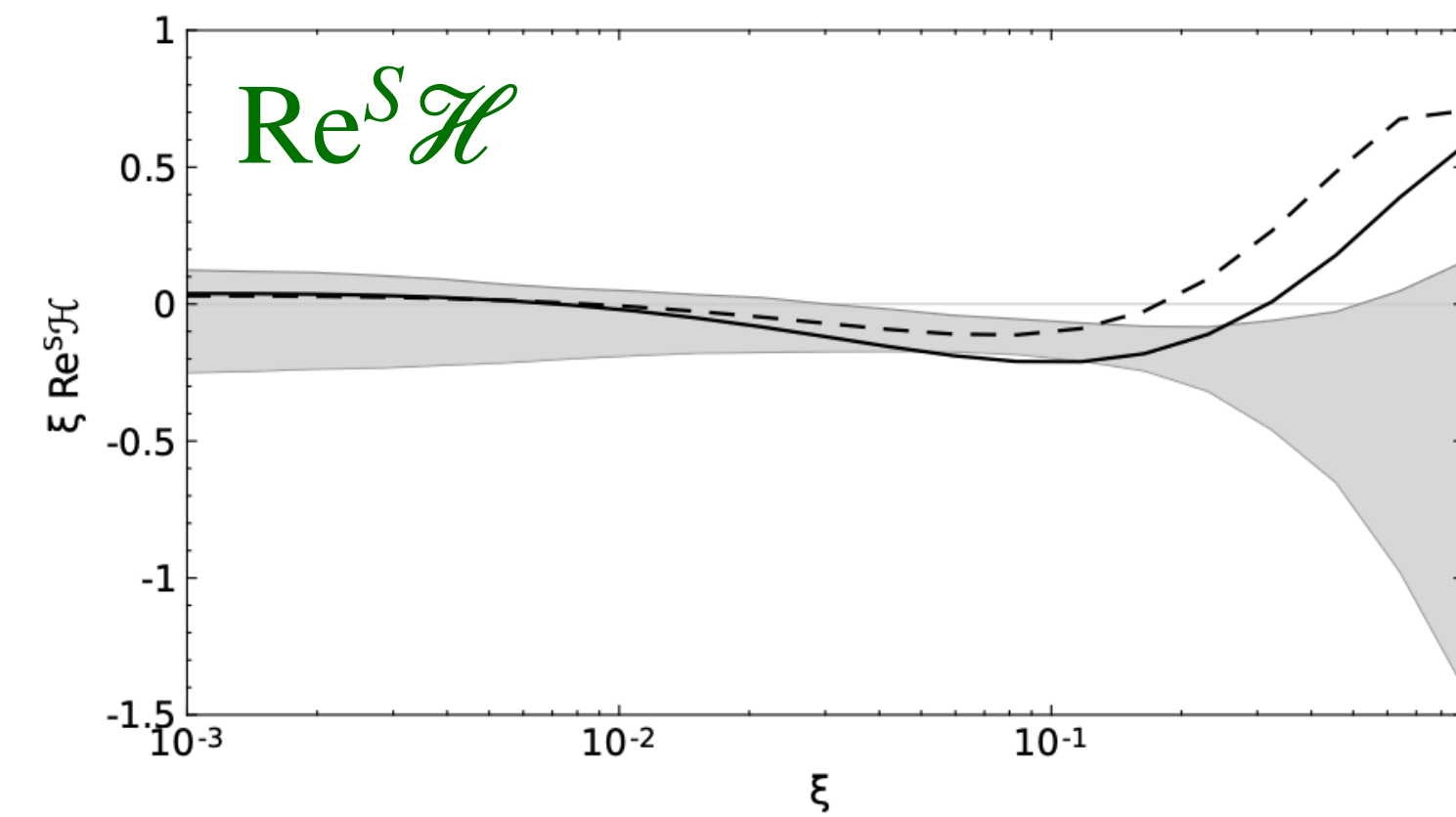
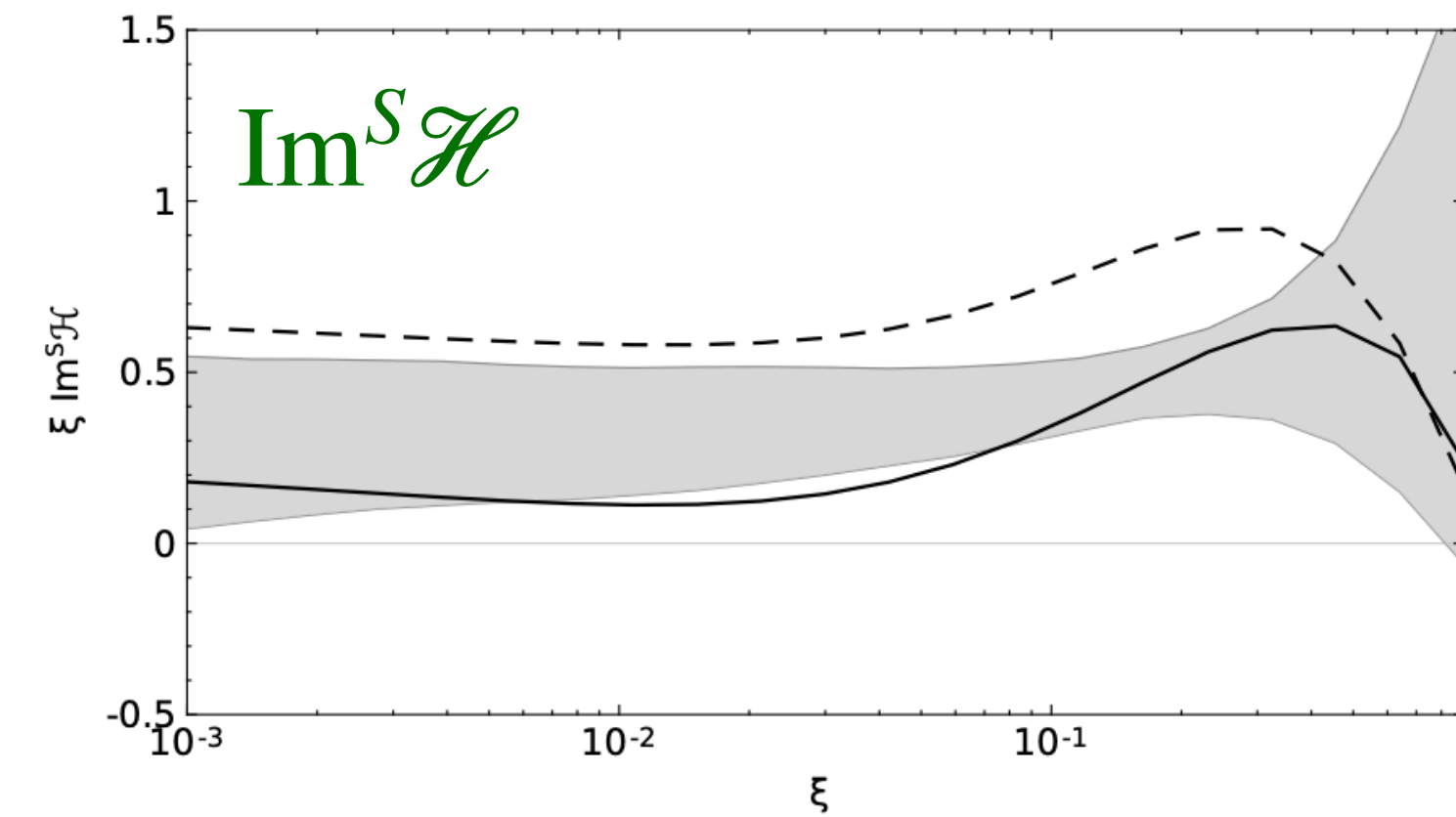
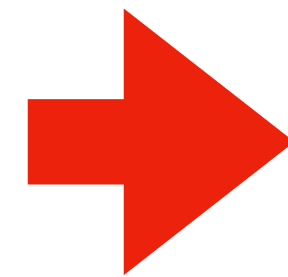
making the deconvolution of CFFs ill-posed problem

We found such GPDs for DVCS for both LO and NLO
(for discussion see also PRD 108 (2023) 3, 036027)

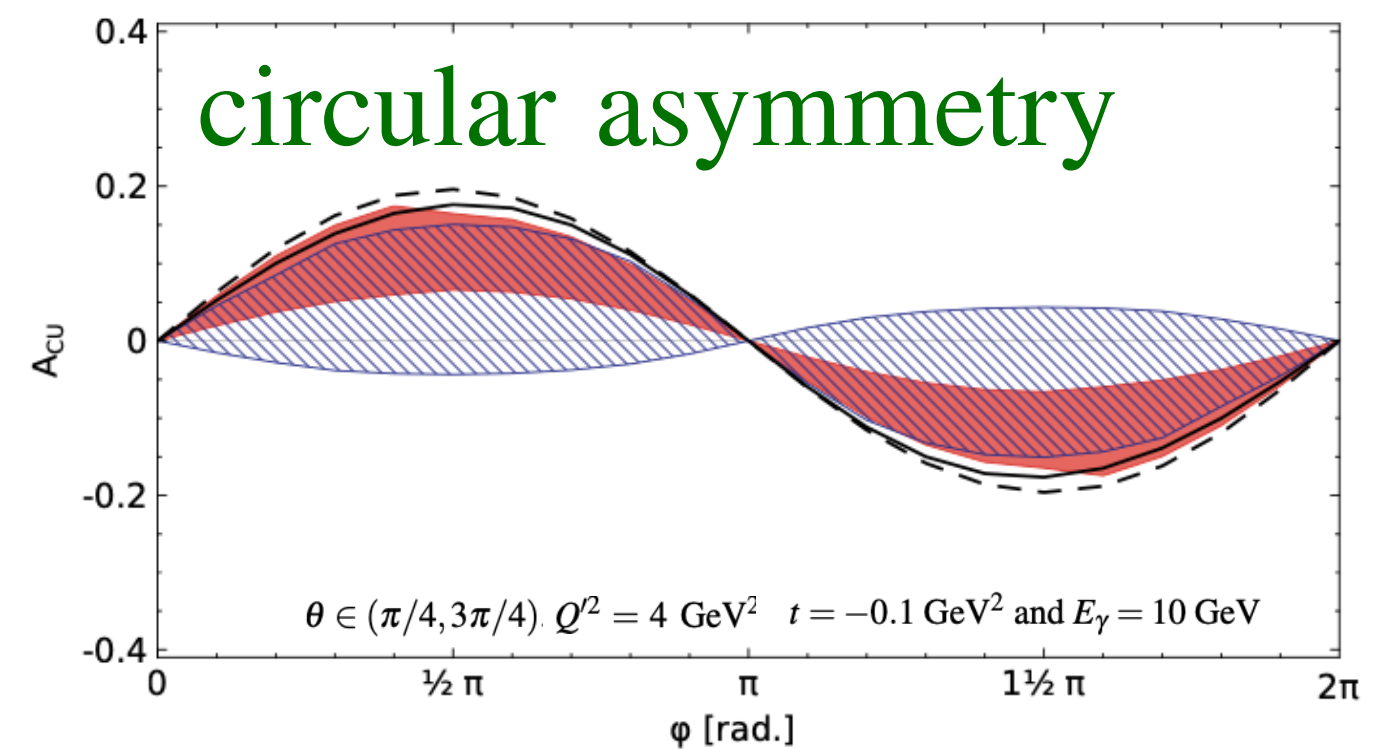
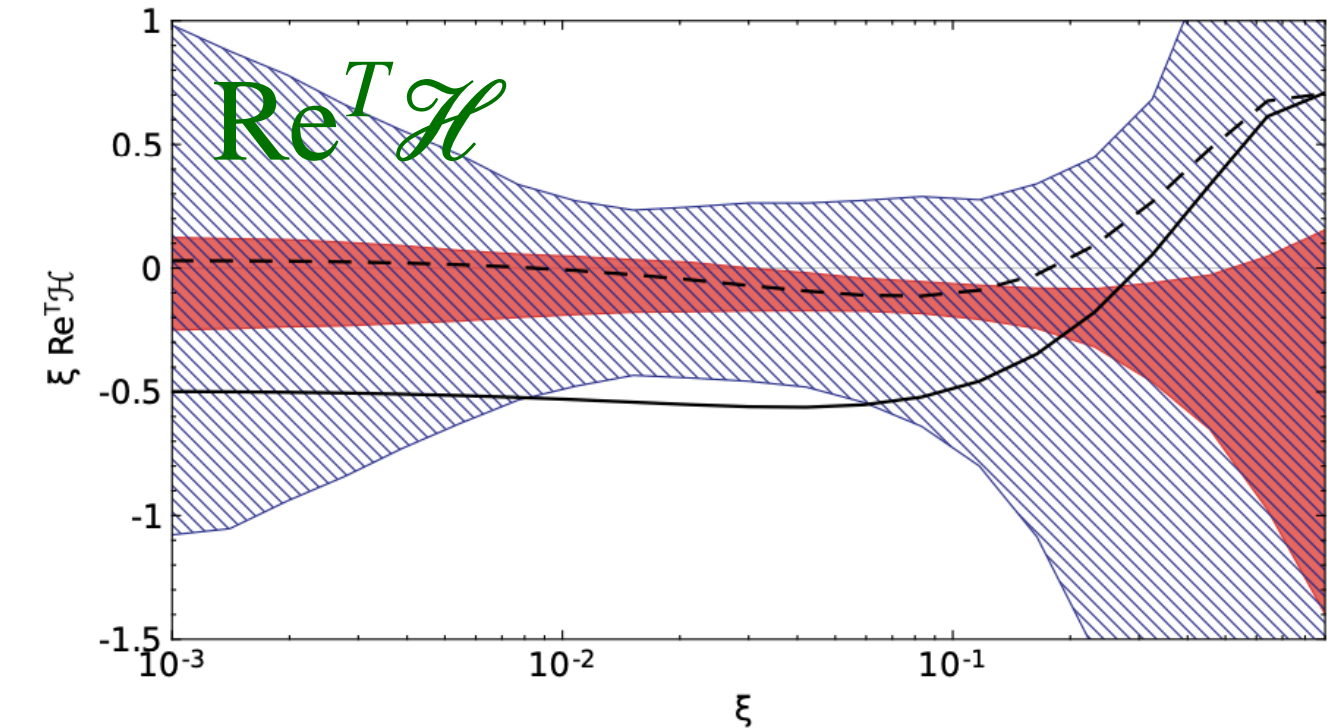
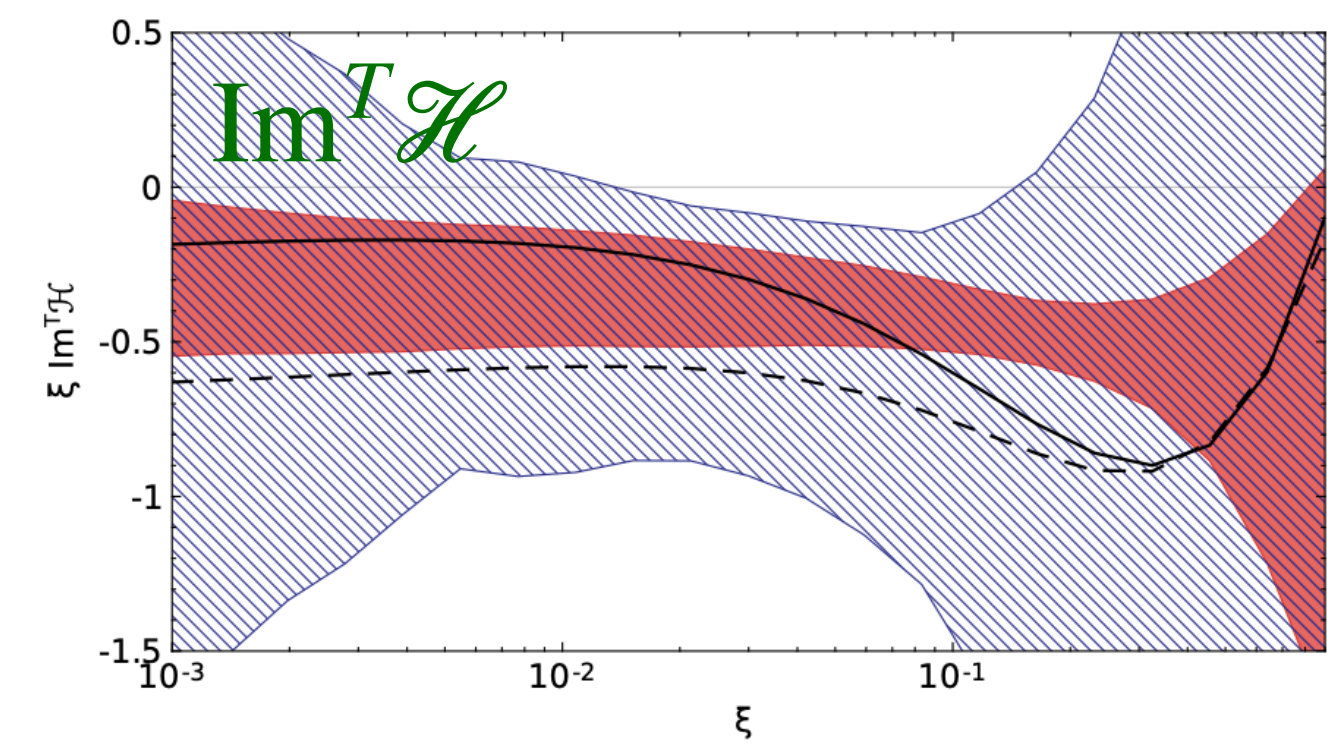


O. Grocholski et al.,
Eur. Phys. J. C 80 (2020) 2, 171

Relation between space-like
and time-like amplitudes



ANN analysis
GK (LO) — GK (NLO)



TCS from DVCS (LO)
TCS from DVCS (NLO)

$$T \mathcal{H} \stackrel{\text{LO}}{=} S \mathcal{H}^*$$

$$T \widetilde{\mathcal{H}} \stackrel{\text{LO}}{=} -S \widetilde{\mathcal{H}}^*$$

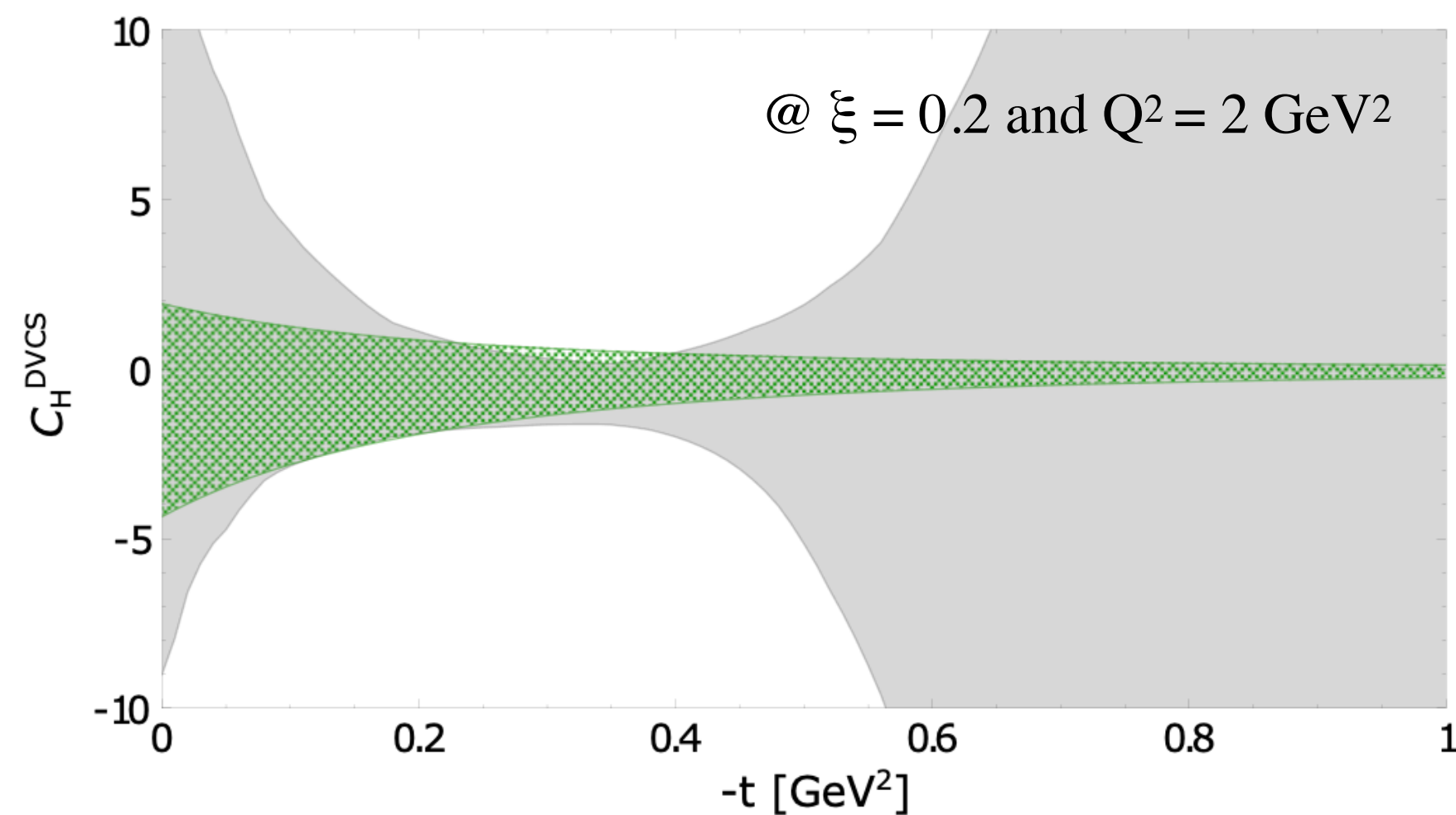
$$T \mathcal{H} \stackrel{\text{NLO}}{=} S \mathcal{H}^* - i\pi Q^2 \frac{\partial}{\partial Q^2} S \mathcal{H}^*$$

$$T \widetilde{\mathcal{H}} \stackrel{\text{NLO}}{=} -S \widetilde{\mathcal{H}}^* + i\pi Q^2 \frac{\partial}{\partial Q^2} S \widetilde{\mathcal{H}}^*$$

- probing nucleon tomography at low-xB (see: [JHEP 09 \(2013\) 093](#))

$$d^3\sigma/(dx_{Bj} dQ^2 dt) \propto (\text{Im}\mathcal{H}(\xi, t))^2 \propto \left(\sum_q e_q^2 H^{q(+)}(\xi, \xi, t) \right)^2 \propto \left(\sum_q e_q^2 H^{q(+)}(\xi, 0, t) \right)^2$$

- extraction of D-term (see: [Nature 570 \(2019\) 7759, E1](#), [EPJC 81 \(2021\) 4, 300](#))



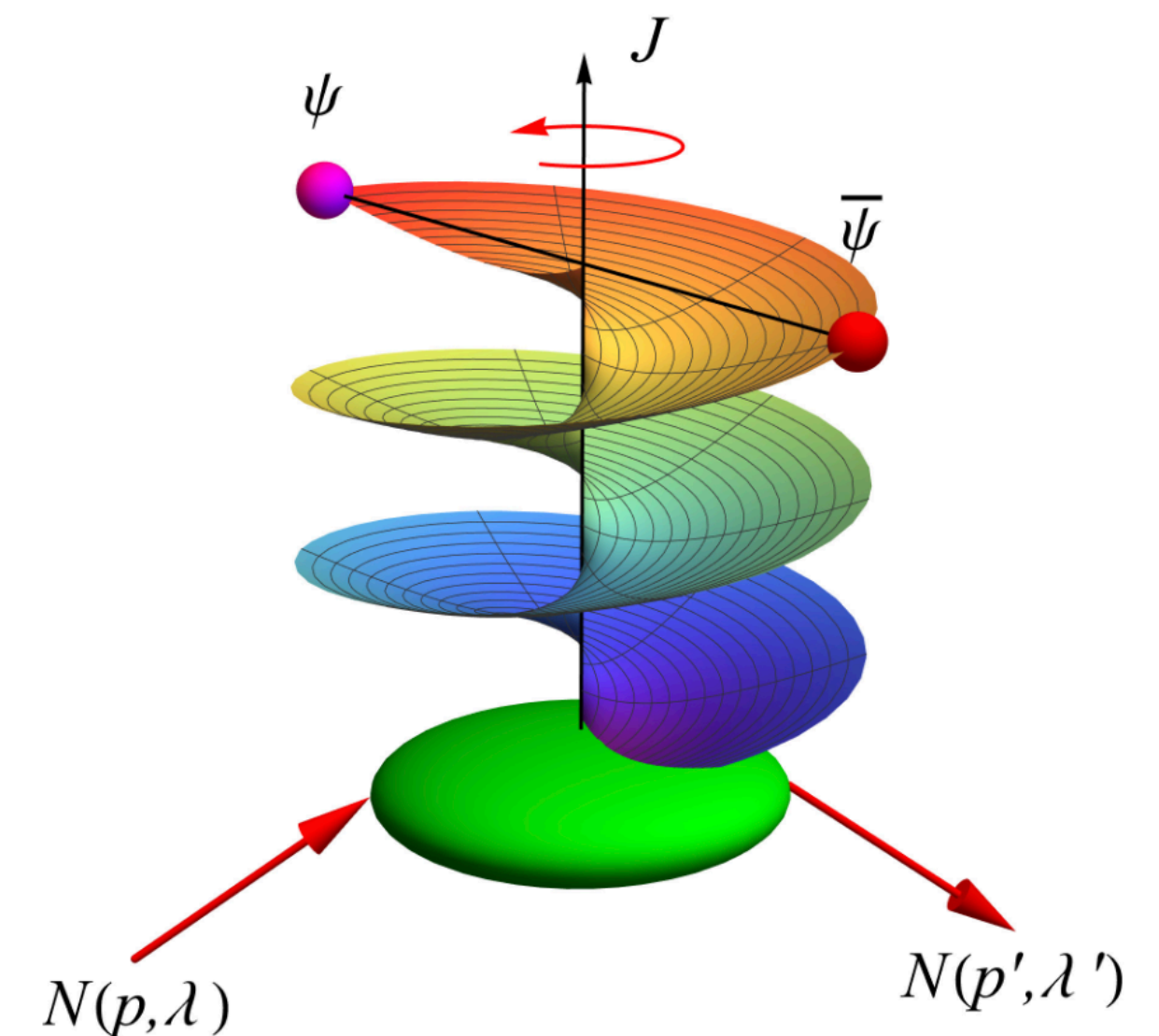
ANN analysis

Model dependent extraction

$$d_1^{uds}(t, \mu_F^2) = d_1^{uds}(\mu_F^2) \left(1 - \frac{t}{\Lambda^2} \right)^{-\alpha}$$

$$\alpha = 3 \quad \Lambda = 0.8 \text{ GeV}$$

- Froissart-Gribov projections (see: [PRD 109 \(2024\) 5, 054010](#))



FG projections are obtained by reconstructing cross-channel partial wave expansion amplitudes from the dispersive representation of the amplitude in the direct channel.

In cross-channel: $\gamma^*(q) + \gamma(-q') \rightarrow h(p') + \bar{h}(-p)$

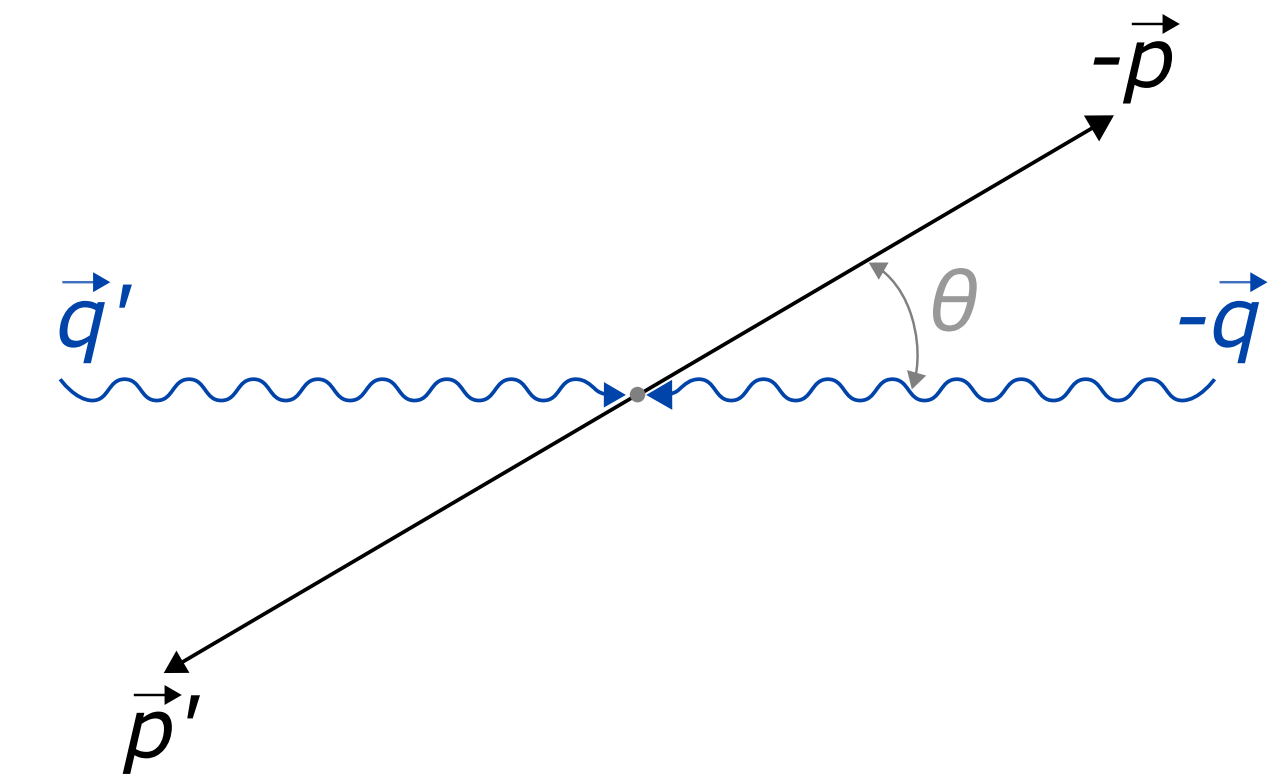
Expansion in the cross channel SO(3) partial waves: $\mathcal{H}_+(\cos \theta_t, t) = \sum_{\substack{J=0 \\ \text{even}}}^{\infty} F_J(t) P_J(\cos \theta_t)$

which gives: $F_J(t) = \frac{2J+1}{2} \int_{-1}^1 d(\cos \theta_t) P_J(\cos \theta_t) \mathcal{H}_+(\cos \theta_t, t)$

In direct-channel: $\gamma^*(q) + h(p) \rightarrow \gamma(q') + h(p')$

Dispersion relation: $\text{Re } \mathcal{H}_+(\xi, t) = \mathcal{P} \int_0^1 dx \frac{2x H_+(x, x, t)}{\xi^2 - x^2} + 4D(t)$

where: $\cos \theta_t \rightarrow -\frac{1}{\xi \beta} + \mathcal{O}(1/Q^2)$ $\beta = \sqrt{1 - \frac{4m^2}{t}}$



$\beta = 1$

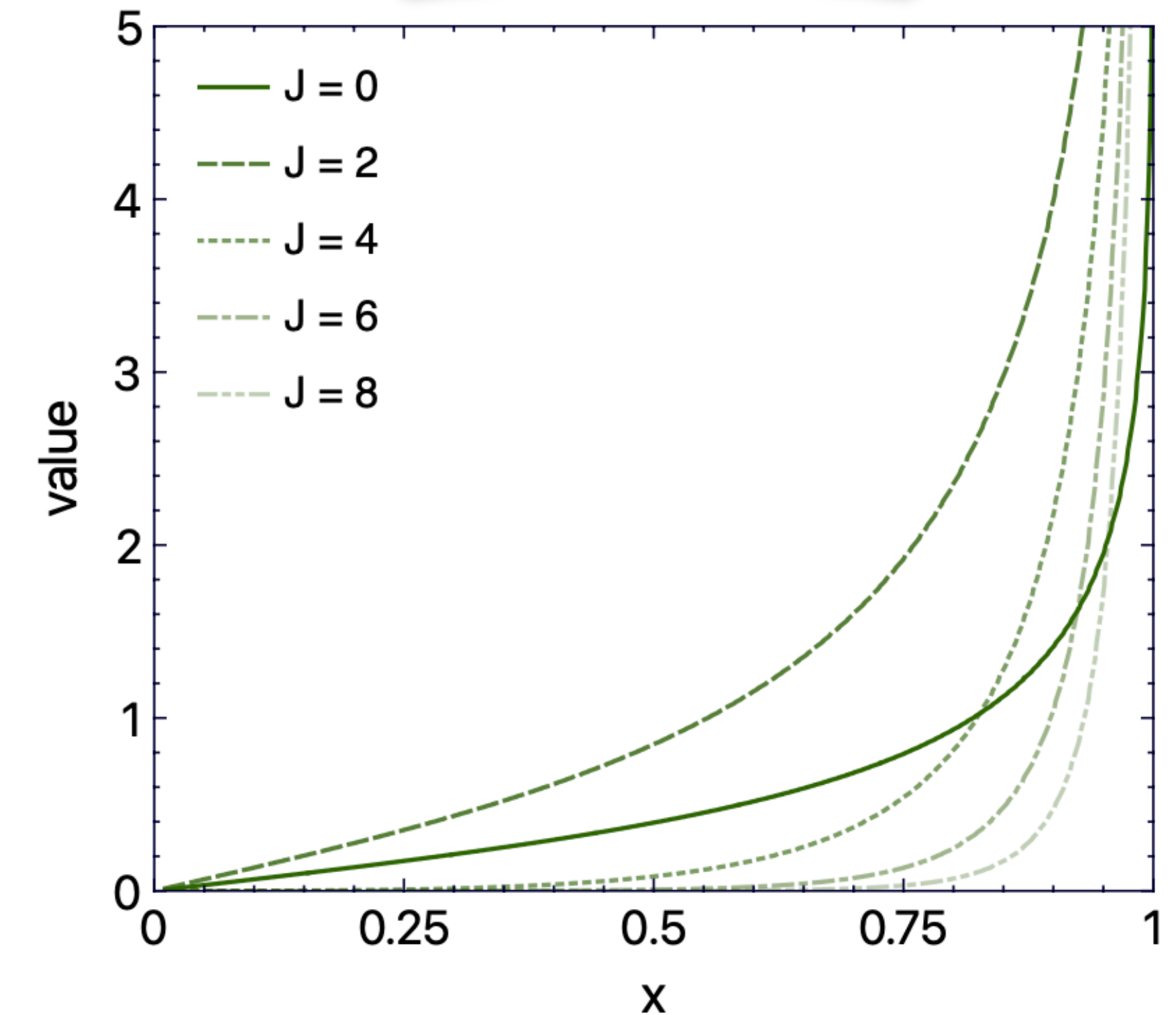
in the current analysis
 (see the publication for
 discussion of
 consequences)

weight functions

Final result:

$$F_{J=0}(t) = 2 \int_0^1 dx \left(\frac{Q_0(1/x)}{x^2} - \frac{1}{x} \right) H_+(x, x, t) + 4D(t)$$

$$F_{J>0}(t) = 2(2J + 1) \int_0^1 dx \frac{Q_J(1/x)}{x^2} H_+(x, x, t)$$



Electric combination:

$$H_{\pm}^{(E)}(x, \cos \theta_t, t) = H_{\pm}(x, \cos \theta_t, t) + \tau E_{\pm}(x, \cos \theta_t, t)$$

$$\tau \equiv t/(4m^2)$$

helicities of $p\bar{p}$ couple to $|\lambda-\lambda'| = 0$

has to be expanded in $P_J(\cos \theta_t)$ rotation function

Magnetic combination:

$$H_{\pm}^{(M)}(x, \cos \theta_t, t) = H_{\pm}(x, \cos \theta_t, t) + E_{\pm}(x, \cos \theta_t, t)$$

helicities of $p\bar{p}$ couple to $|\lambda-\lambda'| = 1$

has to be expanded in $\sin \theta_t P'_J(\cos \theta_t) / \sqrt{J(J+1)}$ rotation function

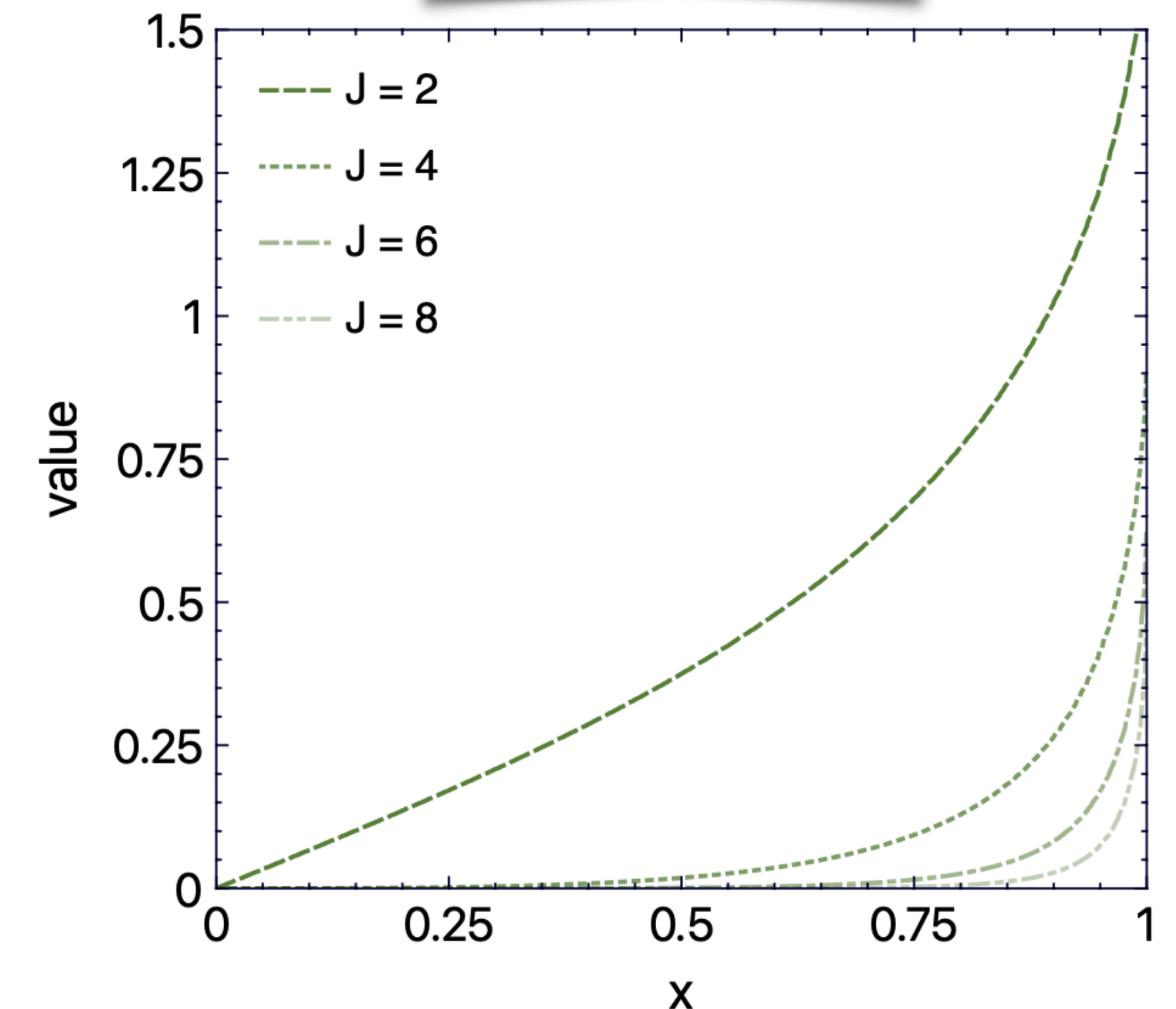
Final result:

$$F_{J=0}^{(E)}(t) = 2 \int_0^1 dx \left[\frac{Q_0(1/x)}{x^2} - \frac{1}{x} \right] H_+^{(E)}(x, x, t) + 4(1 - \tau)D(t)$$

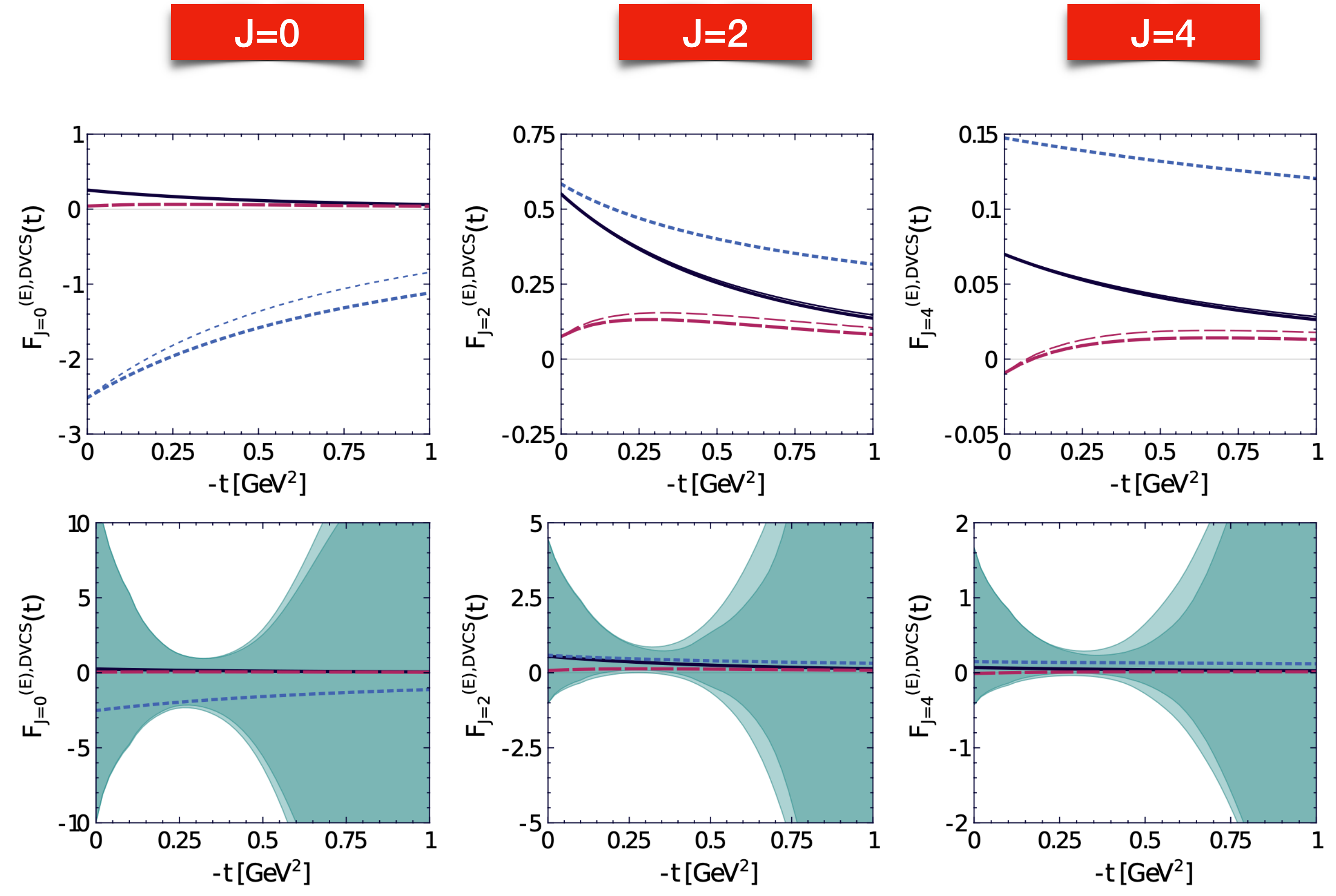
$$F_{J>0}^{(E)}(t) = 2(2J + 1) \int_0^1 dx \frac{Q_0(1/x)}{x^2} H_+^{(E)}(x, x, t)$$

$$F_J^{(M)}(t) = 2 \int_0^1 dx H_+^{(M)}(x, x, t) \frac{2J + 1}{J(J + 1)} \frac{(-1)}{x} \sqrt{\frac{1}{x^2} - 1} Q_J^1(1/x)$$

weight functions
(for $F_J^{(M)}$)



Numerical estimates - electric case:

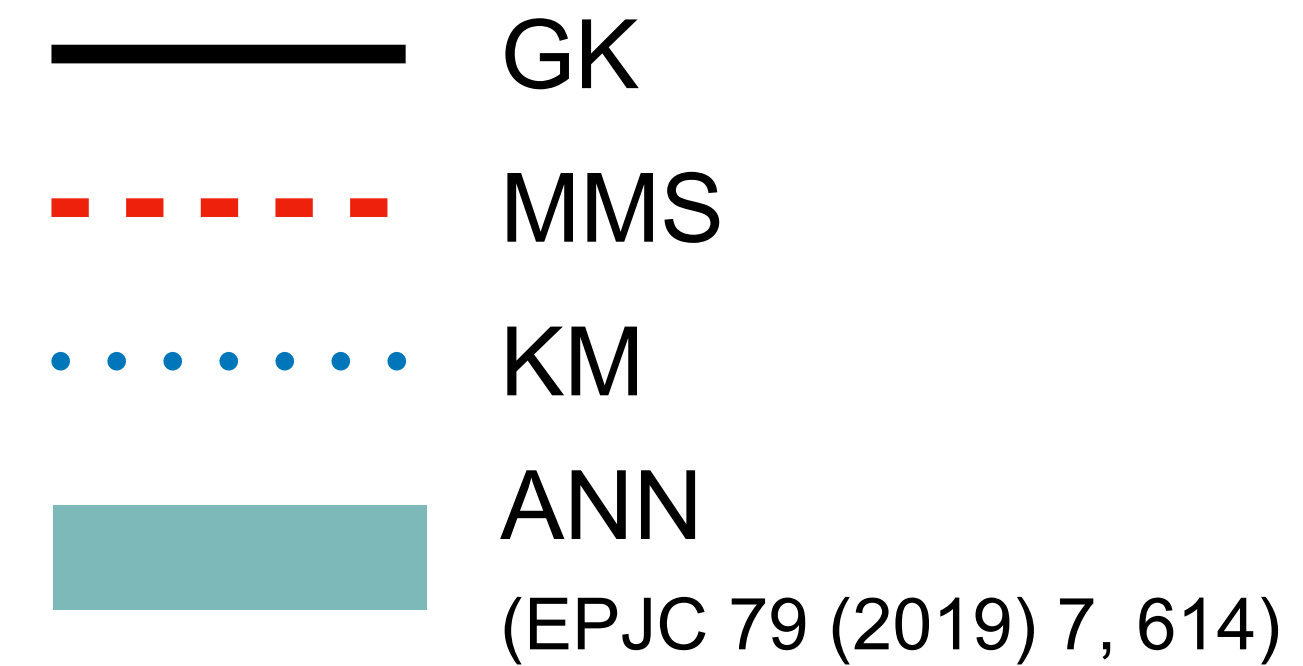
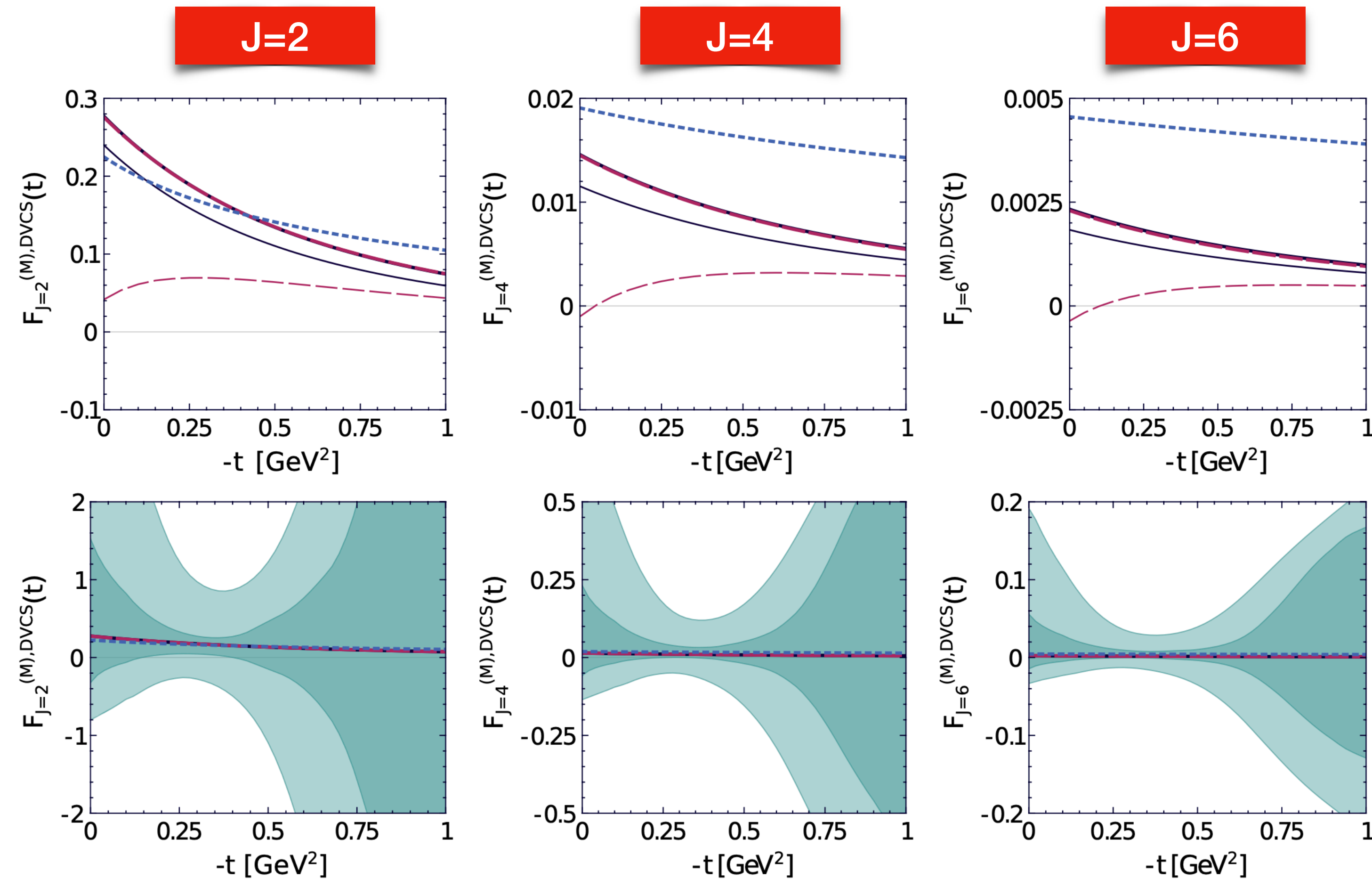


- GK
- MMS
- KM
- ANN
(EPJC 79 (2019) 7, 614)

thin lines and dark bands are estimates for only GPD H

plots for $Q^2 = 2 \text{ GeV}^2$

Numerical estimates - magnetic case:



*thin lines and dark bands
are estimates for only GPD H*

plots for $Q^2 = 2 \text{ GeV}^2$

*See the publication for more,
in particular for sum rules connecting FG projections with Mellin moments*

- The process allows to directly probe GPDs outside $x=\xi$ line, but is much more challenging experimentally

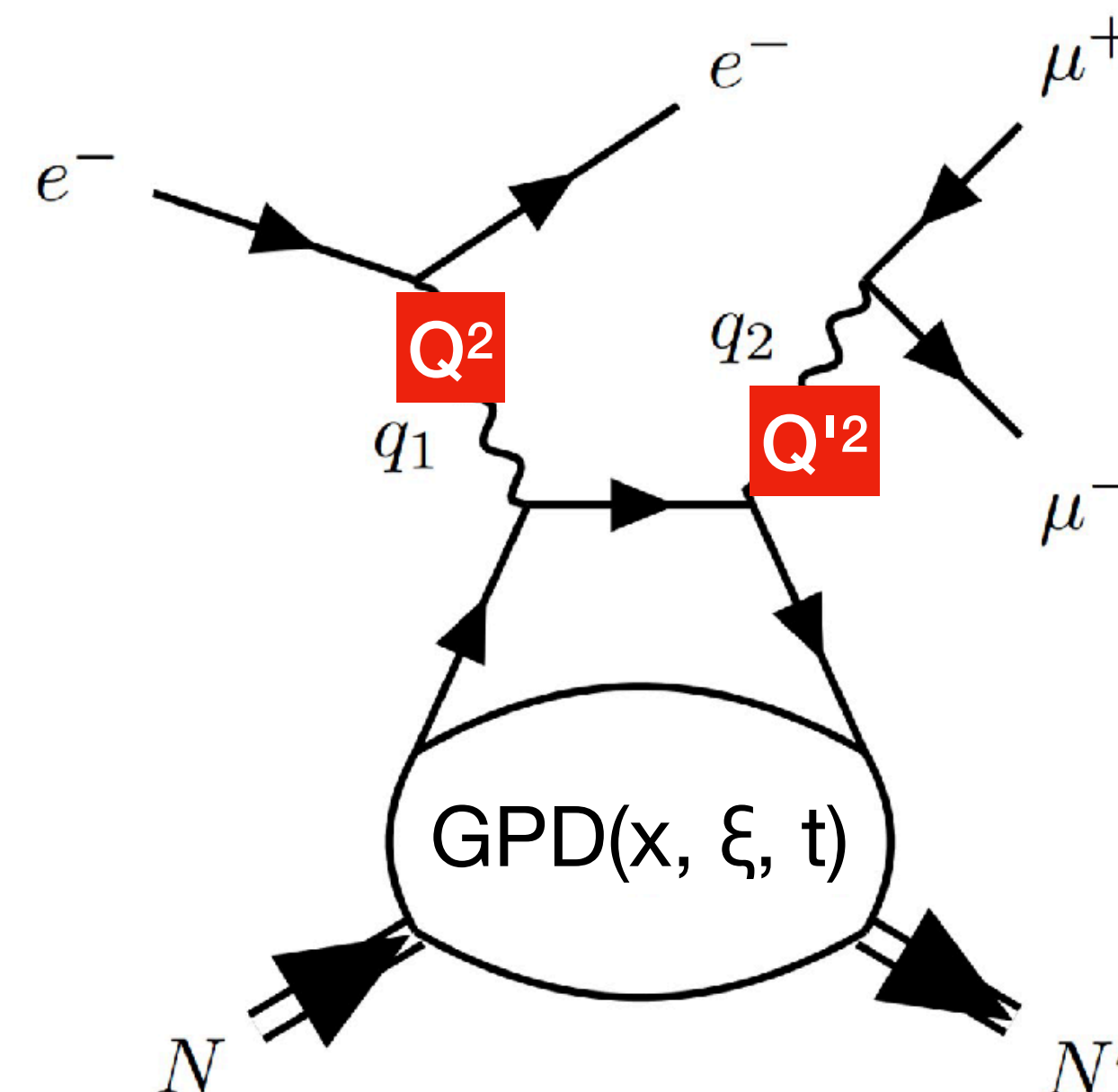
$$(\mathcal{H}, \mathcal{E})(\rho, \xi, t) = \sum_{f=\{u,d,s\}} \int_{-1}^1 dx C_f^{(-)}(x, \rho)(H_f, E_f)(x, \xi, t)$$

$$C_f^{(\pm)}(x, \rho) \stackrel{LO}{=} \left(\frac{e_f}{e}\right)^2 \left(\frac{1}{\rho - x - i0} \pm \frac{1}{\rho + x - i0} \right)$$

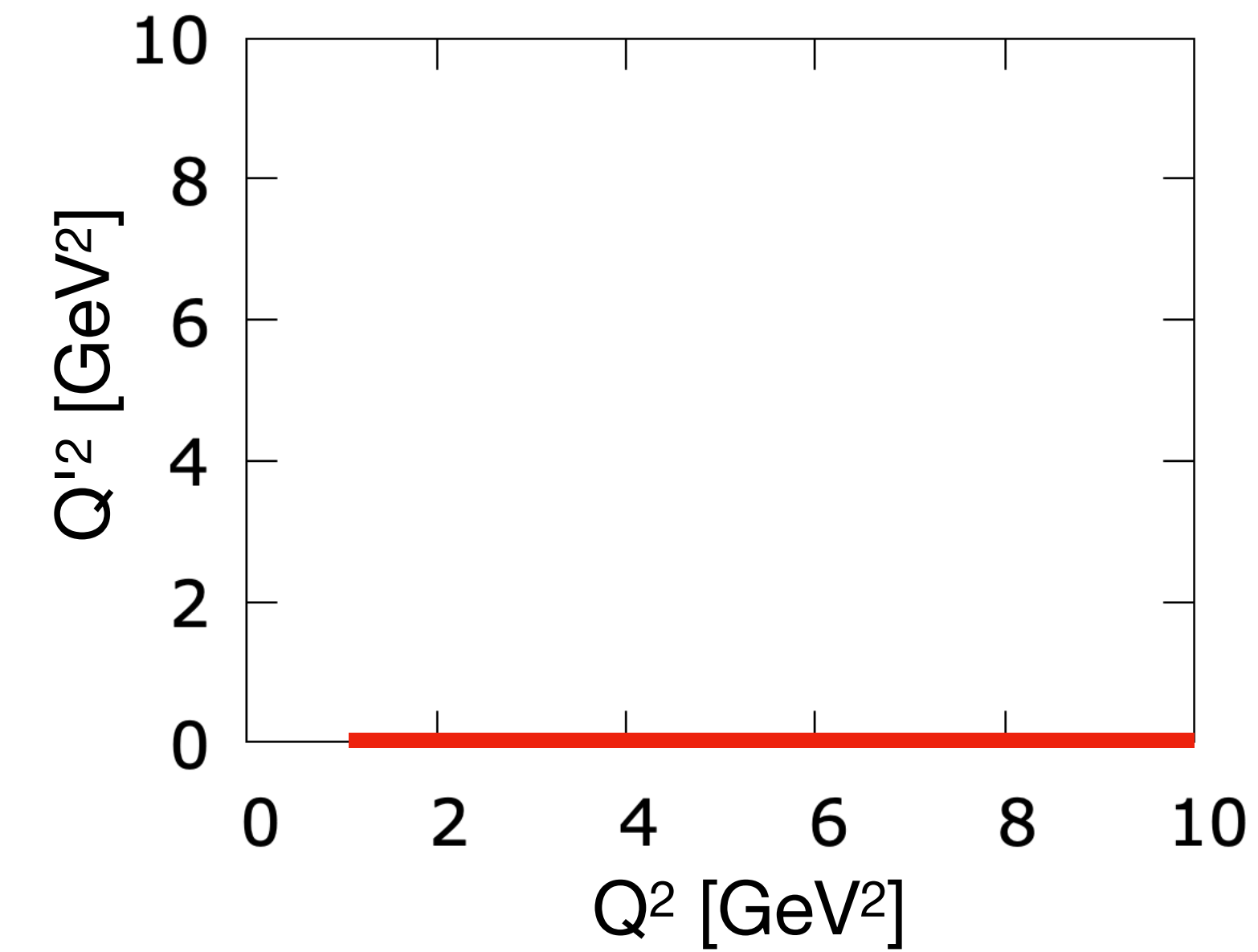
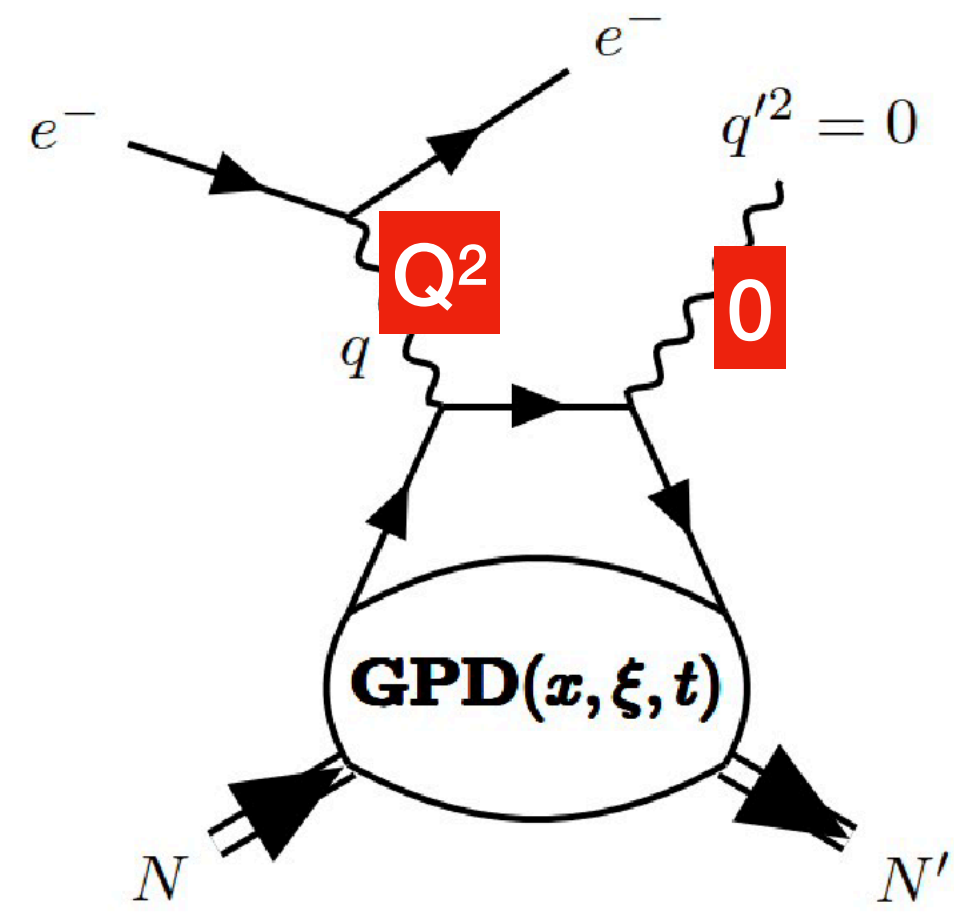
- We revisit DDVCS phenomenology in view of new experiments, including reevaluation of DDVCS and BH cross-sections with Kleiss-Stirling spinor techniques
- Obtained results are available in PARTONS and EpIC MC generator

$$\xi = \frac{Q^2 + Q'^2}{2Q^2/x_B - Q^2 - Q'^2}$$

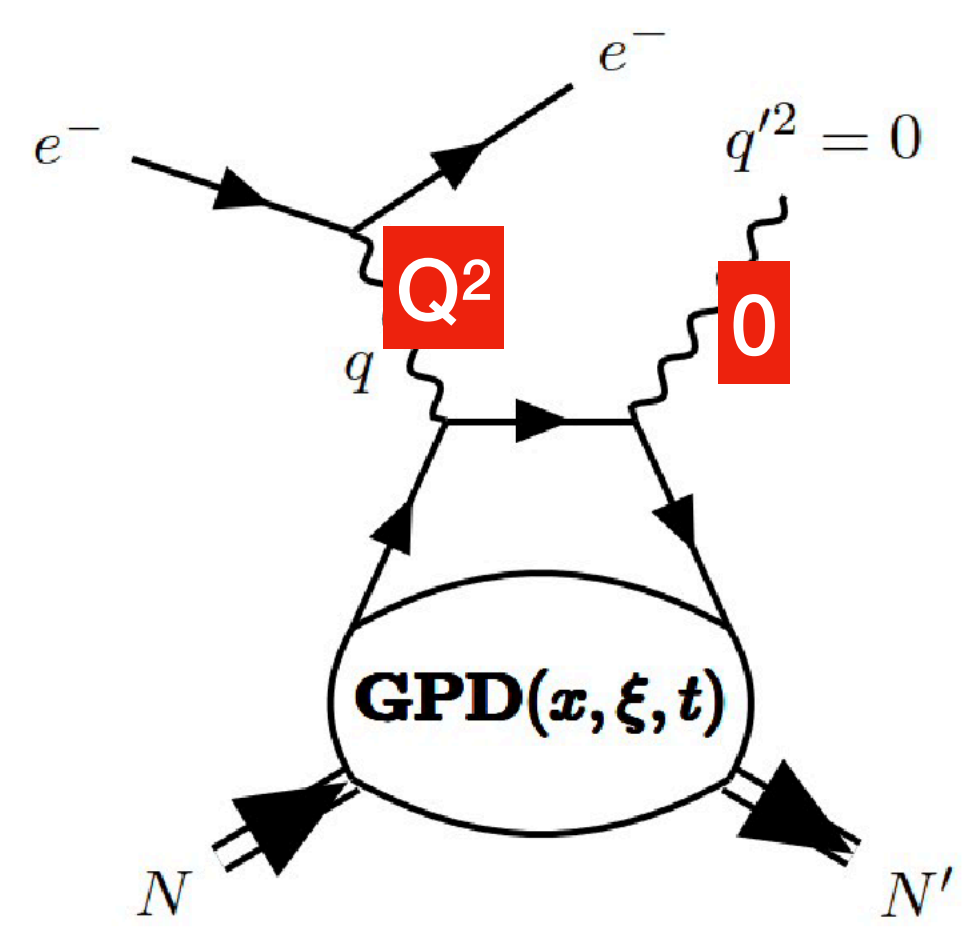
$$\rho = \xi \frac{Q^2 - Q'^2}{Q^2 + Q'^2}$$



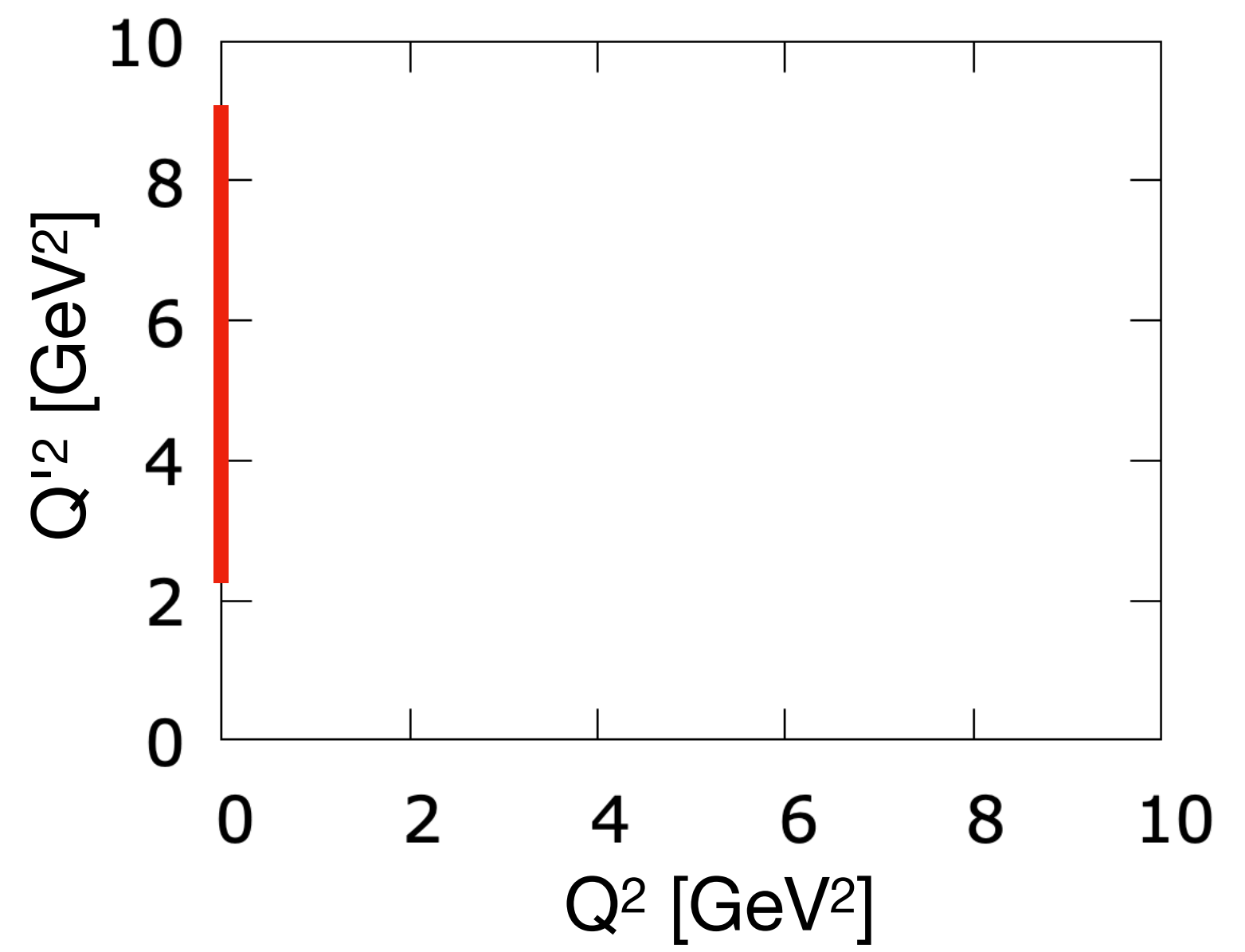
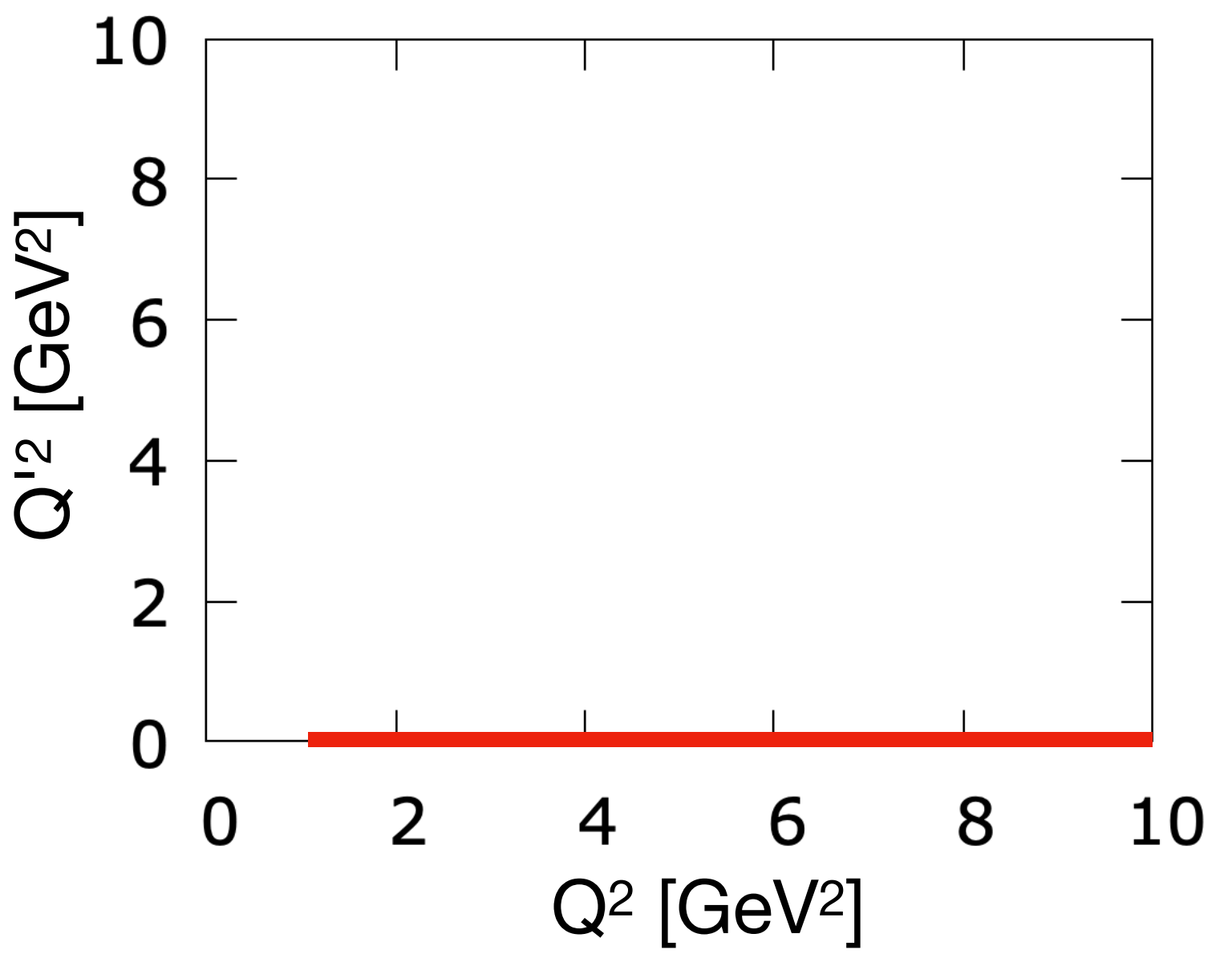
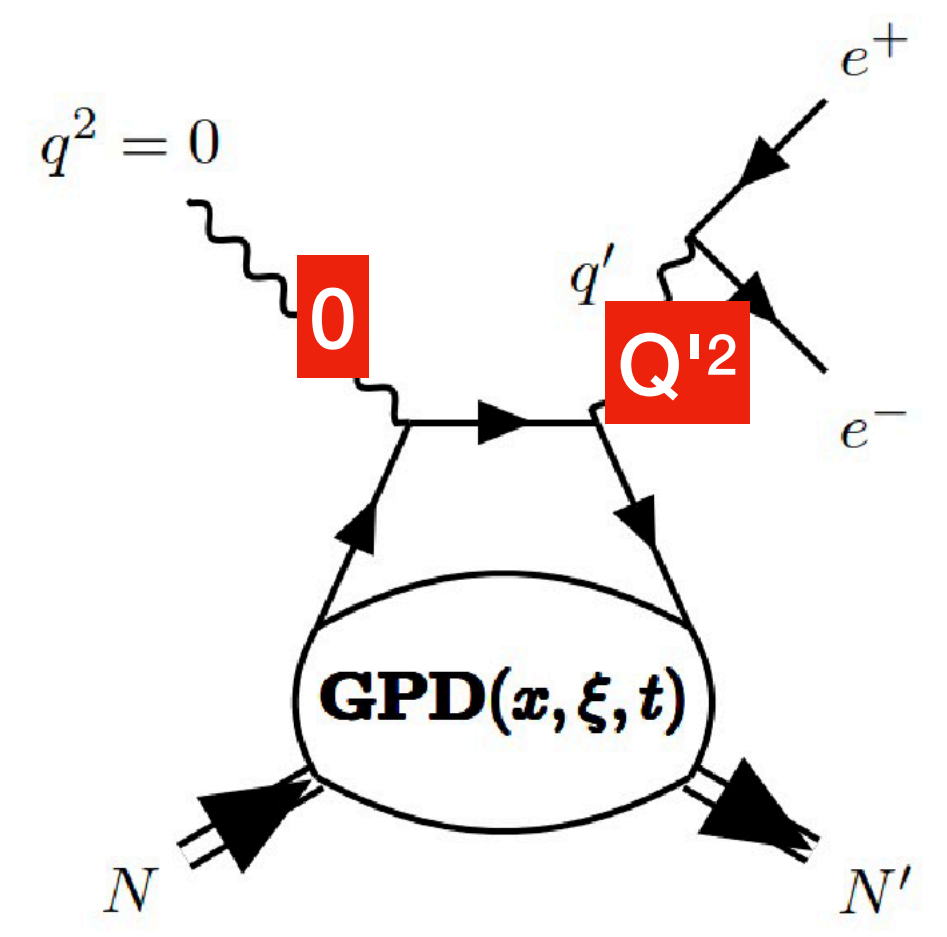
DVCS



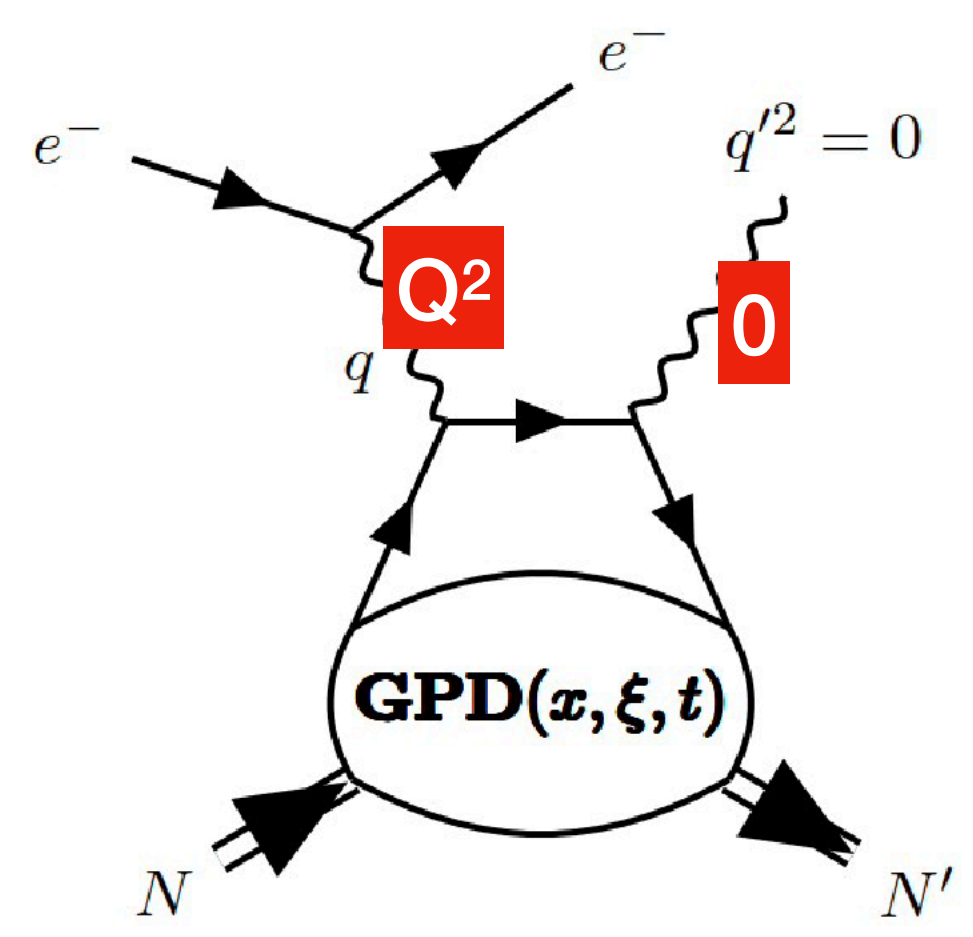
DVCS



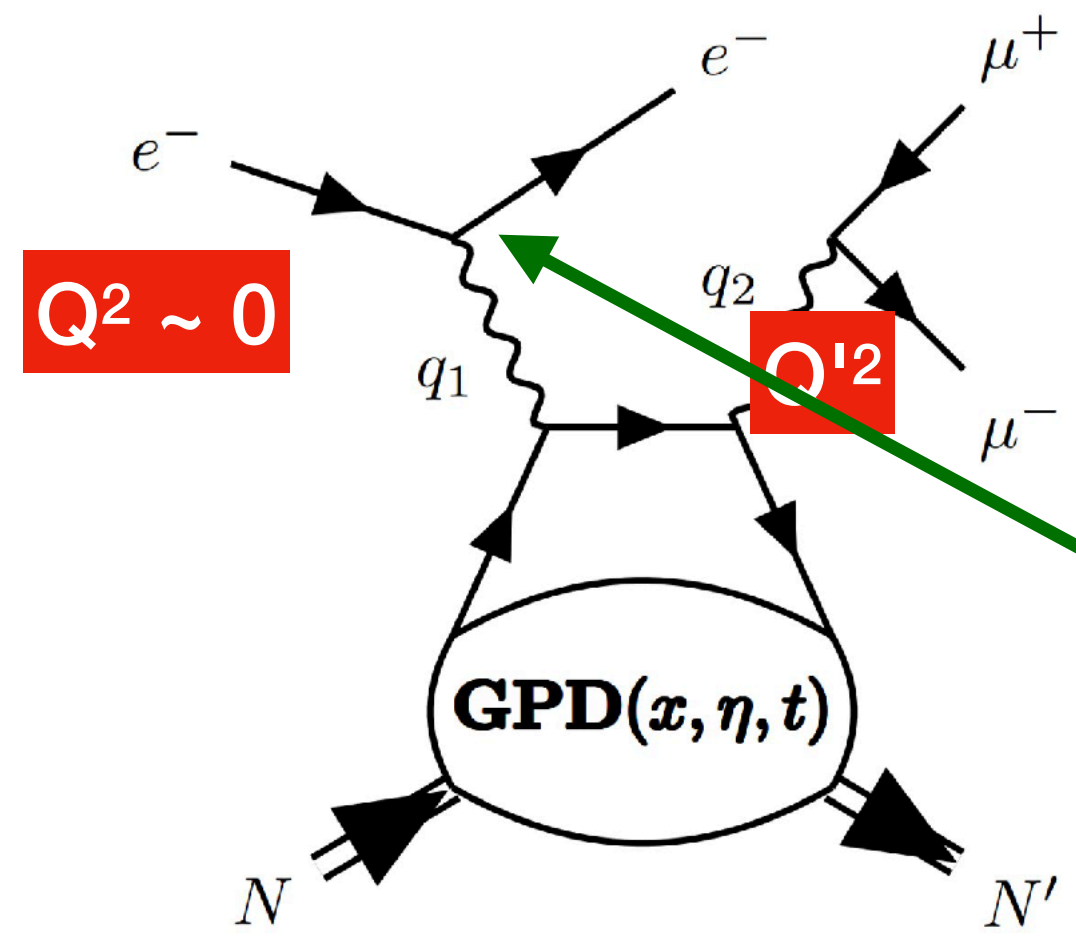
TCS



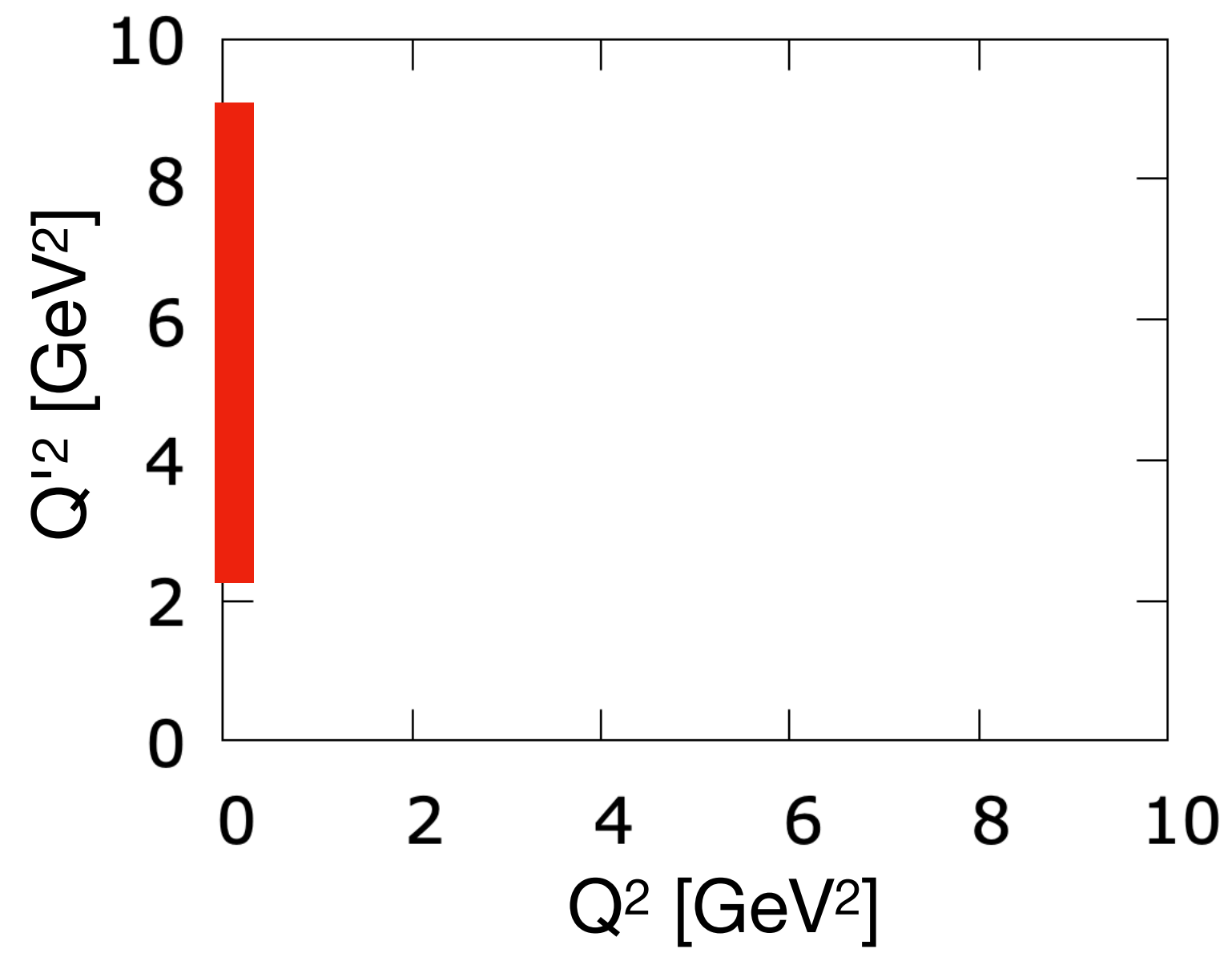
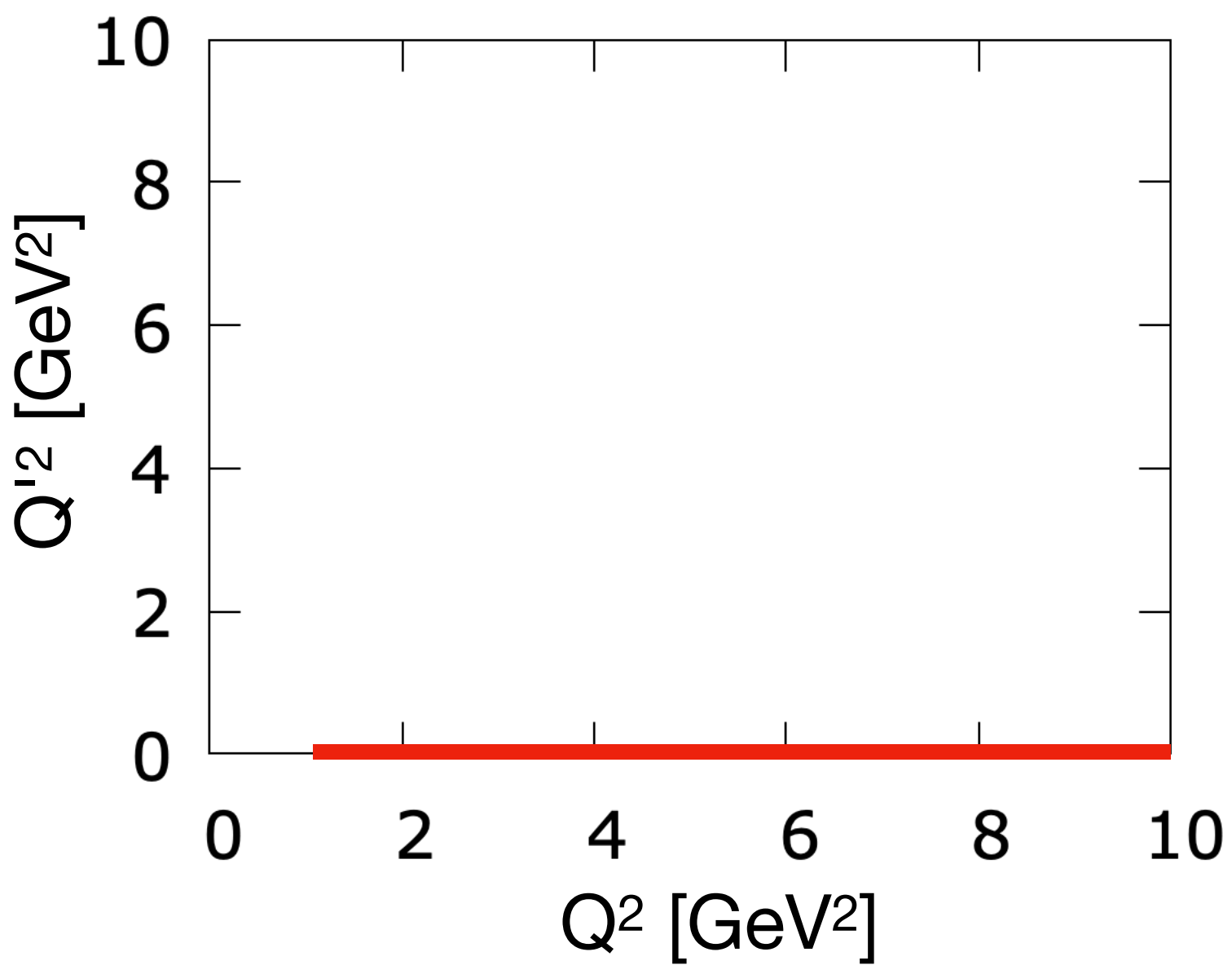
DVCS



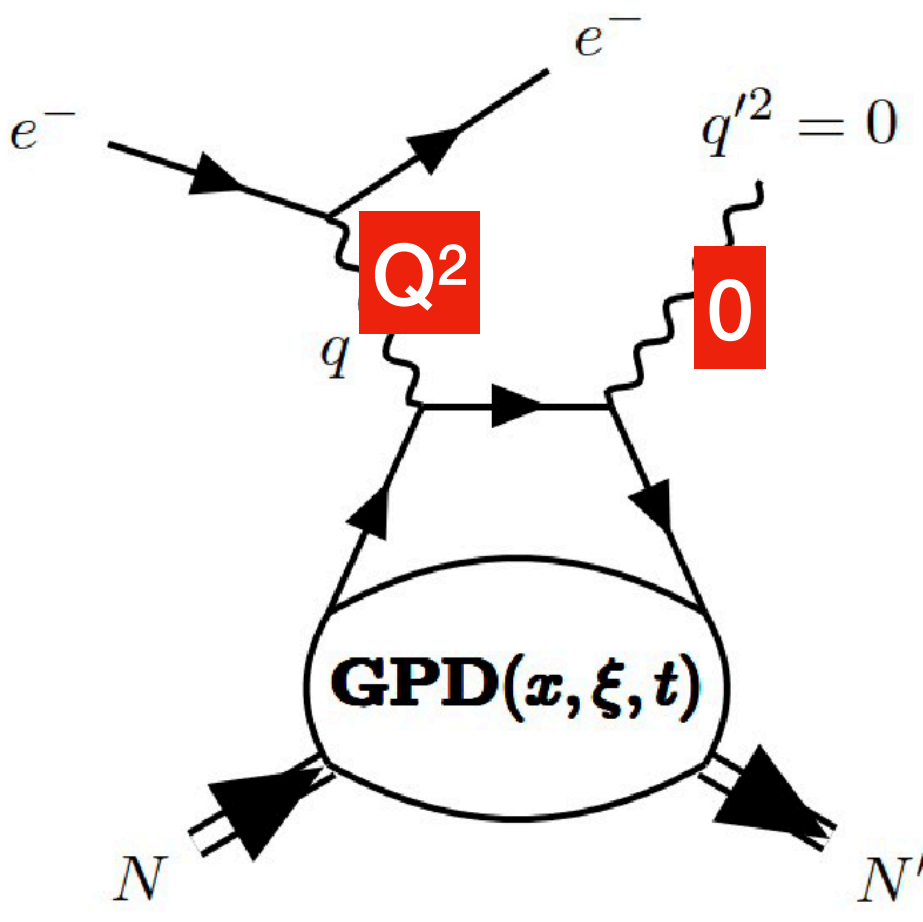
TCS in ep experiments



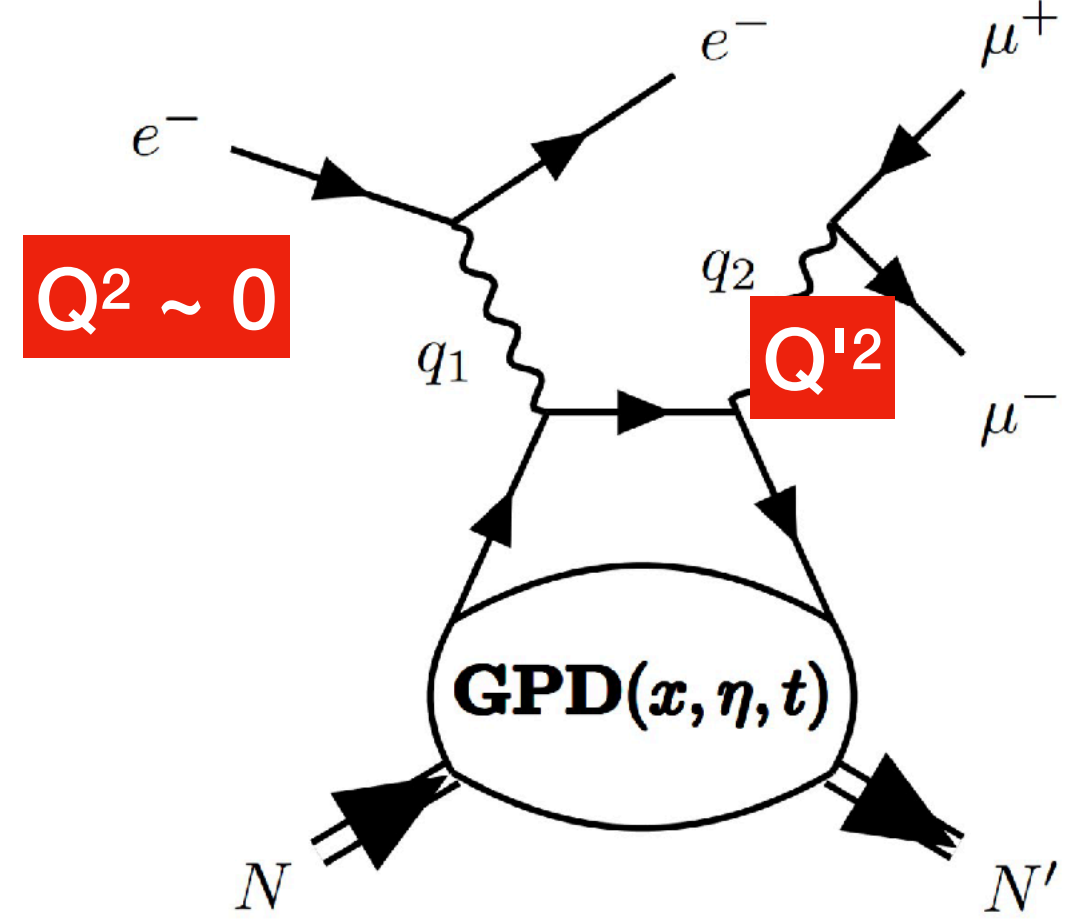
α_{EM} already here (in Γ)!



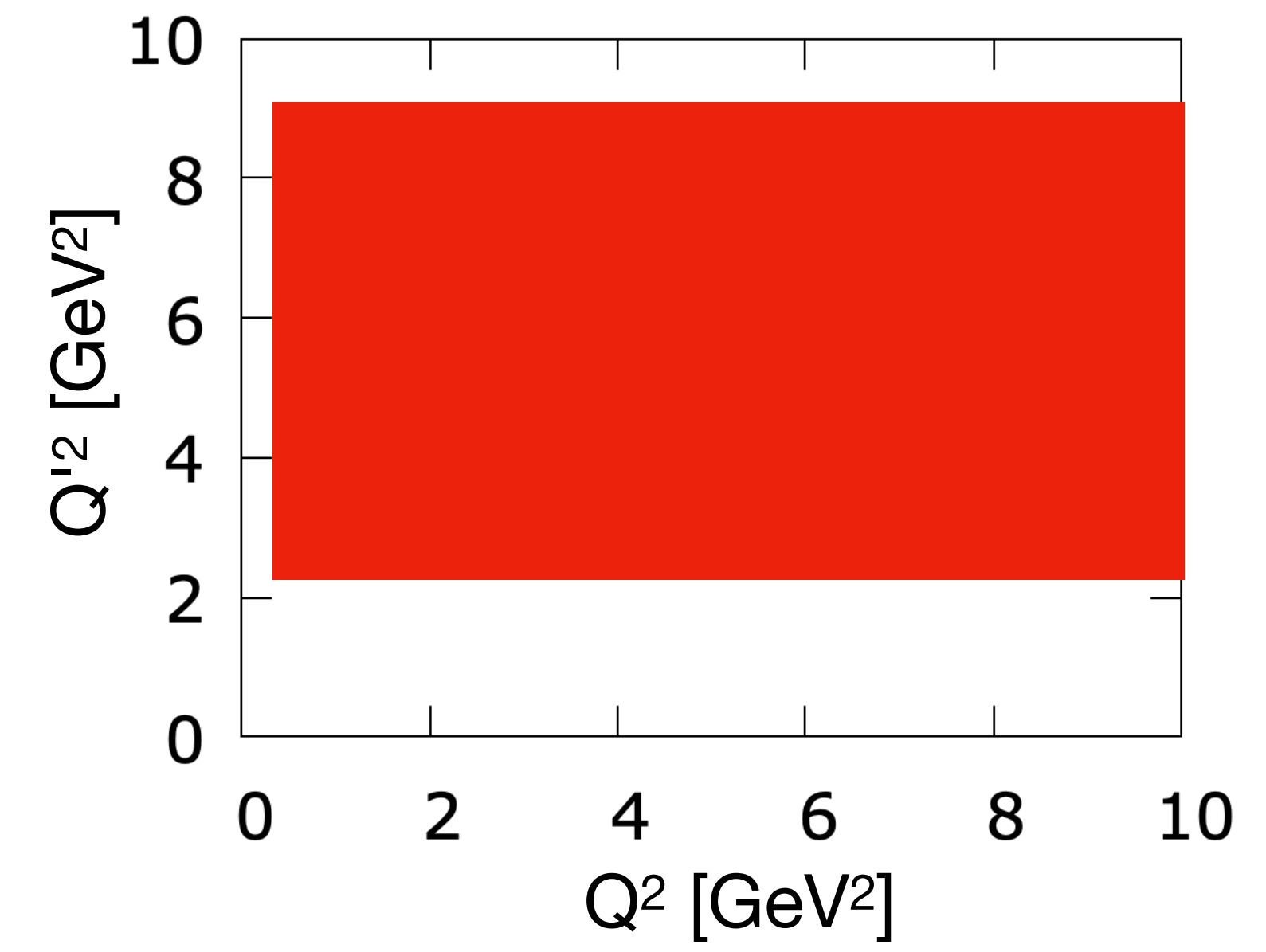
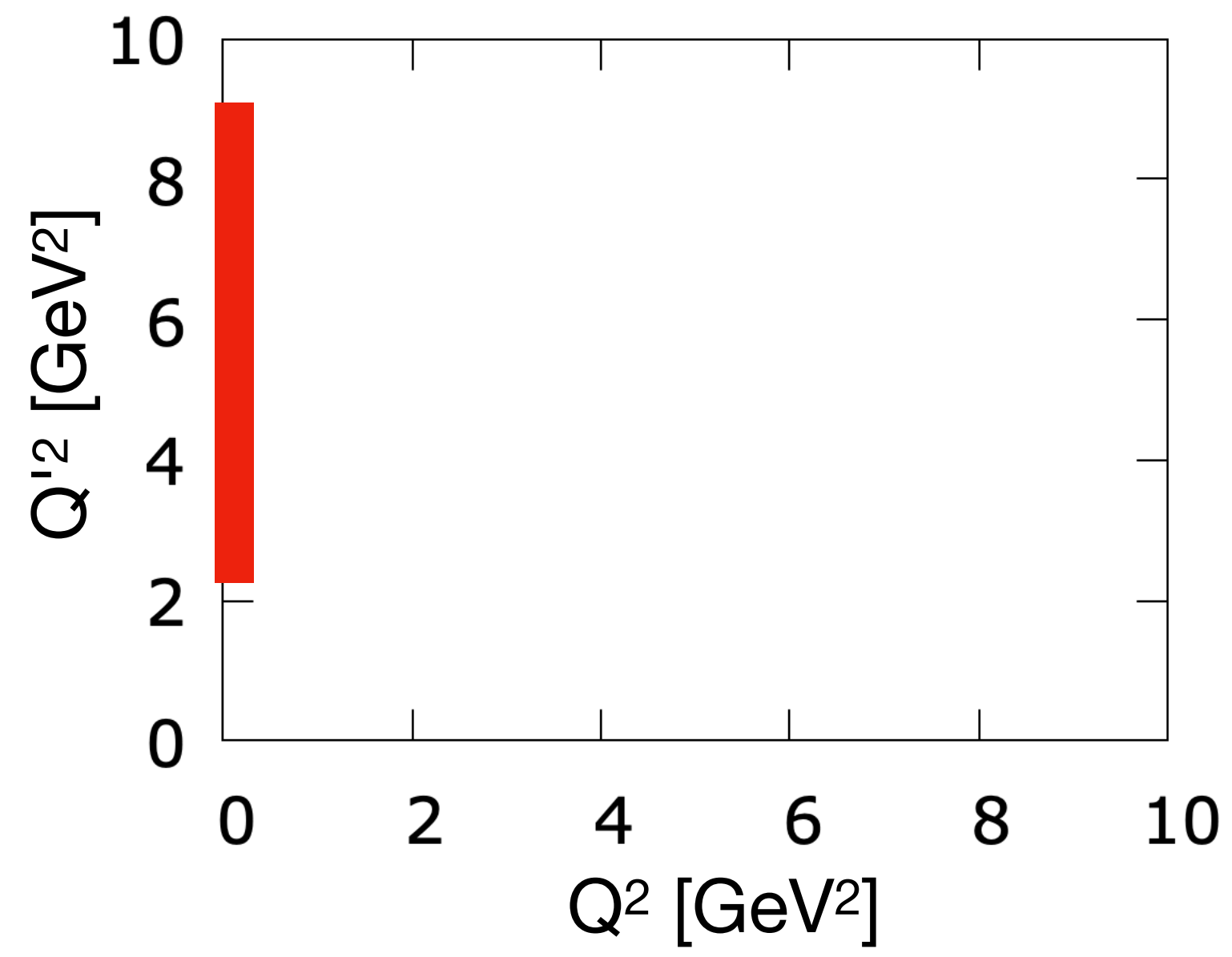
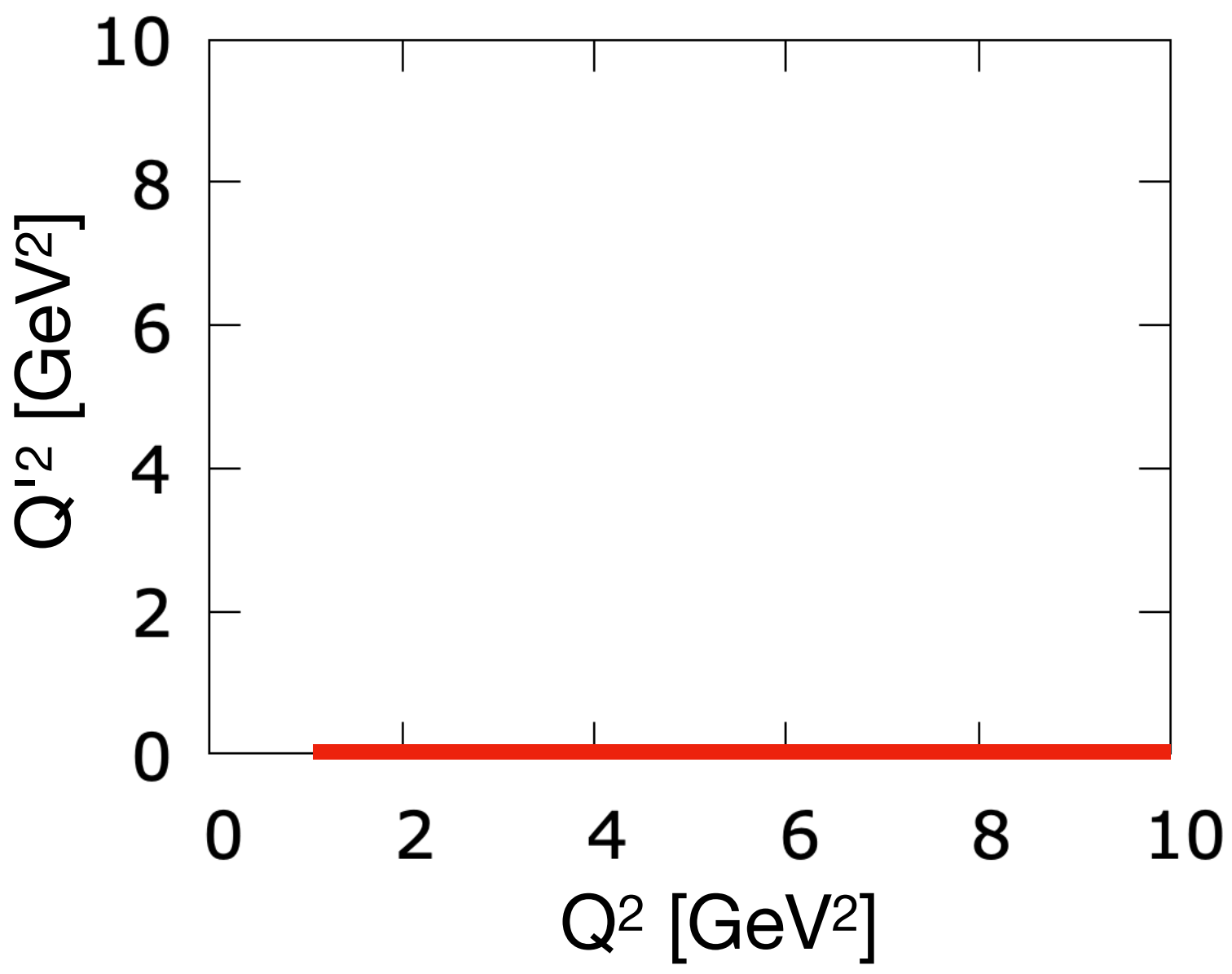
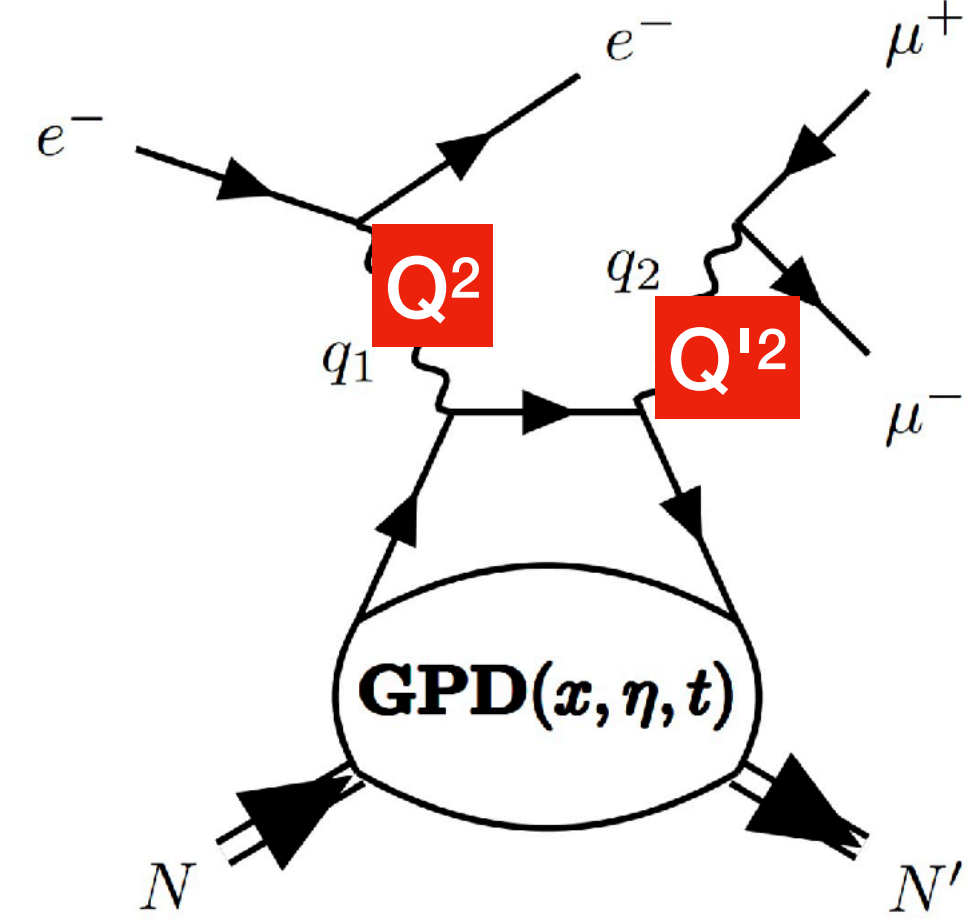
DVCS

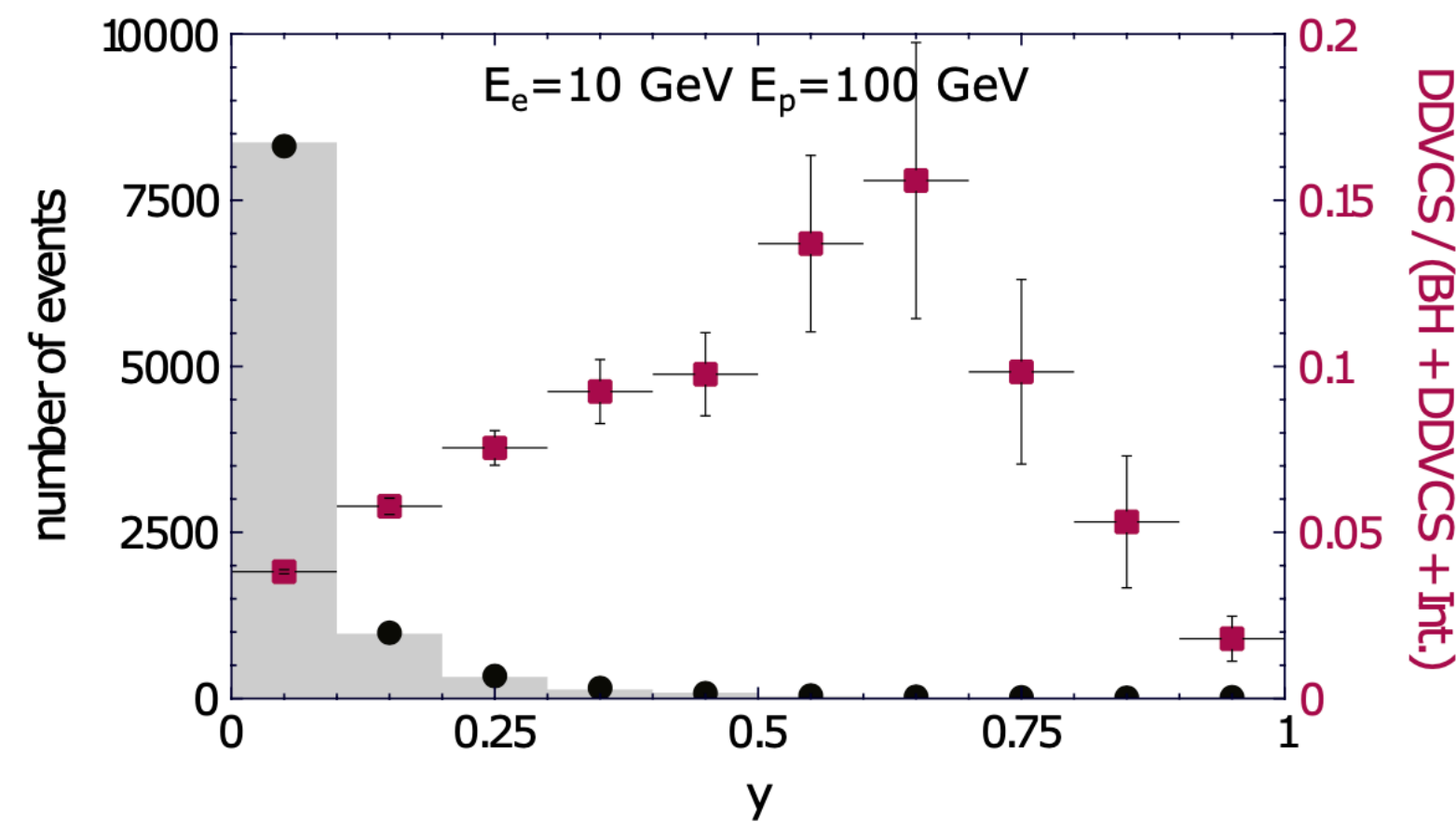
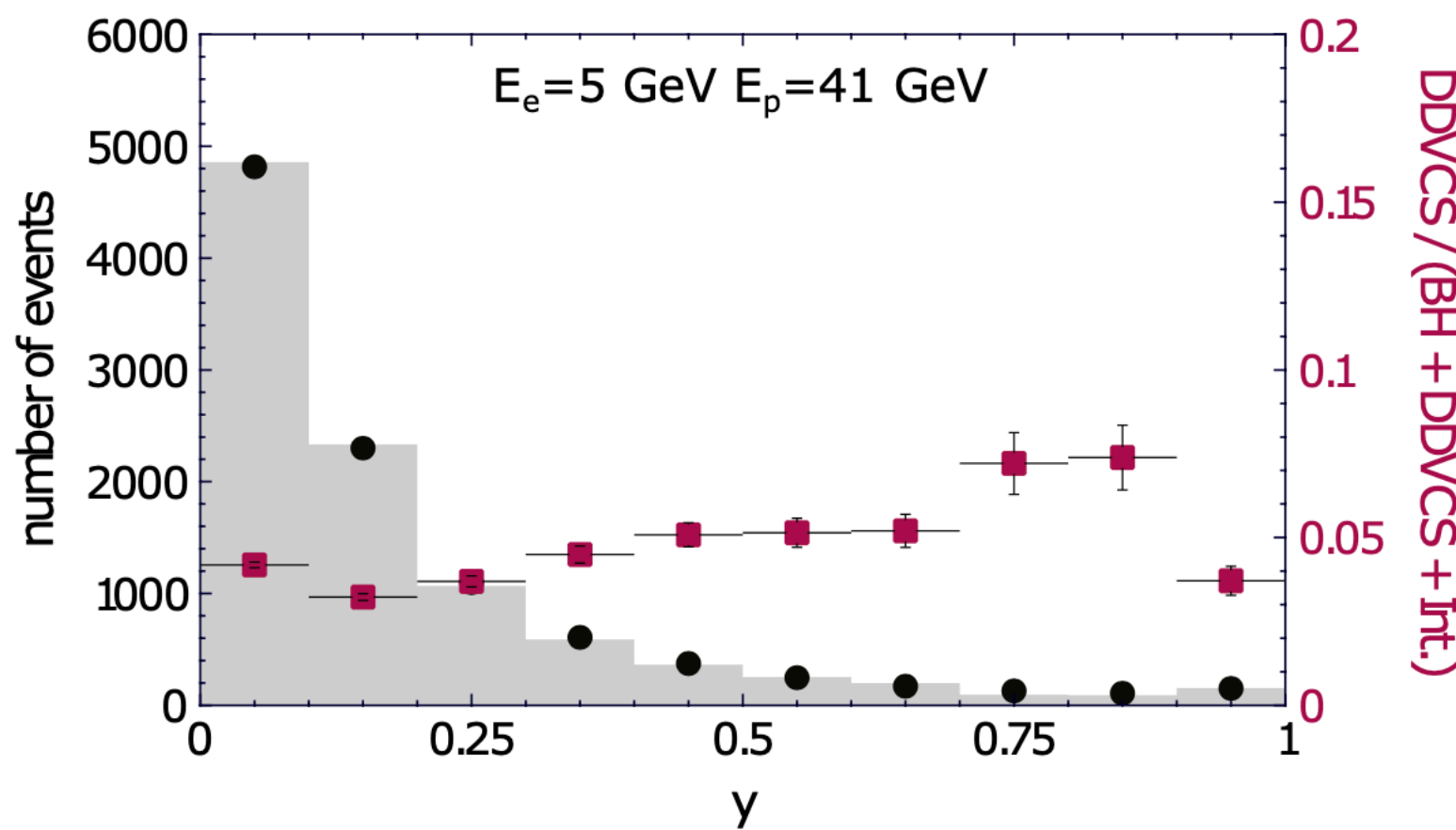
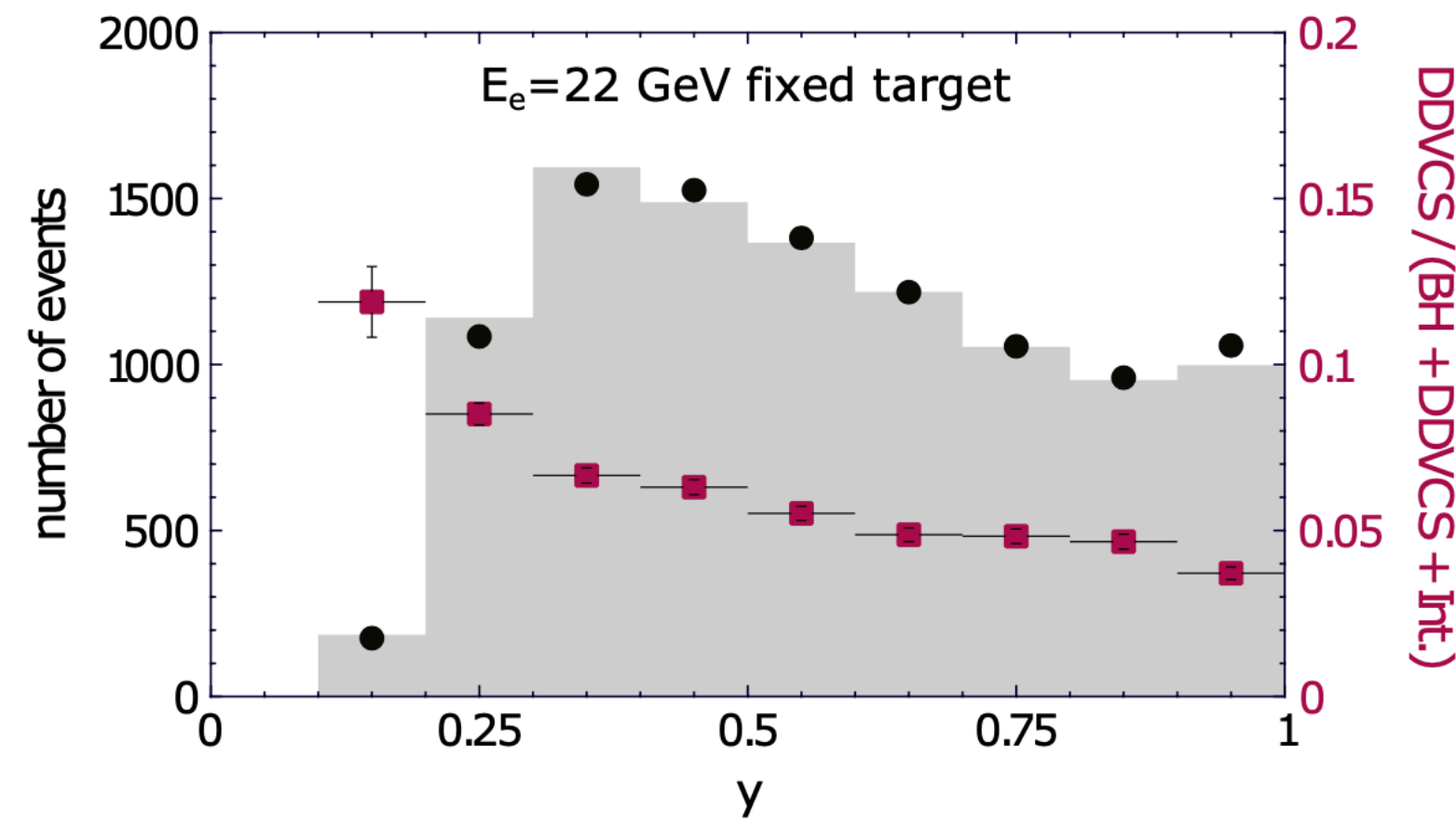
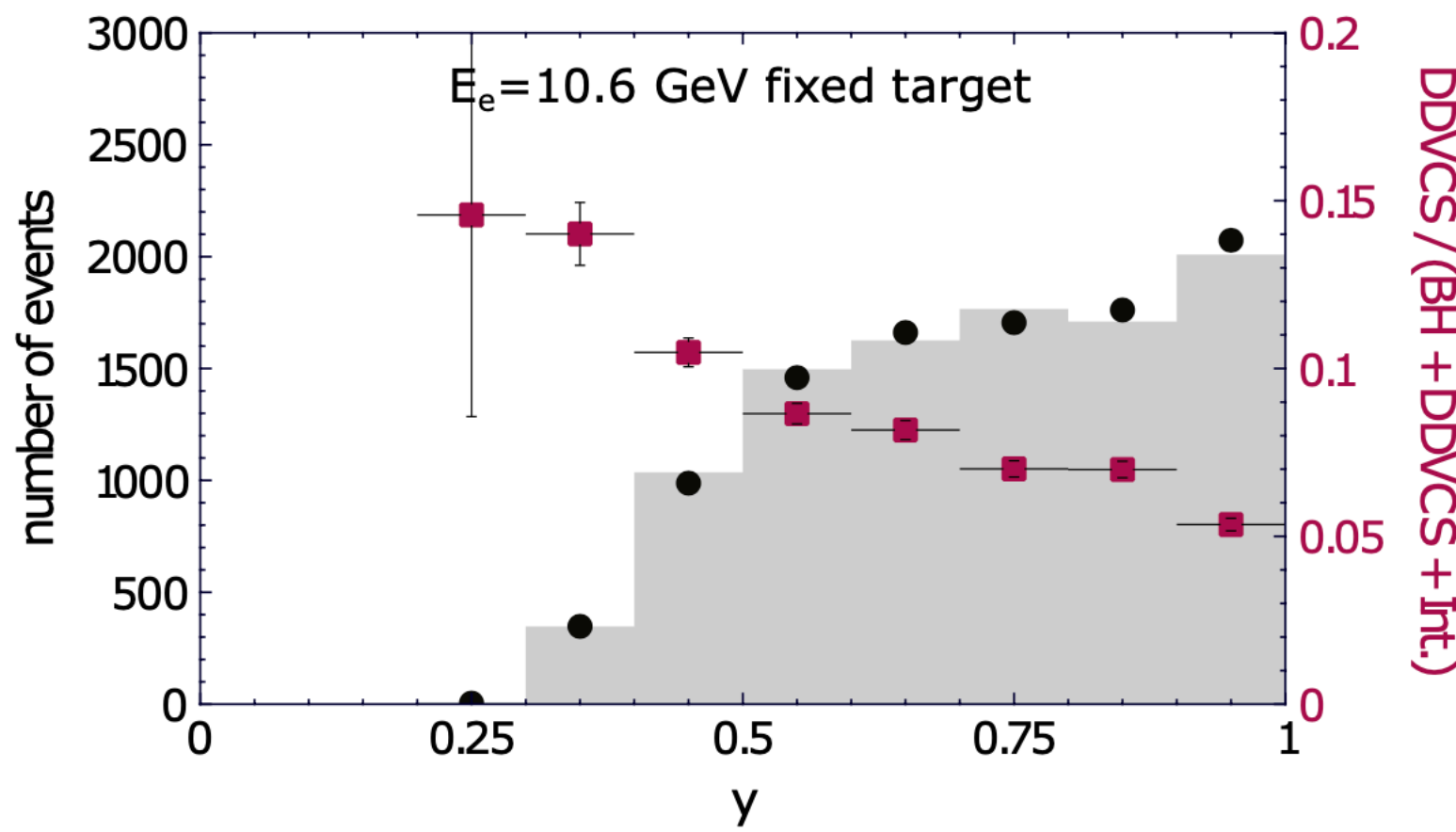


TCS in ep experiments



DDVCS



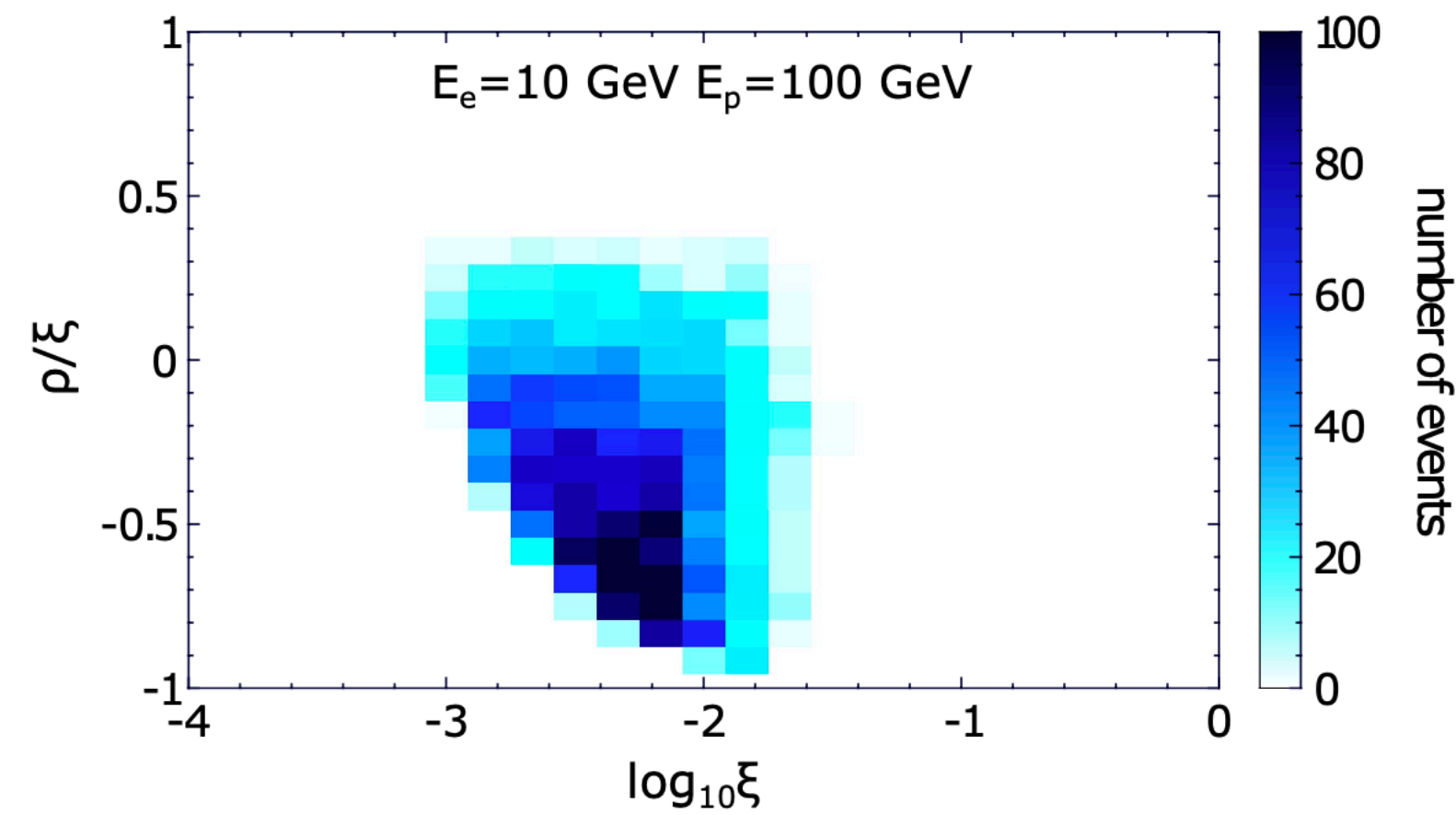
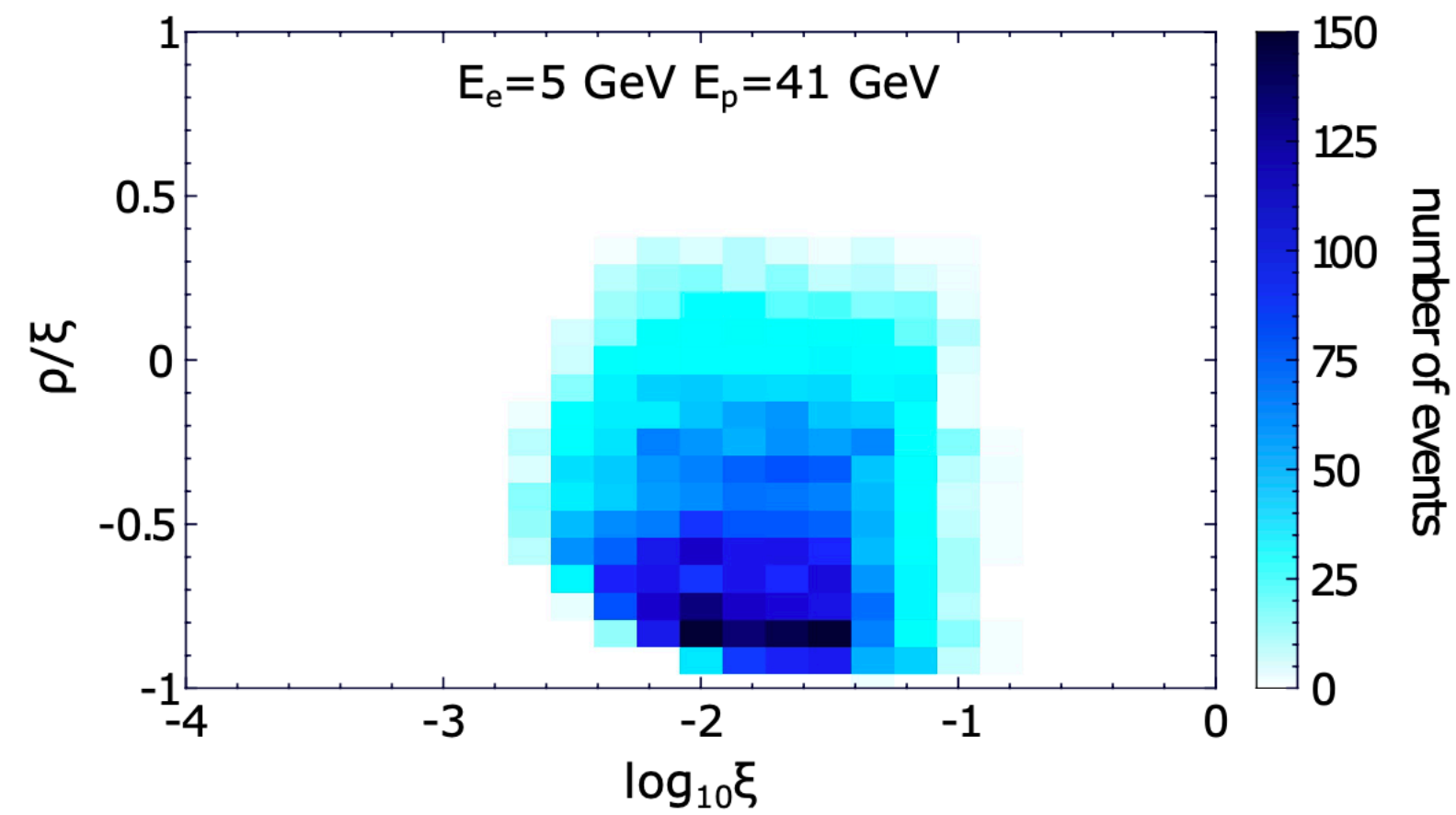
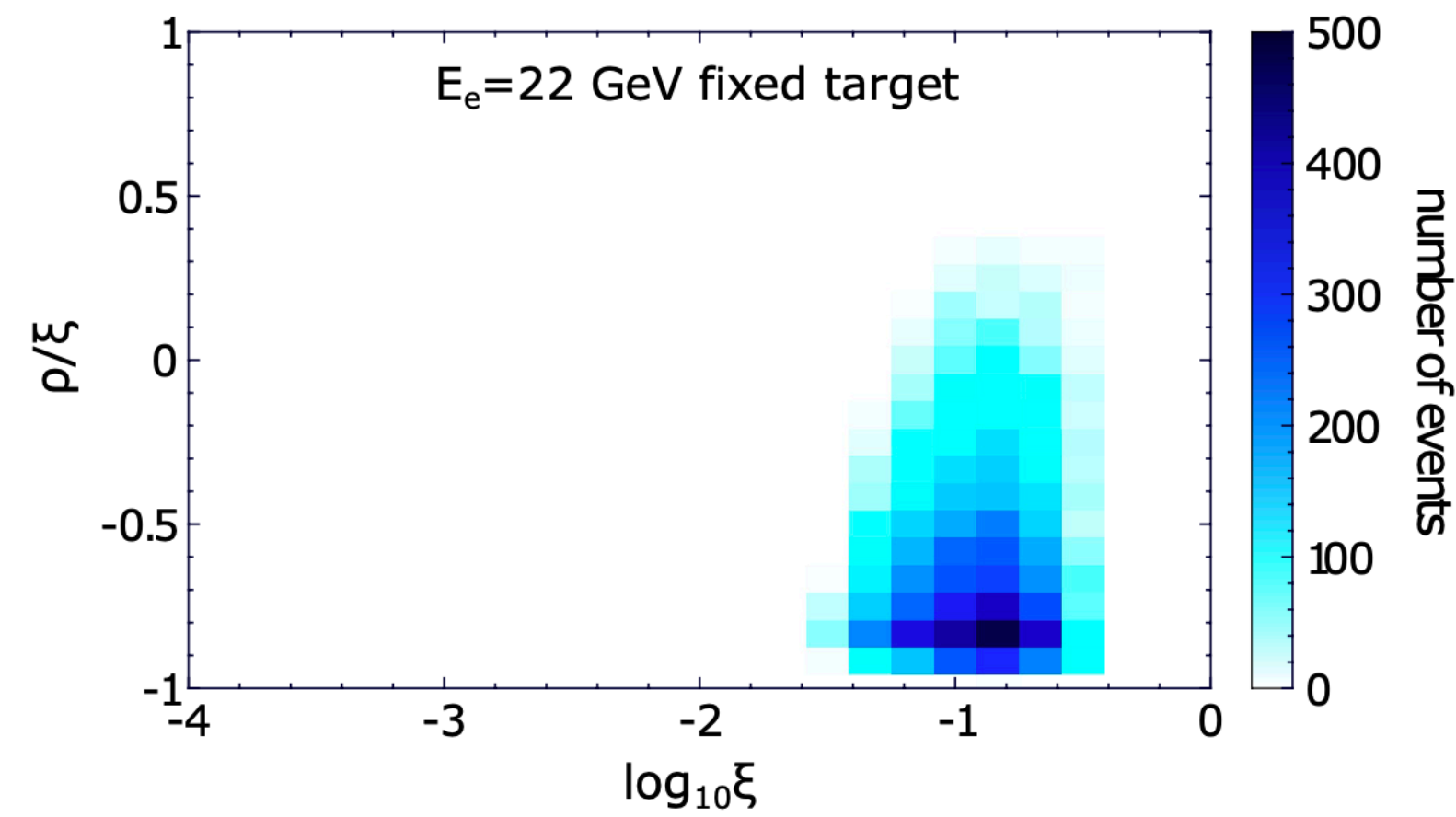
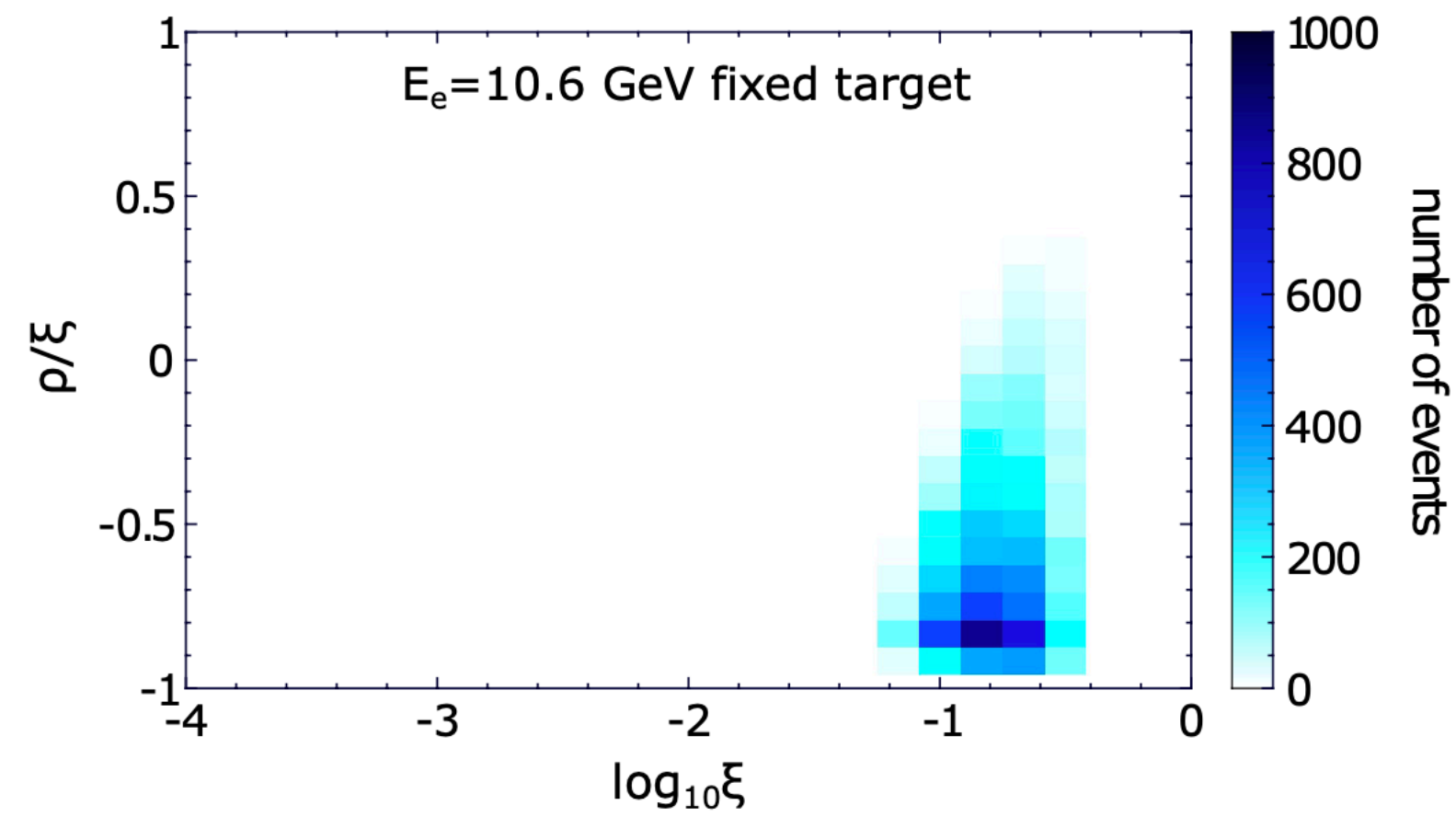


- EpIC MC
- integrated cross-section
- pure DDVCS contribution

Kinematic cuts:

- $0.15 \text{ GeV}^2 < Q^2 < 5 \text{ GeV}^2$
- $2.25 \text{ GeV}^2 < Q'^2 < 9 \text{ GeV}^2$
- $0.1 \text{ GeV}^2 < t < 0.8 \text{ GeV}^2$ (JLab)
- $0.05 \text{ GeV}^2 < t < 1 \text{ GeV}^2$ (EIC)
- $0.1 < \varphi, \varphi_l < 2\pi - 0.1$
- $\pi/4 < \theta_l < 3\pi/4$
- $0.1 < y < 1$ (JLab)
- $0.05 < y < 1$ (EIC)

Experiment	Beam energies [GeV]	Range of $ t $ [GeV ²]	$\sigma _{0 < y < 1}$ [pb]	$\mathcal{L}^{10k} _{0 < y < 1}$ [fb ⁻¹]	y_{\min}	$\sigma _{y_{\min} < y < 1} / \sigma _{0 < y < 1}$
JLab12	$E_e = 10.6, E_p = M$	(0.1, 0.8)	0.14	70	0.1	1
JLab2+	$E_e = 22, E_p = M$	(0.1, 0.8)	0.46	22	0.1	1
EIC	$E_e = 5, E_p = 41$	(0.05, 1)	3.9	2.6	0.05	0.73
EIC	$E_e = 10, E_p = 100$	(0.05, 1)	4.7	2.1	0.05	0.32

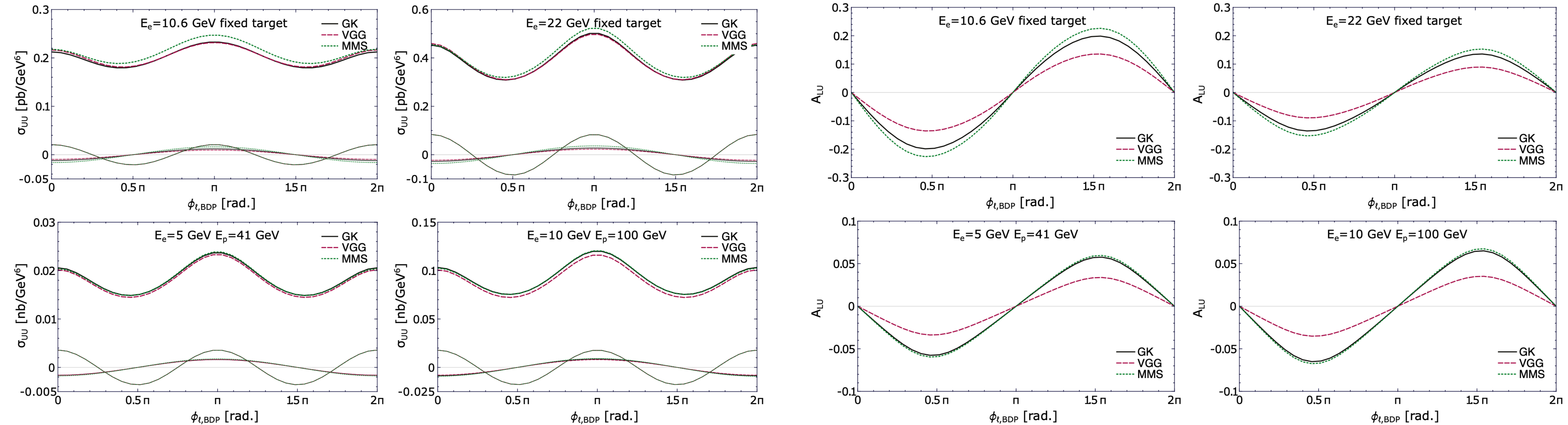


Kinematic cuts:

- $0.15 \text{ GeV}^2 < Q^2 < 5 \text{ GeV}^2$
- $2.25 \text{ GeV}^2 < Q'^2 < 9 \text{ GeV}^2$
- $0.1 \text{ GeV}^2 < t < 0.8 \text{ GeV}^2$ (JLab)
- $0.05 \text{ GeV}^2 < t < 1 \text{ GeV}^2$ (EIC)
- $0.1 < \varphi, \varphi_l < 2\pi - 0.1$
- $\pi/4 < \theta_l < 3\pi/4$
- $0.1 < y < 1$ (JLab)
- $0.05 < y < 1$ (EIC)

Unpolarised cross-section
integrated over
 $0 < \phi < 2\pi$ and $\pi/4 < \theta < 3\pi/4$

corresponding ALU asymmetry

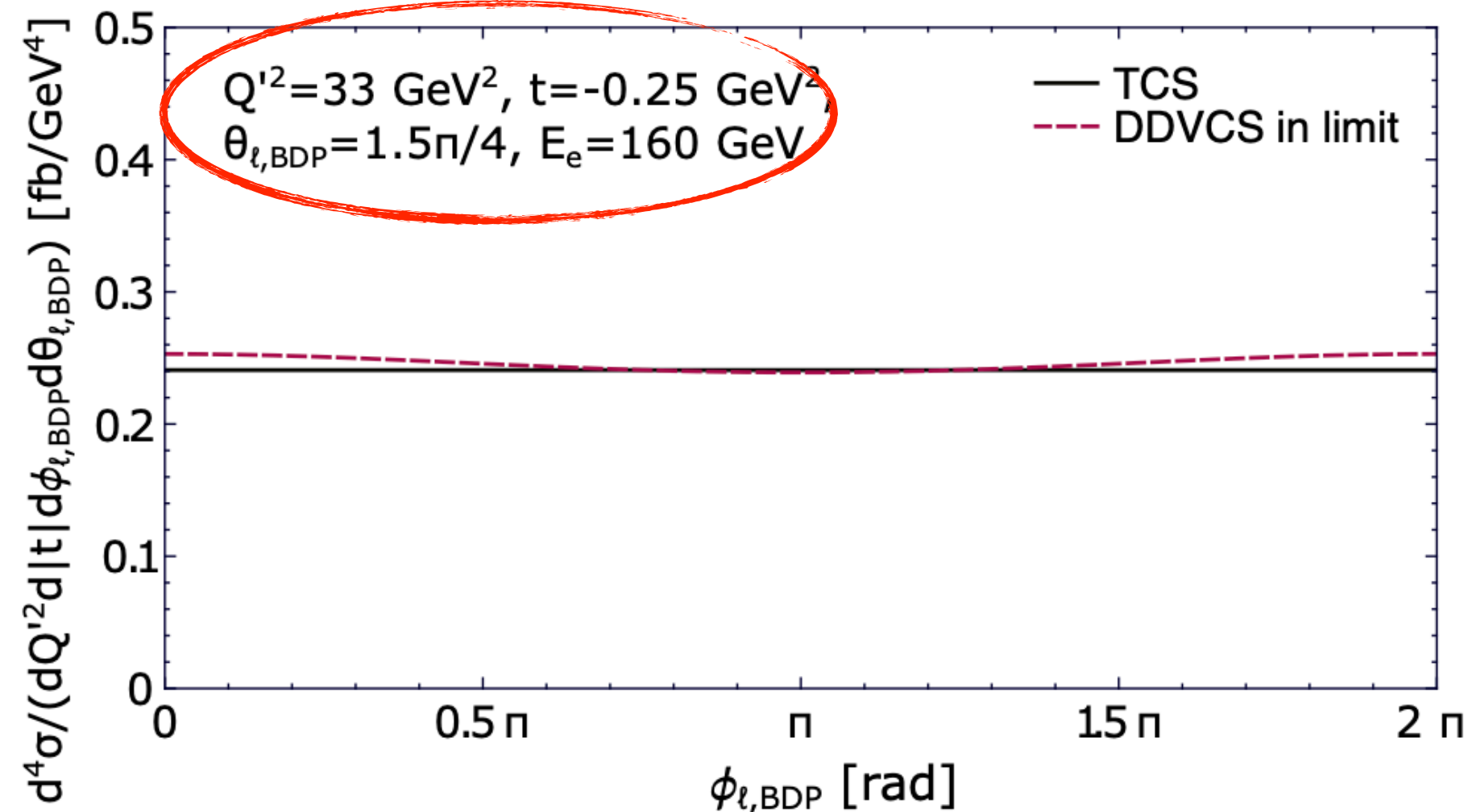
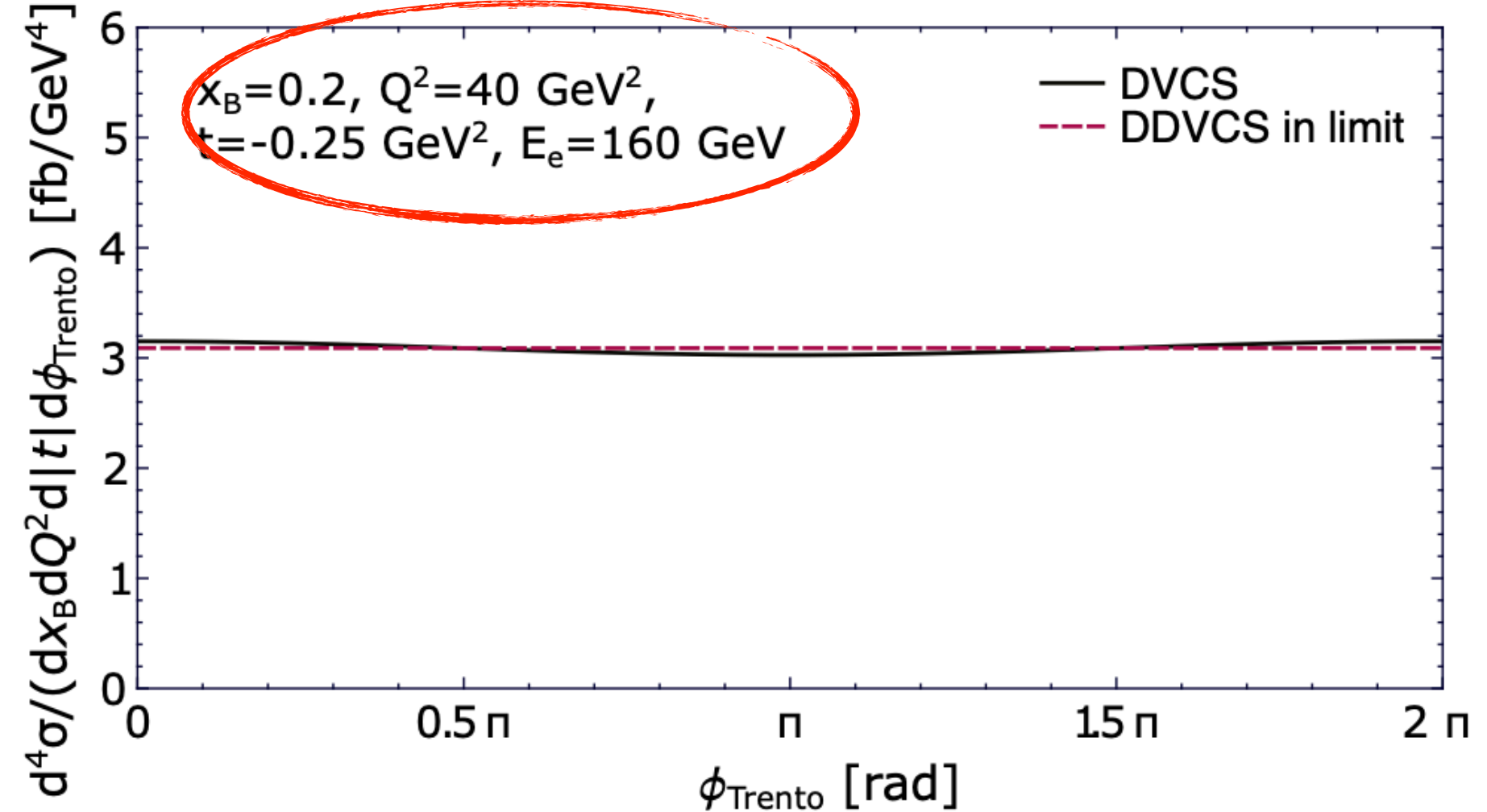
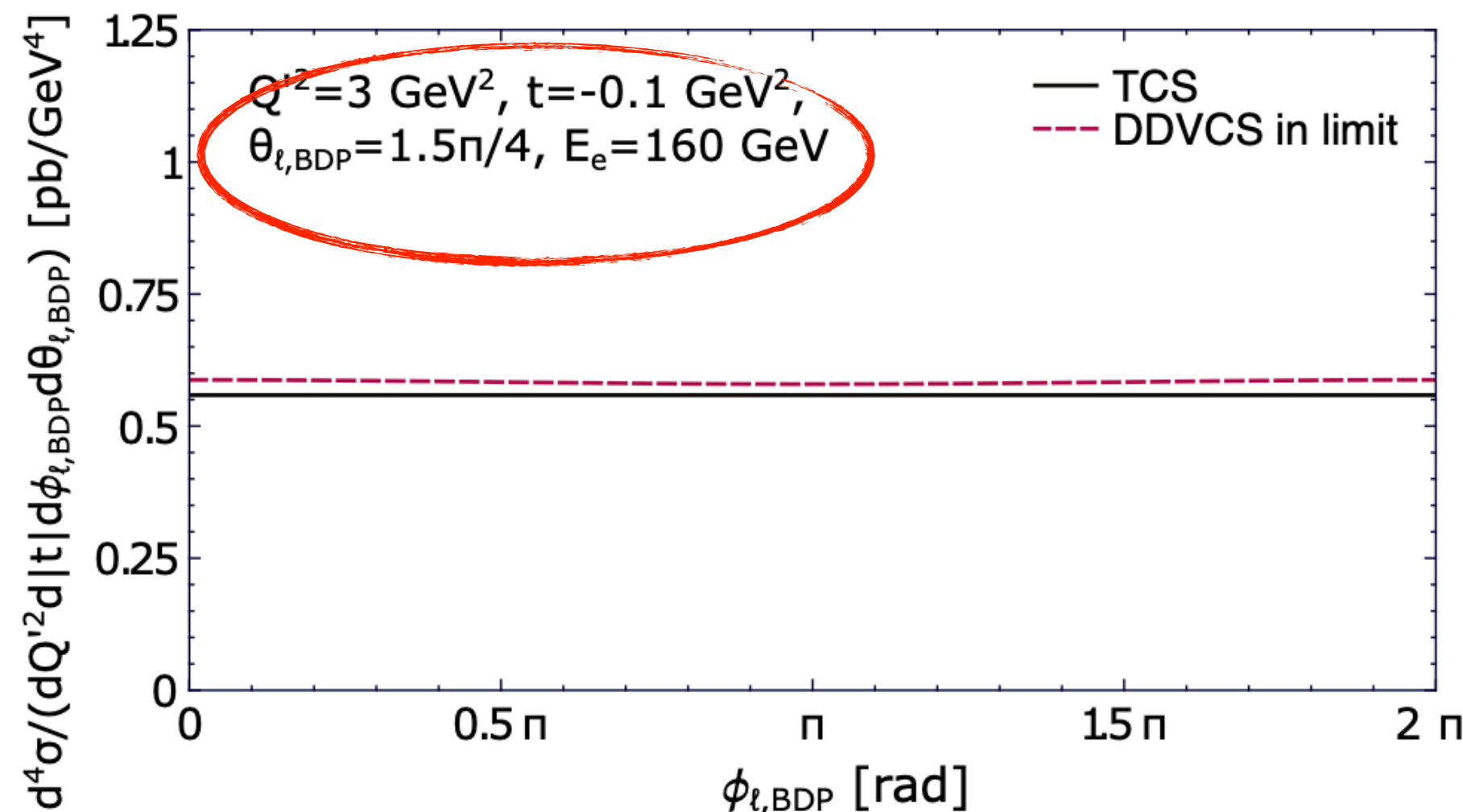
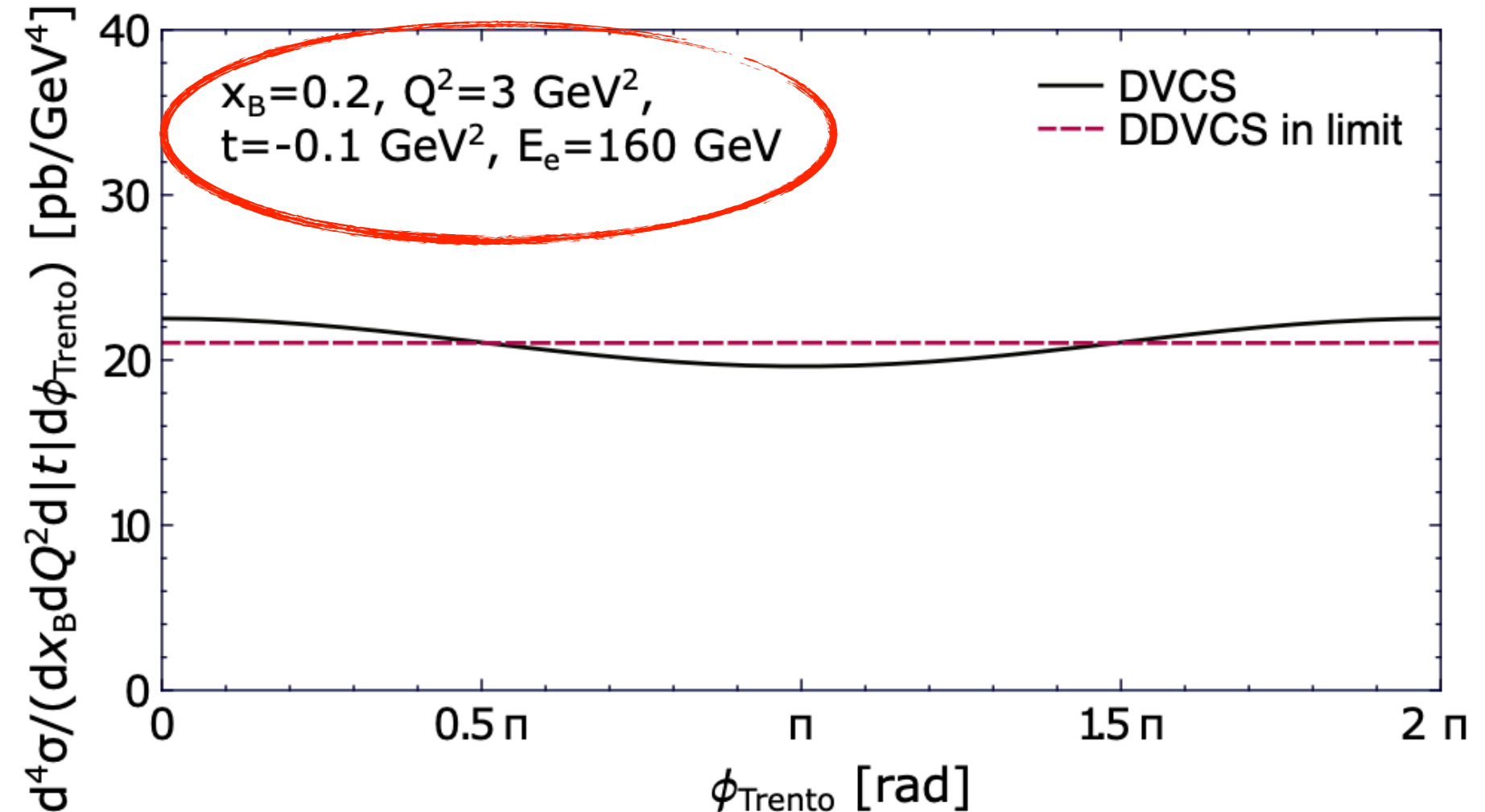


— GK
- - - VGG
... MMS

Experiment	Beam energies [GeV]	y	$ t $ [GeV ²]	Q^2 [GeV ²]	Q'^2 [GeV ²]
JLab12	$E_e = 10.6, E_p = M$	0.5	0.2	0.6	2.5
JLab2+	$E_e = 22, E_p = M$	0.3	0.2	0.6	2.5
EIC	$E_e = 5, E_p = 41$	0.15	0.1	0.6	2.5
EIC	$E_e = 10, E_p = 100$	0.15	0.1	0.6	2.5

DVCS limit

TCS limit



- Starting point: OPE + CFT (Braun-Ji-Manashov result)
(see: JHEP 03 (2021) 051 and JHEP 01 (2023) 078)

$$T^{\mu\nu} = i \int d^4z e^{iq'z} \langle p' | \mathcal{T} \{ j^\mu(z) j^\nu(0) \} | p \rangle$$

$$= \frac{1}{i\pi^2} i \int d^4z e^{iq'z} \left\{ \frac{1}{(-z^2 + i0)^2} \left[g^{\mu\nu} \mathcal{O}(1, 0) - z^\mu \partial^\nu \int_0^1 du \mathcal{O}(\bar{u}, 0) - z^\nu (\partial^\mu - i\Delta^\mu) \int_0^1 dv \mathcal{O}(1, v) \right] + \dots \right.$$

where $\mathcal{O}, \mathcal{O}_1, \mathcal{O}_2$ are matrix elements $\langle p' | \mathcal{O} | p \rangle, \langle p' | \mathcal{O}_1 | p \rangle, \langle p' | \mathcal{O}_2 | p \rangle$ containing information about GPDs

- For spin-0 target:

$$T^{\mu\nu} = \mathcal{A}^{00} \frac{-i}{QQ'R^2} \left[(qq') (Q'^2 q^\mu q^\nu - Q^2 q'^\mu q'^\nu) + Q^2 Q'^2 q^\mu q'^\nu - (qq')^2 q'^\mu q^\nu \right]$$

$$+ \mathcal{A}^{+0} \frac{i\sqrt{2}}{R|\bar{p}_\perp|} \left[Q' q^\mu - \frac{qq'}{Q'} q'^\mu \right] \bar{p}_\perp^\nu - \mathcal{A}^{0+} \frac{\sqrt{2}}{R|\bar{p}_\perp|} \bar{p}_\perp^\mu \left[\frac{qq'}{Q} q^\nu + Q q'^\nu \right]$$

$$+ \mathcal{A}^{+-} \frac{1}{|\bar{p}_\perp|^2} \left[\bar{p}_\perp^\mu \bar{p}_\perp^\nu - \tilde{\bar{p}}_\perp^\mu \tilde{\bar{p}}_\perp^\nu \right] - \mathcal{A}^{++} g_\perp^{\mu\nu},$$

$$R = \sqrt{(qq')^2 + Q^2 Q'^2}$$

$$\begin{aligned}
 \mathcal{A}^{++} &= \mathcal{A}^{++}|_{\text{LT}} + I_{(0)} + I_{(i)} + I_{(ii)} + I_{(iii)} + I_{(iv)} + I_{(v)} + I_{(vi)} + I_{(vii)} \\
 &= \frac{1}{2} \int_{-1}^1 dx \left\{ - \left(1 - \frac{t}{2Q^2} + \frac{t(\xi - \rho)}{Q^2} \partial_\xi \right) \frac{H^{(+)}}{x - \rho + i0} \right. \\
 &\quad + \frac{t}{\xi Q^2} \left[\mathbb{P}_{(i)} + \mathbb{P}_{(ii)} - \frac{\tilde{\mathbb{P}}_{(i)} - \tilde{\mathbb{P}}_{(iii)}}{2} - \frac{\xi(J + L)}{2} \right. \\
 &\quad \left. \left. - \frac{\xi}{x + \xi} \left(\ln \left(\frac{x - \rho + i0}{\xi - \rho + i0} \right) - \frac{\xi + \rho}{2\xi} \ln \left(\frac{-\xi - \rho + i0}{\xi - \rho + i0} \right) - \tilde{\mathbb{P}}_{(i)} \right) \right] H^{(+)} \right. \\
 &\quad \left. - \frac{t}{Q^2} \partial_\xi \left[\left(\mathbb{P}_{(i)} + \mathbb{P}_{(ii)} - \frac{\xi L}{2} - \frac{\xi}{x + \xi} \left(\ln \left(\frac{x - \rho + i0}{\xi - \rho + i0} \right) - \frac{\xi + \rho}{2\xi} \ln \left(\frac{-\xi - \rho + i0}{\xi - \rho + i0} \right) - \tilde{\mathbb{P}}_{(i)} \right) \right) H^{(+)} \right] \right. \\
 &\quad \left. + \frac{\bar{p}_\perp^2}{Q^2} 2\xi^3 \partial_\xi^2 \left[\left(\mathbb{P}_{(i)} + \mathbb{P}_{(ii)} - \frac{\tilde{\mathbb{P}}_{(i)} - \tilde{\mathbb{P}}_{(iii)}}{2} - \frac{\xi L}{2} + \ln \left(\frac{x - \rho + i0}{x - \xi + i0} \right) \right) H^{(+)} \right] \right\} + O(\text{tw-6})
 \end{aligned}$$

$$L = \int_0^1 dw \frac{-4}{x - \xi - w(x + \xi)} \int_0^1 du \ln(\xi - \rho + i0 + \bar{u}(x - \xi - w(x + \xi))) \left[\ln\left(\frac{\bar{u}(1-w)}{1-\bar{u}w}\right) + \frac{1}{1-\bar{u}w} \right]$$

$$J = \tilde{J} - \frac{2(\xi - \rho)}{-\xi - \rho + i0} \frac{1}{x - \xi} \ln\left(\frac{x - \rho + i0}{\xi - \rho + i0}\right)$$

$$\begin{aligned} \tilde{J} = & \frac{2(\xi - \rho)}{-\xi - \rho + i0} \frac{1}{x - \xi} \ln\left(\frac{x - \rho + i0}{\xi - \rho + i0}\right) \\ & + \frac{2(x + \rho)}{(x - \xi)(x + \xi)} \left[-\text{Li}_2\left(-\frac{x + \rho}{-\xi - \rho + i0}\right) - \text{Li}_2\left(\frac{2\xi}{x + \xi}\right) + \text{Li}_2\left(-\frac{x + \rho}{-\xi - \rho + i0} \frac{2\xi}{x + \xi}\right) \right. \\ & \quad + \text{Li}_2\left(\frac{x - \rho}{\xi - \rho + i0}\right) + \text{Li}_2\left(-\frac{x - \xi}{\xi - \rho + i0}\right) + \text{Li}_2\left(\frac{x - \rho}{x + \xi}\right) \\ & \quad - \text{Li}_2\left(\frac{\xi - \rho + i0}{x + \xi}\right) - \text{Li}_2\left(\frac{x + \rho}{x + \xi}\right) + \text{Li}_2\left(-\frac{-\xi - \rho + i0}{x + \xi}\right) \\ & \quad \left. + \text{Li}_2\left(-\frac{x - \xi}{-x - \rho + i0}\right) + \frac{1}{2} \ln^2\left(\frac{-\xi - \rho + i0}{-x - \rho + i0}\right) \right] \\ & + \frac{\xi - \rho}{\xi(x + \xi)} \left[-\text{Li}_2\left(\frac{2\xi}{\xi - \rho + i0}\right) - \text{Li}_2\left(-\frac{2\xi}{-\xi - \rho + i0}\right) + 2\text{Li}_2(1) \right. \\ & \quad - \text{Li}_2\left(\frac{x - \xi}{x + \xi} \frac{-\xi - \rho + i0}{\xi - \rho + i0}\right) - \text{Li}_2\left(\frac{-\xi - \rho + i0}{\xi - \rho + i0}\right) + \text{Li}_2\left(\frac{x - \xi}{x + \xi} \frac{\xi - \rho + i0}{-\xi - \rho + i0}\right) \\ & \quad - \text{Li}_2\left(\frac{\xi - \rho + i0}{-\xi - \rho + i0}\right) - \ln\left(\frac{2\xi}{x + \xi}\right) \ln\left(\frac{-\xi - \rho + i0}{\xi - \rho + i0}\right) \\ & \quad - \ln\left(-\frac{2\xi}{x + \xi} \frac{-\xi - \rho + i0}{\xi - \rho + i0}\right) \ln\left(\frac{-\xi - \rho + i0}{\xi - \rho + i0}\right) - \text{Li}_2\left(\frac{2\xi}{x + \xi} \frac{x - \rho + i0}{\xi - \rho + i0}\right) + \text{Li}_2\left(\frac{2\xi}{x + \xi}\right) \left. \right] \\ & - \frac{\xi + \rho}{\xi(x - \xi)} \left[\text{Li}_2\left(\frac{x - \xi}{x + \xi}\right) - \text{Li}_2\left(\frac{x - \xi}{x + \xi} \frac{\xi - \rho + i0}{-\xi - \rho + i0}\right) + \ln\left(\frac{-\xi - \rho + i0}{\xi - \rho + i0}\right) \ln\left(\frac{2\xi}{x + \xi}\right) \right. \\ & \quad \left. - \ln\left(\frac{x - \rho + i0}{\xi - \rho + i0}\right) \ln\left(\frac{-\xi - \rho + i0}{\xi - \rho + i0} \frac{x - \xi}{x + \xi}\right) \right]. \end{aligned}$$

$$\mathbb{P}_{(i)}(x/\xi, \rho/\xi) = \frac{\xi - \rho}{x - \xi} \text{Li}_2\left(-\frac{x - \xi}{\xi - \rho + i0}\right),$$

$$\tilde{\mathbb{P}}_{(i)}(x/\xi, \rho/\xi) = -\frac{\xi - \rho}{x - \xi} \ln\left(\frac{x - \rho + i0}{\xi - \rho + i0}\right),$$

$$\mathbb{P}_{(ii)}(x/\xi, \rho/\xi) = \frac{\xi - \rho}{x + \xi} \left[\text{Li}_2\left(-\frac{x - \xi}{\xi - \rho + i0}\right) - (x \rightarrow -\xi) \right],$$

$$\tilde{\mathbb{P}}_{(iii)}(x/\xi, \rho/\xi) = -\frac{\xi + \rho}{x + \xi} \ln\left(\frac{x - \rho + i0}{-\xi - \rho + i0}\right).$$

- In $Q^2 \rightarrow 0$ limit (DVCS) expression agrees with Braun-Ji-Manashov result

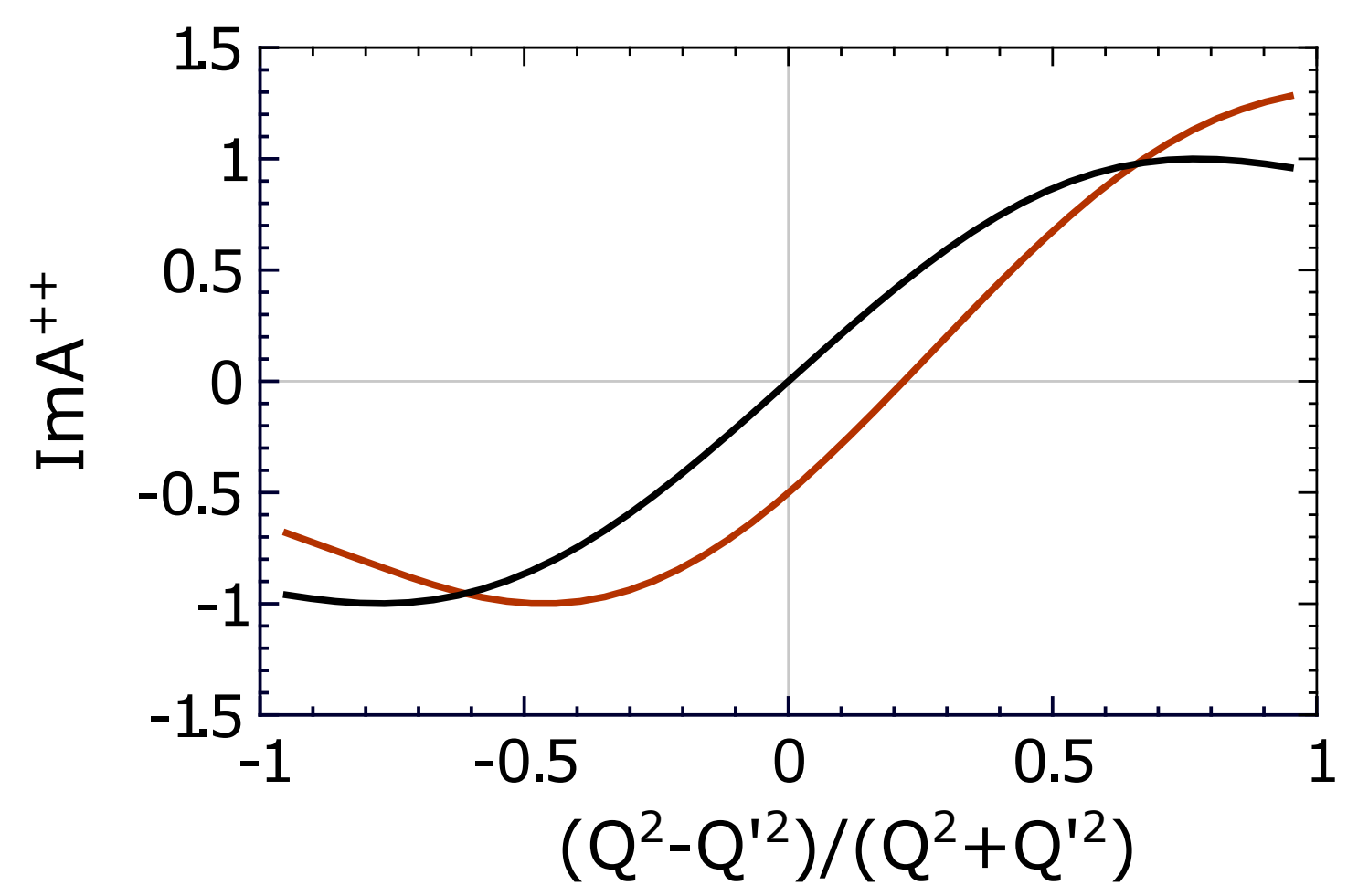
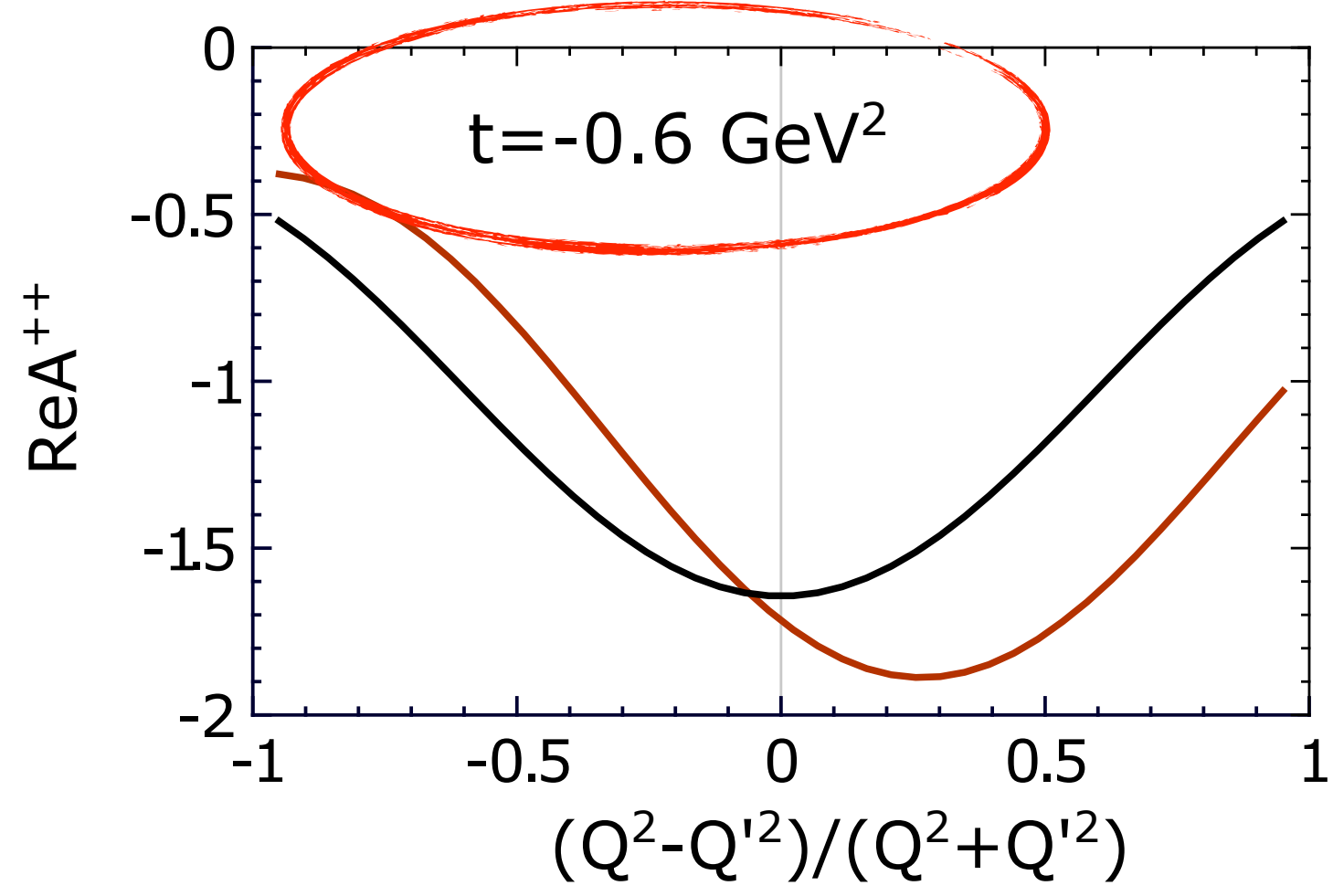
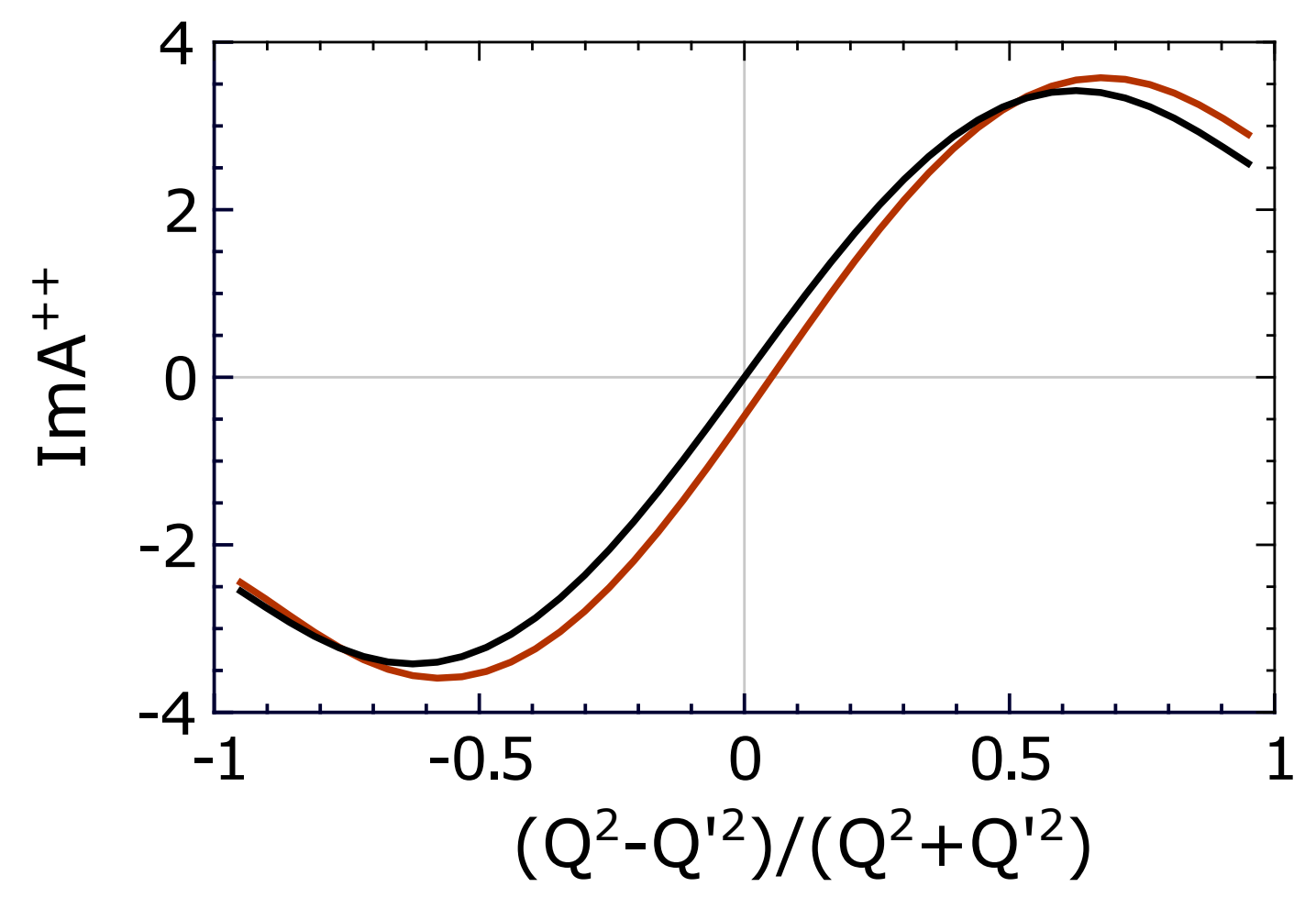
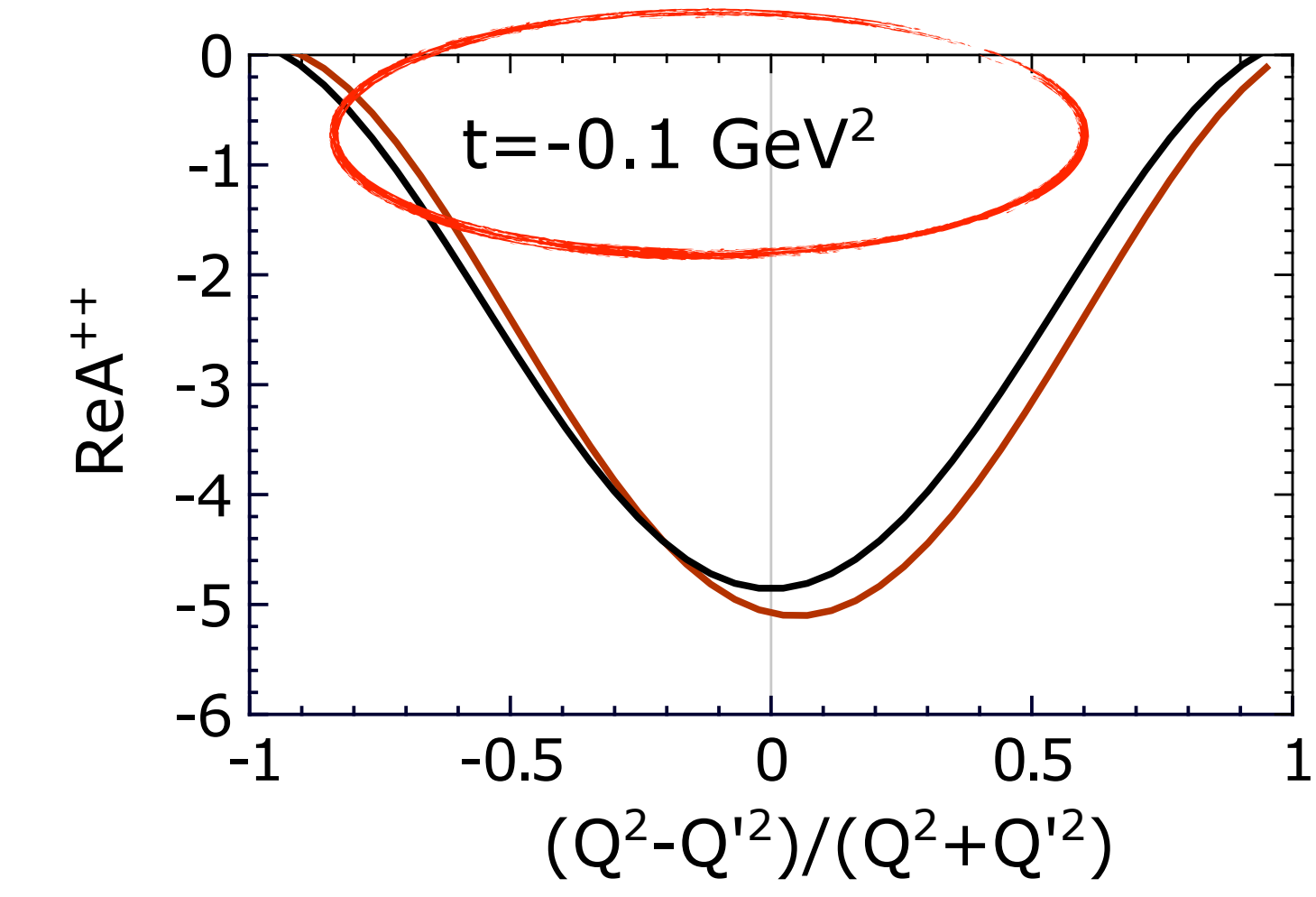
$$\begin{aligned}
 \mathcal{A}_{\text{DVCS}}^{++} &= \lim_{\rho \rightarrow \xi} \mathcal{A}^{++} \\
 &= \frac{1}{2} \int_{-1}^1 dx \left\{ - \left(1 - \frac{t}{2Q_{\text{DVCS}}^2} \right) \frac{H^{(+)}}{x - \xi + i0} \right. \\
 &\quad - \frac{2t}{Q_{\text{DVCS}}^2} \left[\frac{1}{x + \xi} \ln \left(\frac{x - \xi + i0}{-2\xi} \right) + \frac{1}{x - \xi} \left(\text{Li}_2 \left(\frac{x + \xi}{2\xi} \right) - \text{Li}_2(1) \right) \right] H^{(+)} \\
 &\quad + \frac{t}{Q_{\text{DVCS}}^2} \partial_\xi \left[\left(\frac{2\xi}{x - \xi} \left(\text{Li}_2 \left(\frac{x + \xi}{2\xi} \right) - \text{Li}_2(1) \right) + \frac{\xi}{x + \xi} \ln \left(\frac{x - \xi + i0}{-2\xi} \right) \right) H^{(+)} \right] \\
 &\quad \left. - \frac{\bar{p}_\perp^2}{Q_{\text{DVCS}}^2} 2\xi^3 \partial_\xi^2 \left[\left(\frac{2\xi}{x - \xi} \left(\text{Li}_2 \left(\frac{x + \xi}{2\xi} \right) - \text{Li}_2(1) \right) + \frac{\xi}{x + \xi} \ln \left(\frac{x - \xi + i0}{-2\xi} \right) \right) H^{(+)} \right] \right\} \\
 &\quad + O(\text{tw-6}),
 \end{aligned}$$

V. Martínez-Fernández,
B. Pire, PS, J. Wagner
preliminary

- New result for $Q^2 \rightarrow 0$ limit (TCS)

$$\begin{aligned}
 \mathcal{A}_{\text{TCS}}^{++} &= \lim_{Q^2 \rightarrow 0} \mathcal{A}^{++} \\
 &= \frac{1}{2} \int_{-1}^1 dx \left\{ - \left(1 - \frac{5}{2} \frac{t}{Q_{\text{TCS}}^2} \right) \frac{H^{(+)}}{x + \xi(1 - 2t/Q^2) + i0} \right. \\
 &\quad + \frac{2t}{Q_{\text{TCS}}^2} \left[\frac{1}{x - \xi} \text{Li}_2 \left(-\frac{x - \xi}{2\xi} \right) + \frac{1}{x + \xi} \left(\text{Li}_2 \left(-\frac{x - \xi}{2\xi} \right) - \text{Li}_2(1) \right) - \frac{\xi}{4} (L_{\text{TCS}} + J_{\text{TCS}}) \right] H^{(+)} \\
 &\quad - \frac{t}{Q_{\text{TCS}}^2} \partial_\xi \left[\left(\frac{2\xi}{x + \xi + i0} + \frac{2\xi}{x - \xi} \text{Li}_2 \left(-\frac{x - \xi}{2\xi} \right) + \frac{2\xi}{x + \xi} \left(\text{Li}_2 \left(-\frac{x - \xi}{2\xi} \right) - \text{Li}_2(1) \right) - \frac{\xi L_{\text{TCS}}}{2} \right. \right. \\
 &\quad \left. \left. - \frac{\xi}{x - \xi} \ln \left(\frac{x + \xi + i0}{2\xi} \right) \right) H^{(+)} \right] \\
 &\quad + \frac{\bar{p}_\perp^2}{Q_{\text{TCS}}^2} 2\xi^3 \partial_\xi^2 \left[\left(\frac{2\xi}{x - \xi} \text{Li}_2 \left(-\frac{x - \xi}{2\xi} \right) + \frac{2\xi}{x + \xi} \left(\text{Li}_2 \left(-\frac{x - \xi}{2\xi} \right) - \text{Li}_2(1) \right) + \frac{\xi}{x - \xi} \ln \left(\frac{x + \xi + i0}{2\xi} \right) \right. \right. \\
 &\quad \left. \left. - \frac{\xi L_{\text{TCS}}}{2} + \ln \left(\frac{x + \xi + i0}{x - \xi + i0} \right) \right) H^{(+)} \right] \right\} + O(\text{tw-6}),
 \end{aligned}$$

- Numerical estimate:



— LT
— LT+HT corrections
(up to tw-4)

$\xi = 0.2$

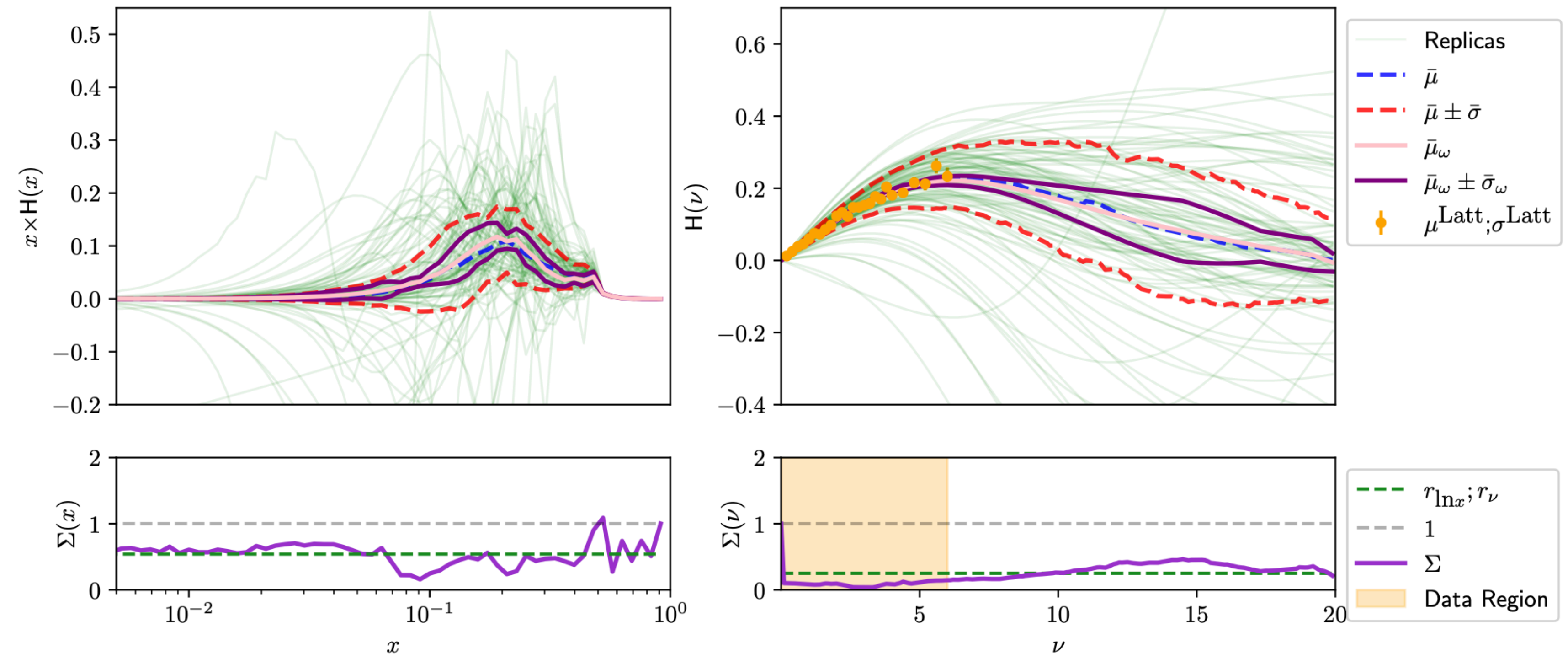
$\mu^2 = 1.9 \text{ GeV}^2$

GPD model from:
PRD 105, 094012 (2022)

M. J. Riberdy, H. Dutrieux, C. Mezrag, PS, EPJC 84 (2024) 2, 201

- Exploratory study to include lattice-QCD results!

Reduction of GPD model uncertainties due to inclusion of pseudo-latticeQCD results



- Take-away messages:
 - virtual Compton scattering processes are important for measuring GPDs.
 - DVCS and TCS only give limited access to GPDs, but still offer a wealth of important information:
 - nucleon tomography at low- x_B
 - "mechanical" properties
 - Froissart-Gribov projections (now also for spin 1/2 target)
 - DDVCS allows to avoid limitations of DVCS and TCS, but is much more difficult to measure
 - new DDVCS description (including pheno. studies) available
 - new evaluation of DDVCS (and also TCS) amplitudes in terms of twist expansion will become available soon
 - new impact studies of lattice QCD data inclusion

Dual parameterisation:

$$H_+(x, \xi, t) = 2 \sum_{\substack{n=1 \\ \text{odd}}}^{\infty} \sum_{\substack{l=0 \\ \text{even}}}^{n+1} B_{n,l}(t) \theta \left(1 - \frac{x^2}{\xi^2} \right) \left(1 - \frac{x^2}{\xi^2} \right) C_n^{3/2} \left(\frac{x}{\xi} \right) P_l \left(\frac{1}{\xi} \right)$$

Coefficients of Mellin moments:

$$\int_0^1 dx x^N H_+(x, \xi, t) = \sum_{\substack{k=0 \\ \text{even}}}^{N+1} h_{N,k}(t) \xi^k$$

where:

$$h_{N,k}(t) = \sum_{\substack{n=1 \\ \text{odd}}}^N \sum_{\substack{l=0 \\ \text{even}}}^{n+1} B_{n,l}(t) (-1)^{\frac{k+l-N-1}{2}} \frac{\Gamma \left(1 - \frac{k-l-N}{2} \right)}{2^k \Gamma \left(\frac{1}{2} + \frac{k+l-N}{2} \right) \Gamma(2-k+N)} \frac{(n+1)(n+2)\Gamma(N+1)}{\Gamma \left(1 + \frac{N-n}{2} \right) \Gamma \left(\frac{5}{2} + \frac{N+n}{2} \right)}$$

E.g.:

$$\int_0^1 dx x H_+(x, \xi, t) = \frac{6B_{1,2}(t)}{5} + \xi^2 \left(\frac{4B_{1,0}(t)}{5} - \frac{2B_{1,2}(t)}{5} \right)$$

This gives:

$$F_{J=0}(t) = 4 \sum_{\substack{n=1 \\ \text{odd}}}^{\infty} B_{n,0}(t) = 4 \sum_{\nu=1}^{\infty} B_{2\nu-1,0}(t)$$

$$F_{J>0}(t) = 4 \sum_{\substack{n=J-1 \\ \text{odd}}}^{\infty} B_{n,J}(t) = 4 \sum_{\nu=0}^{\infty} B_{J+2\nu-1,J}(t)$$

The relations allow us to define "sum rules", e.g. for $\nu = 1$:

$$F_{J=0}(t) = 4(B_{1,0}(t) + \dots) = \frac{5}{3}h_{1,0}(t) + 5h_{1,2}(t) + \left\{ \begin{array}{l} \text{contribution of conformal PWs} \\ \text{with } \nu \geq 2 \end{array} \right\}$$

$$F_{J=2}(t) = 4(B_{1,2}(t) + B_{3,2}(t) + \dots) = -\frac{7}{6}h_{1,0}(t) + 9h_{3,0}(t) + \frac{21}{2}h_{3,2}(t) + \left\{ \begin{array}{l} \text{contribution of conformal PWs} \\ \text{with } \nu \geq 2 \end{array} \right\}$$

Modified dual parameterisation:

$$H_+(x, \xi, t) = 2 \sum_{\substack{n=1 \\ \text{odd}}}^{\infty} \sum_{\substack{l=0 \\ \text{even}}}^{n+1} \beta^l \bar{B}_{n,l}(t) \theta \left(1 - \frac{x^2}{\xi^2} \right) \left(1 - \frac{x^2}{\xi^2} \right) C_n^{3/2} \left(\frac{x}{\xi} \right) P_l \left(\frac{1}{\xi\beta} \right)$$

$$\beta = \sqrt{1 - \frac{4m^2}{t}}$$

Coefficients of Mellin moments:

$$\int_0^1 dx x^N H_+(x, \xi, t) = \sum_{\substack{k=0 \\ \text{even}}}^{N+1} h_{N,k}(t) \xi^k$$

$$h_{N,k}(t) = \sum_{\substack{n=1 \\ \text{odd}}}^N \sum_{\substack{l=0 \\ \text{even}}}^{n+1} \beta^{l+k-N-1} \bar{B}_{n,l}(t) (-1)^{\frac{k+l-N-1}{2}} \frac{\Gamma \left(1 - \frac{k-l-N}{2} \right)}{2^k \Gamma \left(\frac{1}{2} + \frac{k+l-N}{2} \right) \Gamma(2-k+N)} \frac{(n+1)(n+2)\Gamma(N+1)}{\Gamma \left(1 + \frac{N-n}{2} \right) \Gamma \left(\frac{5}{2} + \frac{N+n}{2} \right)}$$

To keep these coefficients regular at $t=0$ one has to assume:

For $\beta \neq 1$ FG projections get admixture from higher spins

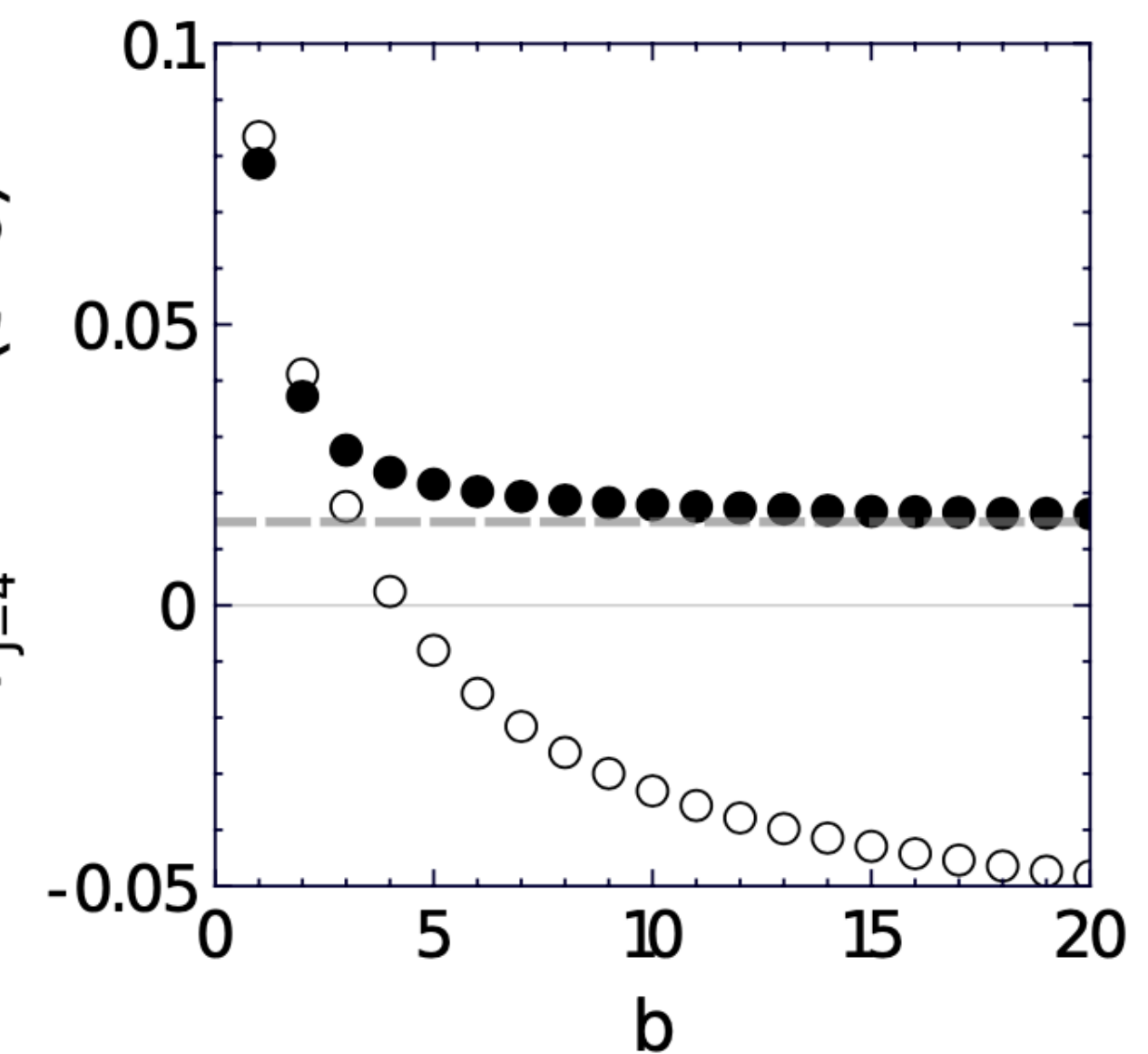
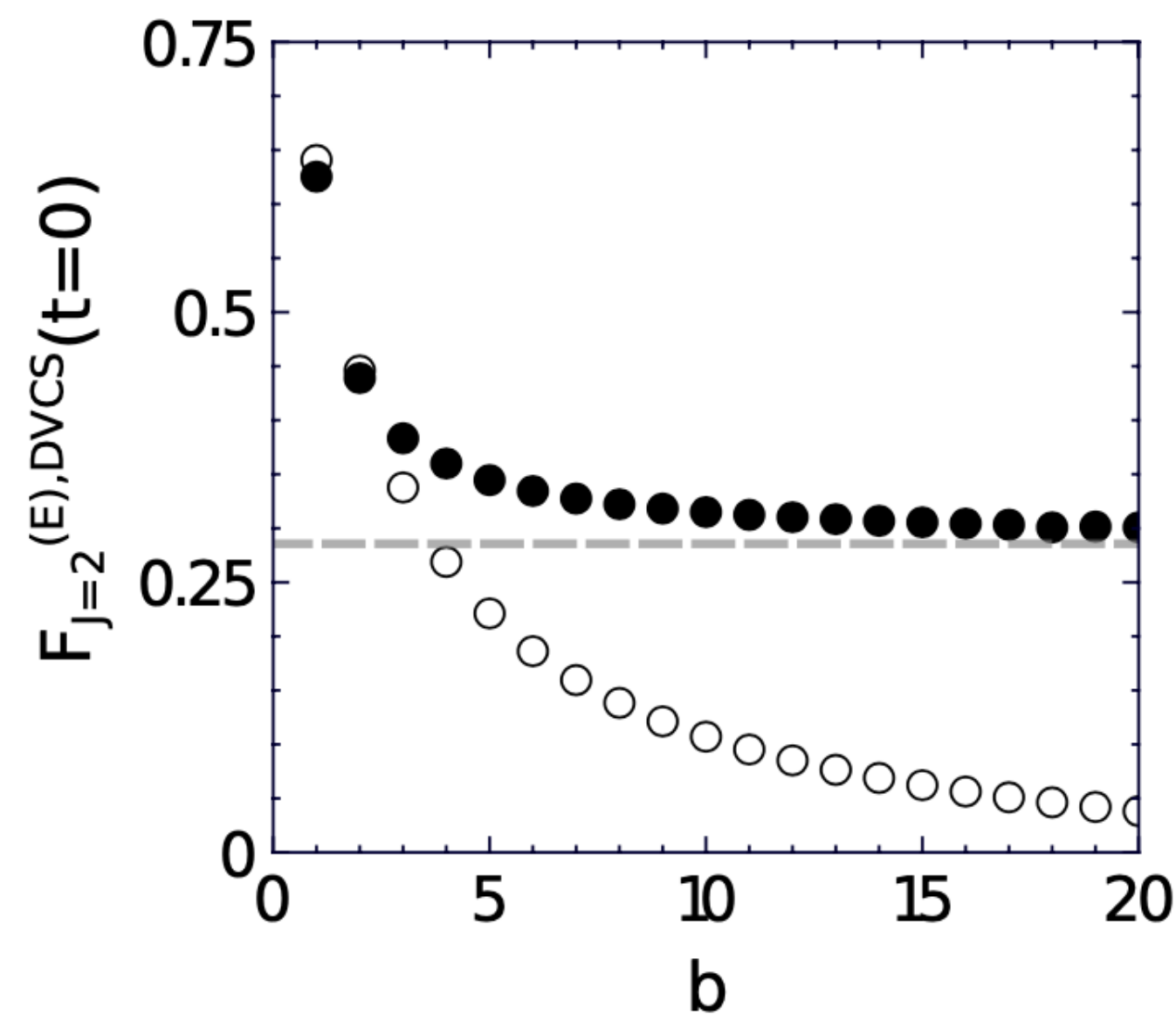
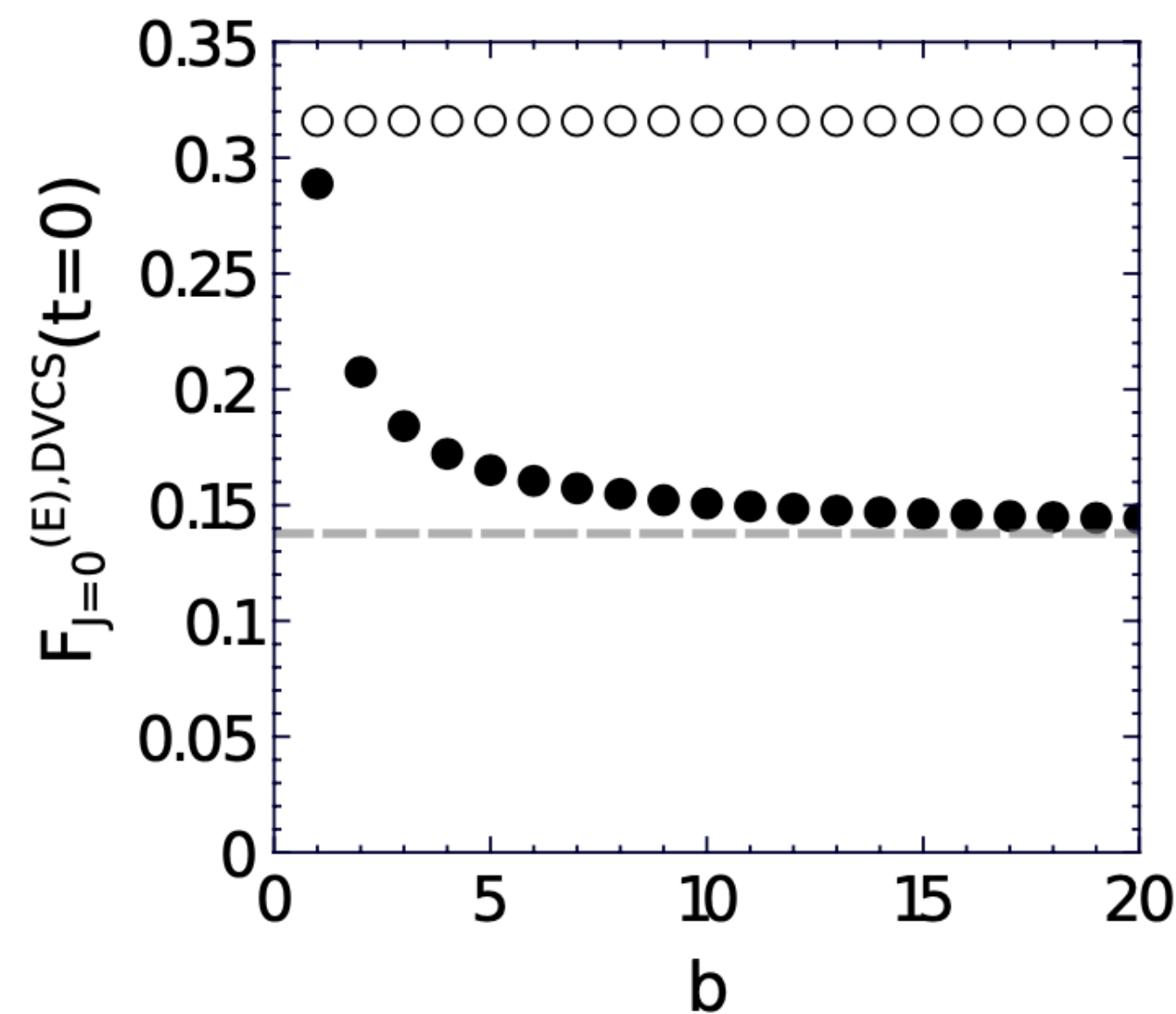
$$B_{n,n+1}(t) = \bar{B}_{n,n+1}(t)$$

$$B_{n,n-1}(t) = \bar{B}_{n,n-1}(t) - (1 - \beta^2) \left(\frac{1}{2} - n \right) \bar{B}_{n,n+1}(t)$$

spin J=n-1
spin J=n+1

Sensitivity of FG projections on the shape of DD profile function

$$H(x, \xi, t=0) = \int_{-1}^1 d\beta \int_{-1+|\beta|}^{1-|\beta|} d\alpha \delta(\beta + \xi\alpha - x) q(\beta) \frac{\Gamma(2b+2)}{2^{2b+1}\Gamma^2(b+1)} \frac{((1-|\beta|)^2 - \alpha^2)^b}{(1-|\beta|)^{2b+1}}$$



- projections from GPD $b \rightarrow \infty$ limit (no skewness effect)
- projections from sum rules (i.e. from certain Mellin moments) for $\nu = 1$